Stone Mountain Technologies, Inc.

Development & Validation of a Gas-Fired Residential Heat Pump Water Heater
DE-EE0003985

Final Report
January 21, 2013

Prepared For:
Jim Payne, Project Officer
U.S. DOE/Golden Field Office
Golden, Colorado

Prepared By:
Michael Garrabrant
Stone Mountain Technologies, Inc.
Unicoi, TN 37692

Team Members:
A.O. Smith Corporation
Milwaukee, WI

Gas Technology Institute
Chicago, Ill

Georgia Institute of Technology
Atlanta, GA

ACKNOWLEDGMENTS

The work presented in this report is the result of the hard work and dedication of dozens of individuals and small businesses. Roger Stout, David Firestine and Chuck Culver designed, assembled and tested solution pumps, breadboard heat pump systems, and the packaged prototype. Janice Fitzgerald of A.O. Smith designed and tested prototype storage tank/heat exchanger prototypes and oversaw EF testing and data analysis at AO Smith's laboratories. Paul Glanville of GTI completed combustion system development, burner design and EF testing. Chris Keinath of the Georgia Institute of Technology completed cycle modeling, heat exchanger design and breadboard testing. Eugene, Jason and Michael Brackins (Brackins Machine; Erwin TN) and Rich Albert (ARS Solutions; Dayton OH) provided invaluable prototype fabrication and assembly services.

SMTI also thanks the Department of Energy for funding and supporting this work regarding this breakthrough water heating technology.

EXECUTIVE SUMMARY

For gas-fired residential water heating, the U.S. and Canada is predominantly supplied by minimum efficiency storage water heaters with Energy Factors (EF) in the range of 0.59 to 0.62. Higher efficiency and higher cost ($700 - $2,000) options serve about 15% of the market, but still have EFs below 1.0, ranging from 0.65 to 0.95. To develop a new class of water heating products that exceeds the traditional limit of thermal efficiency, the project team designed and demonstrated a packaged water heater driven by a gas-fired ammonia-water absorption heat pump. This gas-fired heat pump water heater can achieve EFs of 1.3 or higher, at a consumer cost of $2,000 or less.

Led by Stone Mountain Technologies Inc. (SMTI), with support from A.O. Smith, the Gas Technology Institute (GTI), and Georgia Tech, the cross-functional team completed research and development tasks including cycle modeling, breadboard evaluation of two cycles and two heat exchanger classes, heat pump/storage tank integration, compact solution pump development, combustion system specification, and evaluation of packaged prototype GHPWHs.

The heat pump system extracts low grade heat from the ambient air and produces high grade heat suitable for heating water in a storage tank for domestic use. Product features that include conventional installation practices, standard footprint and reasonable economic payback, position the technology to gain significant market penetration, resulting in a large reduction of energy use and greenhouse gas emissions from domestic hot water production.

TABLE OF CONTENTS

1.0 Introduction 5

2.0 Scope of Work & Project Tasks 8

3.0 Task 2: Cycle Design & Optimization 10

4.0 Task 3: Storage Tank Design/CFD 16

5.0 Task 4: Heat Exchanger Design 22

6.0 Task 8: Solution Pump Development 26

7.0 Task 5: Combustion System Design..... 28

8.0 Task 6: Breadboard Testing 40

9.0 Task 7: Evaluation 45

10.0 Tasks 9 & 10: Alpha Packaged Prototype 46

11.0 Task 11: Beta Packaged Prototypes 51

12.0: Task 12: Water Heating System Application Modeling 63

13.0 Summary & Technology Status 79

14.0 References 80

15.0 List of Acromyms 83

1.0 INTRODUCTION

For gas-fired residential water heating, the U.S. and Canada is predominantly supplied by minimum efficiency gas-fired storage water heaters. Popular due to their low cost, the atmospheric center-flue design represents the majority. The most common size, a 40 gallon unit, will typically have an Energy Factor (EF) in the range of 0.59 to 0.62. For consumers, their options for higher efficiency gas water heating options are threefold:

- Upgrade to a non-condensing storage EnergyStar® water heater, with an EF of 0.67-0.70, which with the current generation of models requires electrical power service.

- Upgrade to a condensing storage water heater, requiring a venting upgrade and power service. These commercial water heaters are rated as greater than 90% thermal efficiency, non-certified laboratory testing has suggested that their performance would result in an EF of less than 0.80 (Davis, 2012).

- Convert to a condensing or non-condensing tankless water heater with EFs typically between 0.82 and 0.95. In addition to requiring a venting upgrade and power service, an up-sizing in the gas service from ½" to ¾" is required. The validity of these efficiency metrics for tankless units is currently in dispute, as the impact of cyclic/startup losses, which due to hot water draw intermittency have lead several groups to "de-rate" the efficiency of units by up to 9% (RESNET 2012).

As approximately half of water heaters sold in the U.S. and Canada for residential and small commercial applications are natural gas fired storage water heaters, it is critical to look beyond these options for high-efficiency, low-installed cost products.

Initial development of a gas-fired residential heat pump water heater with a primary fuel efficiency 2.4 times higher than conventional gas storage water heaters, and 2.1 times higher than electric heat pump water heaters was completed during this project. The heat pump system extracts low grade heat from the ambient air and produces high grade heat suitable for heating water in a storage tank for domestic use. Product features that include conventional installation practices, standard footprint and reasonable economic payback, position the technology to gain significant market penetration, resulting in a large reduction in greenhouse gas emissions from domestic hot water use.

The project team consists of ***Stone Mountain Technologies, Inc***., and major sub-contractors Dr. Srinivas Garimella from the ***Georgia Institute of Technology***, ***A.O. Smith Corporation*** (OEM partner), and the ***Gas Technology Institute***. Project tasks included heat pump thermodynamic cycle optimization, modeling of the heat pump to storage tank interface, heat and mass exchanger design, solution pump development/testing, and system application modeling, followed by the construction and testing of full scale prototypes.

A gas-fired residential heat pump water heater with an Energy Factor (EF) approaching 1.5 offers substantial energy use reduction compared to both 'standard' 0.62 EF gas storage type and 0.82 EF tankless, at a cost target ($1,800) roughly equivalent to tankless technologies. With a primary energy efficiency greater than one (150%), gas heat pump water heaters contribute positively to DOE's net-zero energy home goals.

Current State of Technology: Current residential water heater technologies, both existing and under development, have primary energy efficiencies less than one. The energy efficiency of residential water heaters is given by an Energy Factor (EF), which accounts for both the heating efficiency and passive losses to the ambient (stand-by). Typical values of EF and installed cost are provided in the Table 1. Note that even new electric heat pump water heaters making their way into the market this year with an EF of 2.0, as well as fully condensing tankless models, have a primary energy efficiency less than one. In order to meet our nation's goal of improving building sustainability and achieving significantly reduced carbon footprint, a cost-effective residential water heater system is needed that has a primary energy efficiency much greater than one. Solar Thermal systems provide sustainable energy efficiencies, but their system complexity and high installed cost remain barriers for large market penetration. A gas-fired residential heat pump water heater, using a simple absorption cycle and condensing combustion, can provide primary energy efficiencies of 150% while retaining conventional installation simplicity and envelopes, at an installed cost that yields excellent economic payback. These features provide for a product that can establish significant market penetration, potentially cutting the carbon footprint of residential hot water use in half.

Table 1: Residential Water Heater Efficiecy and Installed Cost

	EF	Primary Energy EF (1)	Installed Cost (2)
Non-Condensing Gas Storage	0.60	**0.60**	$967
Condensing Gas Storage	0.82	**0.82**	$2,200 (3)
Non-Condensing Gas Tankless	0.82	**0.82**	$1,902
Condensing Gas Tankless	0.92	**0.92**	$2,258
Electric Storage	0.95	**0.33**	$786
Electric Heat Pump	2.00	**0.70**	$1,475
Gas-Fired Heat Pump	1.50	**1.50**	$1,800 (4)

(1) Grid Electric Power Provided at 35% Efficiency

(2) Preliminary Technical Support Document: Energy Efficiency Program for Consumer Products, DOE, 01/05/09

(3) Value not profided in DOE Report, Author's Estimate (4) Target Value

Heat activated absorption cycles, using a wide variety of working fluids, have been utilized to provide cooling, refrigeration, and heating for many years. Absorption cycles utilize thermal energy as the primary energy source instead of mechanical work (electric motor driven compressor) utilized by vapor-compression cycles. The most common working fluids for absorption cycles are ammonia-water (NH_3-H_2O) and lithium bromide-water (LiBr-H_2O), although there are many other combinations. Since water is used as the refrigerant for LiBr-H_2O systems, these cycles cannot be used for heat pump applications.

Historically, the hurdles to commercialization of absorption heat pump equipment for the residential HVAC market have been high cost and large footprint. Prior research and development programs have targeted space cooling and heating applications, with capacities of 36,000 – 100,000 Btu/hr (10 - 30 kW). Numerous cycles to achieve cooling and heating from these absorption systems have been proposed and investigated in research laboratories throughout the world. In general, research has taken the path of embracing increasingly complex cycle configurations (e.g., double-, triple-, and even quadruple- effect cycles, GAX cycles, Branched GAX cycles, and Vapor-Exchange GAX cycles) to improve system efficiencies.

While these approaches have indeed yielded progressively smaller increases in efficiency, they have, in most cases, proven to be unviable due to the high levels of system complexity, difficult-to-implement control systems, and excessive component and system footprints with correspondingly high costs that cannot be justified in the marketplace. The commercial success of a thermally activated residential heat pump water heater hinges upon the use of a simple, reliable cycle and the availability of efficient, manufacturable and economical heat and mass exchangers. The development of a compact, heat and mass exchanger technology that could be applied to a variety of heat and mass transfer processes such as

desorption, condensation, evaporation, absorption, and recuperative heat exchange, and a highly efficiency combustion system (condensing) would enable the deployment of the subject water heating system. Additionally, by integrating an absorption heat pump system with a storage tank, which acts as a thermal battery providing a large quantity of thermal energy when needed on an intermittent basis, a very small, low capacity heat pump system can be used, minimizing size and cost.

Project Performance Goals: The end result of the project is a ***proof-of-concept*** gas-fired absorption heat pump residential water heater with an approximate 3 kW (10,000 Btu/hr) heating capacity, combined with a conventional residential water storage tank (60 – 80 gallons) to provide a first hour rating of at least 50, with a consumer cost approximately equivalent to an electric heat pump water heater or condensing tankless model. The heat pump system efficiency is expected to be 150-160%, resulting in an EF of 1.3 to 1.5 taking into account parasitic and stand-by losses.

The heat pump module will be mounted directly on top of the storage tank (Figure 1). Capacity and storage volume align with electric heat pump models currently in the market. The heat pump module will utilize a simple NH_3-H_2O cycle and high efficiency heat and mass exchangers to keep the footprint small and the refrigerant charge very low (below the requirement for small NH_3 systems in mechanical codes).

Figure 1: Residential Gas Heat Pump Water Heater

2.0 SCOPE OF WORK AND PROJECT TASKS

Scope of Work: The scope of work began with thermodynamic cycle model application optimization, and CFD analysis of heat pump cycle-storage tank heat exchange options. The resulting cycle state points provided input to component design algorithms. Two sets of heat exchangers were designed and tested, one using microscale geometries, the other using small-scale shell-tube, concentric-tube or plate-fin geometries. A solution pump suitable for the application was designed, fabricated and tested. An Alpha and three Beta packaged prototypes were fabricated and tested. In-kind cofunded work scope performed by GTI developed a model of this water heater for incorporation into whole house water heating system simulation tools, along with recommendations for ASHRAE Method of Test Standard development.

Task 1.0 Project Management Plan

Task 2.0 Thermodynamic Cycle Modeling: Single-effect and GAX ammonia-water heat pump cycles were modeled (using EES software platform) and optimized for performance over a range of operating conditions suitable for the water heating application. Mass, species and energy balances at each component were performed, together with the component heat transfer resistances using heat exchanger effectivenesses, overall heat transfer conductances, or closest approach temperature differences CAT, as appropriate. This resulted in a set of cycle state points (temperature, pressure, flow rate, species concentration and physical state) and heat exchanger performance parameters (Q, UA, LMTD and effectiveness), used to design the prototype components in Task 3, as well as provide estimated system performance over the range of anticipated operational ambient and water temperatures.

Task 3.0 CFD Modeling of Storage Tank Heat Exchange: A CFD model (using Fluent® Software) was developed to model and understand the transfer of heat from the heat pump cycle and condensing combustion system to the storage tank. The temperature of the water inside the storage tank varies as water is drawn from the tank (under an infinite number of draw patterns) and slowly loses heat to the ambient through the tank insulation (standby loss). The water temperature in the tank is preferably stratified, hotter at the top and colder at the bottom, but the degree of stratification changes over time according to the draw pattern and stand-by losses. Heat will be transferred from the heat pump using a pumped working fluid that collects the condenser and absorber heat and transfers it to the stored water. Both internal and external (tank) coils were evaluated based on performance and estimated cost.

Task 4.0 Heat Exchanger Design and Fabrication: Heat exchangers for a nominal 3 kW heating system will were designed per the cycle state points developed in Task 2, using both microscale (GIT) and conventional geometries (SMTI), and coupled heat and mass transfer modeling techniques developed by both GIT and SMTI from prior work. Microscale manufacturing techniques and costs were evaluated.

Task 5.0 Combustion System Development: A low-NOx condensing combustion system was evaluated, designed and selected. GTI developed CFD models for the burner and combustion chamber, simulating heat transfer to the burner-side heat exchanger and NOx production. GTI and SMTI tested and evaluated several burner/blower/gas valve combinations.

Task 6.0 Breadboard Testing: Components designed and fabricated in Task 4 were installed in laboratory breadboard systems (microscale at GIT, conventional at SMTI) to determine performance and operational characteristics. Cycle state points (temperatures, flow rates, pressures) were measured as appropriate. For breadboard testing, the evaporator load was provided by a heated hydronic loop and the heat loads rejected to a chilled water loop maintained at the appropriate temperature. Design changes based on performance were identified and implemented on the breadboard systems prior to design and fabrication of the Alpha packaged prototype.

Task 7.0 Component Evaluation: Results of the breadboard testing were assessed based on performance, projected component cost estimates and packaged system size constraints. Optimum component designs were selected for a packaged system.

Task 8.0 Solution Pump Design and Testing: Absorption cycles require a small positive pressure pump to move solution from the low pressure to the high pressure side of the cycle. Since the solution is often at or near saturation, slow moving diaphragm or piston pumps that can handle a two-phase mixture are typically used. Due to the unique requirements of this application, cost effective pumps are not commercially available for volume heat pump production. Low internal pressure losses and the ability to pull solution into the pump, especially at low ambients where the low side pressure may be close to, or below atmospheric, is also critical.

Solution pump designs used on prior or similar systems were evaluated for, performance over a wide range of ambient conditions, reliability, manufacturing complexity, and cost. A suitable pump was designed and prototypes fabricated and tested to confirm performance over the desired range of conditions.

Task 9.0 Alpha Packaged System Design and Fabrication: A packaged system (heat pump and gas water heater storage tank), representative of a commercial product, was designed and fabricated using the components selected in Task 7. Auxiliary components and sub-systems were obtained from commercial vendors. A PLC control system was designed and fabricated.

Task 10.0 Alpha Packaged System Testing: The Alpha prototype was performance tested over a variety of operating conditions and per the DOE Residential Water Heater Efficiency Test. System components and control methods were modified to improve performance where possible.

Task 11 Beta Packaged System: Based on results and lessons learned from the Alpha unit, three Beta units were fabricated and tested (one at AOS, one at GTI, and one at SMTI). Performance and operational characteristics were determined over a range of expected operating conditions and per the DOE test procedure. Preliminary design specification package was completed and manufacturing costs estimated.

Task 12 Water Heating System Application Modeling & Test Method Development: GTI performed these in-kind cofunded activities under the Residential Water Heater Program project sponsored by the California Energy Commission (CEC). This task develop system-level analytical tools and addressed current test methods for gas-fired water heaters. Under the broader CEC work scope, the goal was to implement a simplified equation-based simulation model of gas-fired water heaters using modern programming tools, based on the detailed modeling performed under Tasks 2 and 3 and the experimental data generated from Tasks 5, 7, 9 and 10.

The secondary goal was to improve the methods of test for gas-fired residential water heaters. Through inclusion of validated modeling tools for gas-fired heat pump water heaters, this task supported the revision of ASHRAE SPC 118.2, Method of Testing for Rating Residential Water Heaters (MOT), so that it will be capable of testing all advanced residential water heaters (currently, gas-fired heat pump water heater models are not covered). The ASHRAE test procedure may be adopted by the Department of Energy for their Energy Factor rating procedure.

Task 13 Final Project Report: Results, findings, conclusions and recommendations for future work were documented in the Final Project Report.

3.0 Task 2: THERMODYNAMIC CYCLE MODELING

Thermodynamic cycle models of a single-effect ammonia-water absorption system (Figure 2) and a Generator-Absorber heat eXchange (GAX) system (Figure 5) were developed in *Engineering Equation Solver* (EES) software. Both systems were modeled with a direct gas-fired counter-flow desorber, an ambient coupled evaporator, and a water tank coupled condenser and absorber. In the GAX cycle, increased internal heat recuperation reduces the required heat input while maintaining the heating capacity obtained in the single-effect cycle. The improvement in system performance comes with the penalty of increased system complexity and control requirements.

Baseline models were developed for both systems where coupling fluid (water) entered the absorber and condenser at 90˚F and exited at 105˚F, and the ambient source temperature was 68˚F at a relative humidity of 0.5. During model development, heat transfer resistances were taken into account with the specification of overall heat conductance, *UA,* for each heat exchanger. Baseline *UA* values for each component were calculated initially using reasonable assumptions for the closest approach temperature (*CAT*) or heat exchanger effectiveness for each component. The resulting *UA* values were then used as specifications for the system model.

After an analysis of the baseline system, parametric analyses were conducted to maximize the system *COP*. System response to changes in *UA* values and other key parameters was assessed to achieve progressive improvements in *COP*. Each parameter was varied by ±15% with the remaining inputs held constant. Plots of system response to variations in each parameter were used to select the final *UAs* and other key parameter values. The parameter values selected with this process were then used to investigate system response to changes in the water inlet temperature and ambient temperatures. Additional details are provided in the appropriate model sub-section.

Single-Effect Absorption Cycle

Performance of the single-effect system was investigated for a water inlet temperature range of 58 to 120˚F and an ambient temperature range of 35 to 100˚F. For the initial parametric study, the inlet to outlet temperature rise was set, and the water flow rate was allowed to change accordingly. Investigation showed that maintaining 15˚F water temperature steps at the design ambient required an increase in the absorber/condenser coupling fluid flow rate from 1.17 to 1.34 gpm. Plots were developed to allow for the investigation of trends and overall system performance.

Figure 3 is a plot of the heating cycle *COP* for the water inlet and ambient temperature ranges investigated. The plot shows that system performance increases with decreased water inlet temperatures and increased ambient temperatures. At decreased water and increased ambient temperature conditions, the system is able to utilize more low grade heat from the ambient, resulting in higher heating loads and *COP*s.

Additional studies were performed to investigate the impact of higher and lower absorber/condenser coupling fluid flow rates on the performance of the system. The water flow rates investigated were 1.0, 1.23 and 1.5 gpm. The full range of water temperatures at ambient temperatures of 40, 68 and 90˚F was investigated for each flow rate. This investigation showed that increased water flow rates allowed for increased *COPs,* heating duties and reduced differential pressures. Based on this result, the water flow rate was selected to be 1.5 gpm for the final optimized single-effect model. The final optimization resulted in a theoretical cycle *COP* and heating duty of 1.74 and 2.79 kW, respectively. Optimized baseline conditions are presented in Table 2.

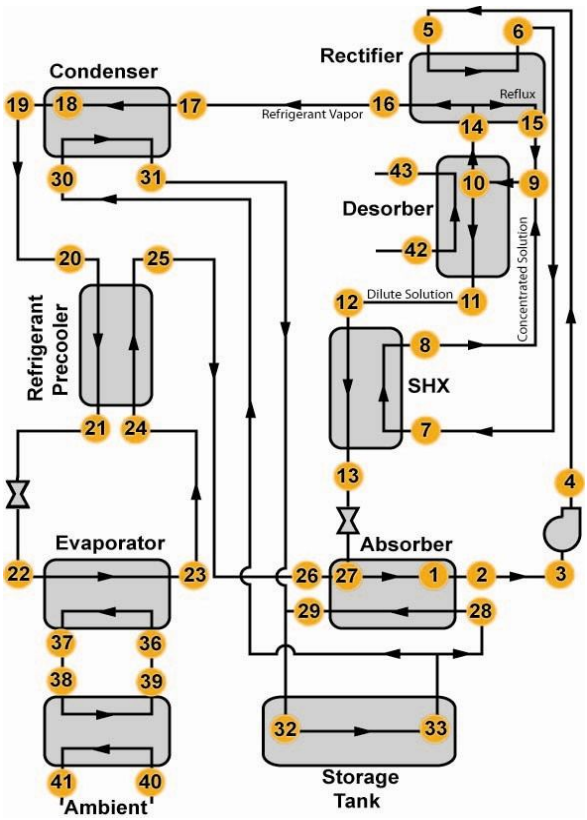

Figure 2: Single-effect Cycle Model Schematic

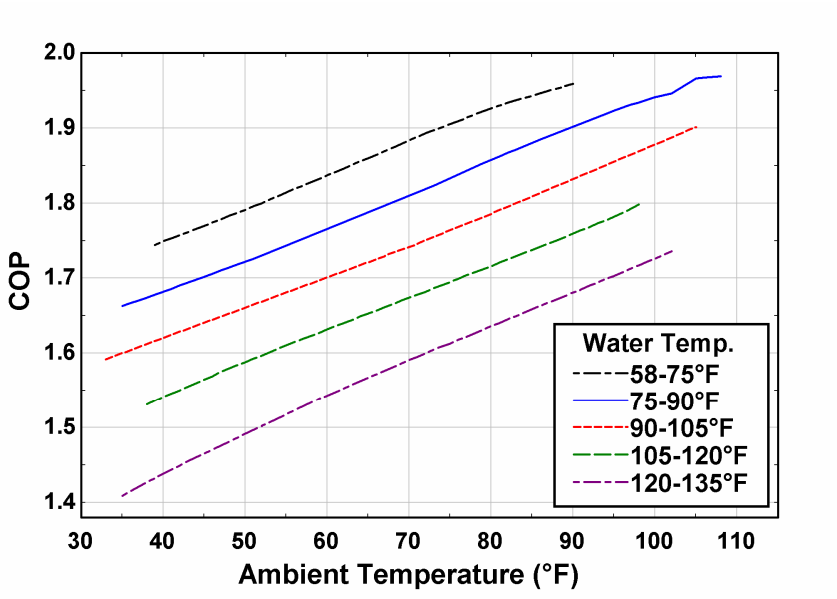

Figure 3: Single-effect cycle COP, Function of Water Inlet and Ambient Temperature

Table 2: Single-effect Cycle Design Specifications

Component	UA [W-K^{-1}]	Coupling Fluid		Duty [W]
		Flow Rate [kg-s^{-1}]	Inlet Temperature [°C]	
Absorber	137	0.047	32.22	**1,617**
Ambient Heat Exchanger	800	0.096	**14.02**	**1,178**
Condenser	251	0.047	32.22	**1,170**
Desorber	2.97			**1,605**
Evaporator	475	0.096	**17.05**	**1,178**
Rectifier	4.44			**0.1325**
Refrigerant Heat Exchanger (RHX)	20.2			**88.17**
Solution Heat Exchanger (SHX)	17.9			**448.1**
Solution Pump				**2.997**
*The bold values are not set parameters; they are calculated based on the set parameters.				

As the water in the storage tank is heated, the differential pressure increases several fold, while the (modeled) cycle flow rates remain about the same (Figure 4). This is due to the high side pressure being tied to the (increasing) water temperature, while the low side pressure is tied to the ambient temperature (relatively constant). The large change in differential pressure within a single heat pump operating cycle differs significantly from a space conditioning application where the high and low side pressure are both substantially tied to the ambient temperature (relatively constant during an operating cycle), which results in a fairly constant differential pressure over the course of a heating or cooling cycle. Since the refrigerant and weak solution flow rates are a function of the differential pressure, controls are a more important factor for achieving optimum performance over the entire heating cycle.

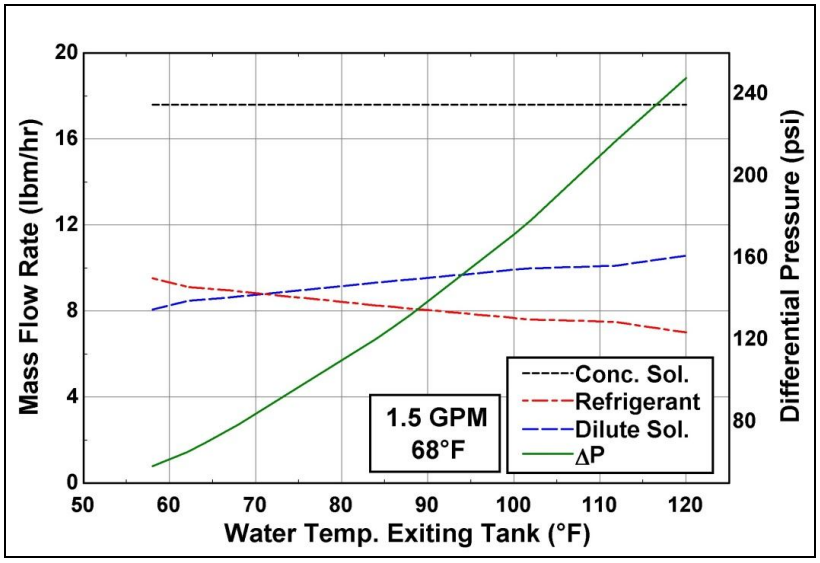

Figure 4: SE Cycle State Points as Function of Water Temperature

GAX Absorption Cycle

A GAX cycle offers higher cycle efficiencies compared to a single effect cycle with an associated penalty of larger heat exchanger sizes (UA) and increased complexity (higher cost). In a GAX cycle, the temperature at the bottom of the Desorber (weak solution exit) is increased to the point where there is temperature overlap between the absorber and desorber components. Simply, energy recovered in a portion of the Absorber can used to generate ammonia vapor in the Desorber. Efficiencies approaching a double-effect cycle can be realized, without the penalty of very high pressures.

The modeled GAX cycle diaphragm is shown below in Figure 5. Compared to the single effect cycle, the Solution Heated Desorber (SHD) replaces the Solution Heat Exchanger (SHX), and two new components are added, the Solution Cooled Absorber (SCA) and GAX Absorber. In an actual system, the SCA and GAX absorbers can be combined into a single heat exchanger (SCAGAX Absorber).

As for the Single Effect cycle, a baseline model was developed at 68° F ambient and 90/105° F water temperatures, using representative heat pump cycle temperatures, flow rates, pressures and concentrations. Development of the baseline GAX cycle resulted in a cycle *COP* and heating capacity of 2.4 and 2.8 kW, respectively. Performance of the GAX system was investigated for a water inlet temperature range of 58 to 120˚F and an evaporator coupling fluid temperature range of 35 to 90˚F. Plots were developed for these parametric studies to allow for the investigation of trends and overall system performance, which showed trends similar to the single-effect cycle (Figure 6). Optimized baseline conditions are presented in Table 3.

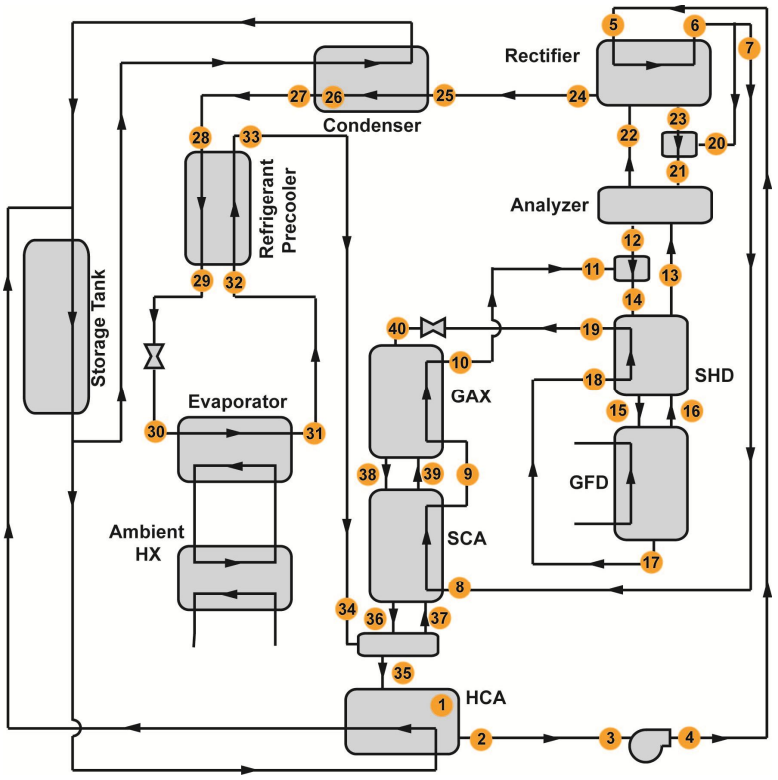

Figure 5: GAX Cycle Model Schematic

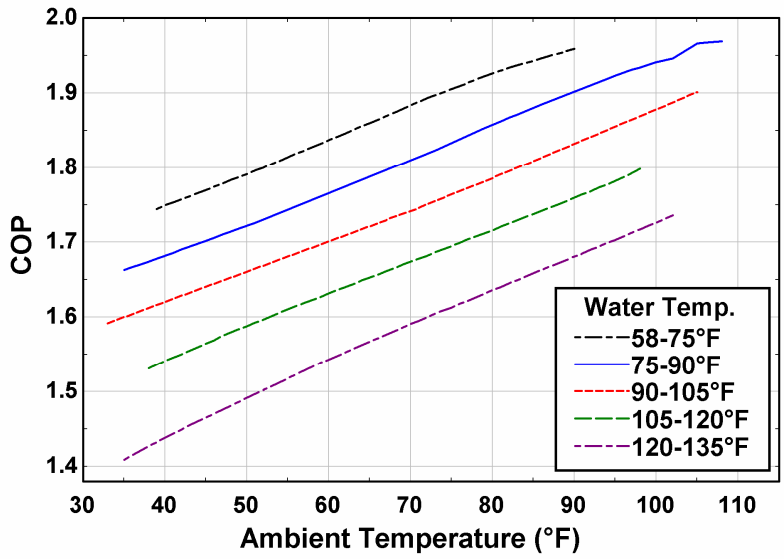

Figure 6: GAX Cycle COP, Function of Water Inlet and Ambient Temperature

Table 3: GAX Cycle Design Specifications

Component	UA [kW-K^{-1}]	Coupling Fluid		Duty [W]
		Flow Rate [kg-s^{-1}]	Inlet Temperature [°C]	
Rectifier	2.4			**96**
Solution Heated Desorber	12.6			**334**
Desorber	2.2			**1,166**
Condenser	372.5	0.051	32.2	**1,678**
Precooler	25.0			**152**
Evaporator	684.9	0.117	**15.6**	**1,627**
SCA/GAX	128.7			**1,505**
Hydronically Coupled Absorber	181.8	0.032	32.2	**1,120**
Ambient Sink	645.8	0.117	**12.2**	**1,627**
Solution Pump				**4.1**
*The bold values are not set parameters; they are calculated based on the set parameters.				

At this point, the project plan called for a decision to be made regarding which cycle to move forward with for component design and breadboard testing. Points of evaluation included:

- **Cycle Efficiency:** The GAX cycle provides a much higher theoretical COP (2.4 vs 1.7) at the baseline temperatures (68/90/105). Accounting for flue and ambient heat losses, the single effect cycle may not provide the target water heater EF of 1.5. The GAX cycle can potentially provide water heater EF's well above 1.5.

- **Component Size/Cost:** The total UA of the Single Effect Cycle is 0.9 W/K compared to 1.4 W/K for the GAX cycle, a 55% increase. Although the relationship between total UA and cost is not a 1:1 relationship, the GAX cycle will require larger and potentially more expensive heat exchangers.

- **Complexity:** The GAX cycle requires one additional heat exchanger (SCAGAX) than the single effect and it must be a counter-flow design (vapor and solution flow in opposite directions).

Although this is not a significant issue when using conventional heat exchangers, it does create significant challenges when applying micro channel geometries.

- **Consumer Payback:** Depending upon the installation, an EF of 1.5 will provide approximate annual energy savings to the consumer of $125 – 175 compared to a standard 0.6 EF water heater. An EF of 2.0 will provide an additional $25-50 savings. Given the heat exchanger costs are not yet known, it is difficult to determine if the additional GAX cycle efficiency will increase or decrease the payback.

The project plan called for Georgia Tech to design/build a breadboard system using micro channel heat exchanger technology and for SMTI to design/build a system using more conventional heat exchangers. This provided an opportunity to evaluate both cycle scenarios so that the cycle decision can be made at a later date when actual performance and projected cost data is available.

Therefore, Georgia Tech (GT) proceeded to develop a breadboard system using micro channel heat exchangers and the single effect state points. Georgia Tech also sized (but did not build) micro channel heat exchangers per the GAX cycle state points so that we will have projected cost information. Conversely, SMTI developed a breadboard system using the GAX state points while also sizing (but not building) conventional heat exchangers for the single effect cycle.

4.0 Task 3: Storage Tank Design/CFD

In Task 3, the inter-relationship between the heat pump and the storage tank was modeled using CFD, with the results used to drive the design of the heat exchangers that transfer heat from the heat pump (hydronic and flue gas) to the water in the storage tank.

For initial modeling, representative heat fluxes from hydronic tank and flue gas heat exchangers were integrated into a standard 75 gallon gas-fired water heater storage tank using ANSYS CFD software. The hydronic flow rate and flue gas energy availability inputs were derived from the initial results of thermodynamic cycle modeling. A satisfactory solid model mesh was defined and an initial case of heating a cold tank of water (58 F) to 135 F was completed (Figure 7).

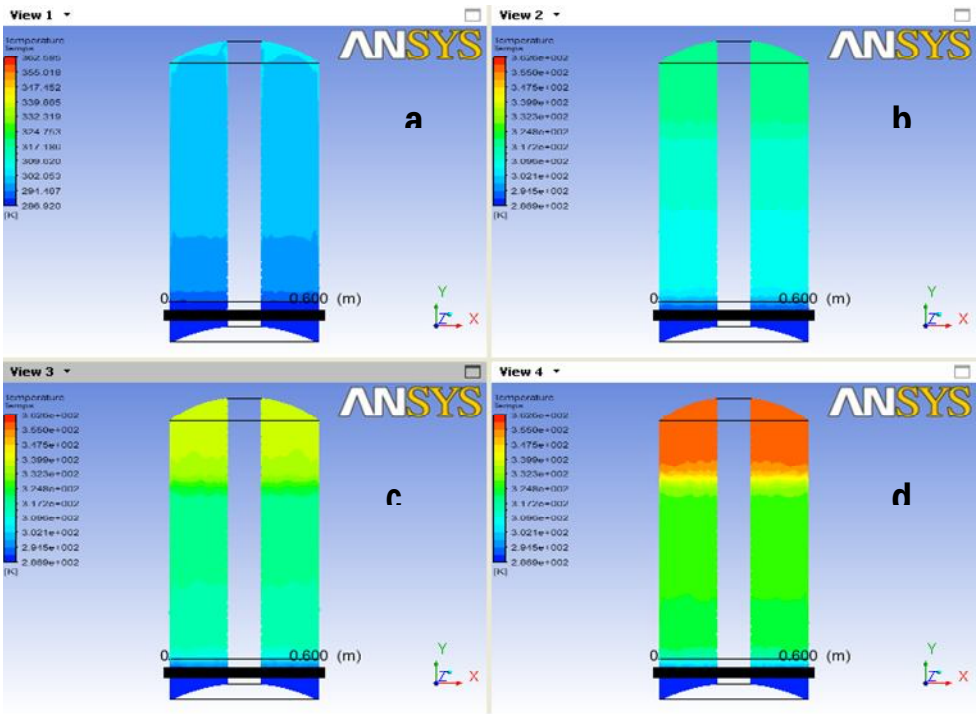

Figure 7: Tank Heating CFD Simulation

Modeling transitioned from using a representative heat flux through the tank wall to one where the heat flux is through the walls of an external coil heat exchanger. The heat exchanger design was based on the design used in the current AO Smith 80 gallon residential electric heat pump water heater (Figure 8). A transient simulation using a High Resolution Advection Scheme with a Second Order Backward Euler Transient Scheme was performed. The transient simulation used one second time steps to capture the buoyant flow characteristics in the water volume. Transient results were logged at ten minute real time intervals. All calculations were performed with double-precision. The model was meshed with a ten layer boundary layer as shown in Figure 9. The final mesh included 311,798 nodes and 860,109 elements.

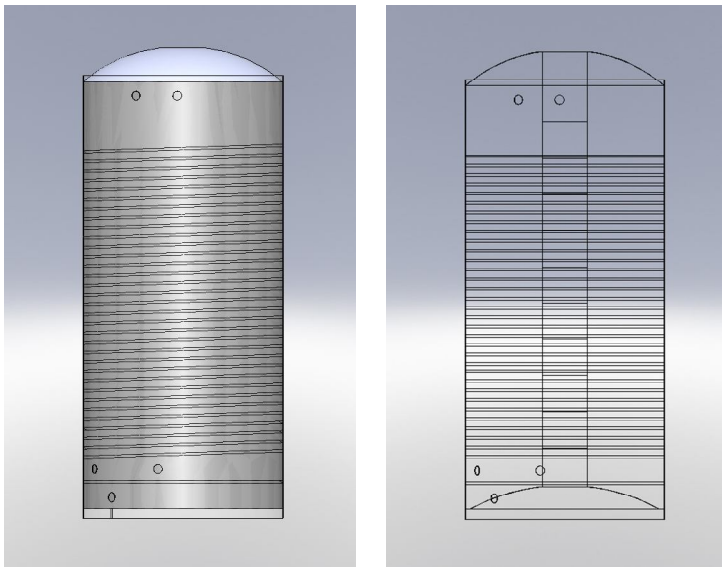

Figure 8: External Tank Coiled Heat Exchanger

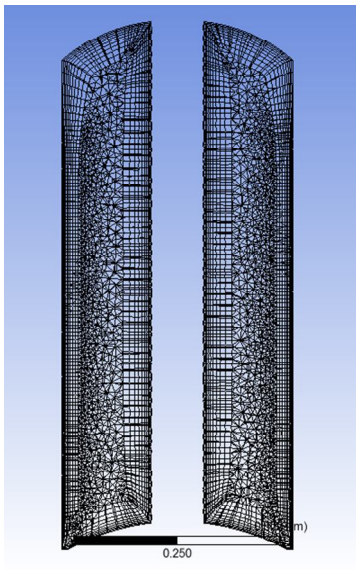

Figure 9: CFD Tank Model Mesh

Modeling Conditions: Cold start up: Initial tank temperature of 58°F, no water drawn. Water is heated to a final temperature of 135°F.

Boundary Conditions: The total contact surface area of the heat exchange coil is 0.44 m^2. Based on a flow rate of 1.28 gpm and temperatures of 105°F from the heat pump and 90°F returning to the heat pump, an initial heat flux of 573 W/m^2-K was applied to the coil surfaces. The simulation was halted at 10 minute real-time intervals to adjust the boundary condition to match the rising tank temperatures. Unfortunately, this simulation was quite slow, with 10 minutes of real time requiring > 18 hours of simulation time. The simulation was stopped after simulating 83.5 minutes of heat up due to the length of run-time (Figure 10). This simulation did not produce significantly better results than the simpler simulation using a uniform tank jacket heat flux, so future modeling was performed using heat flux on the jacket walls, modified to account for the difference in heat exchanger surface areas.

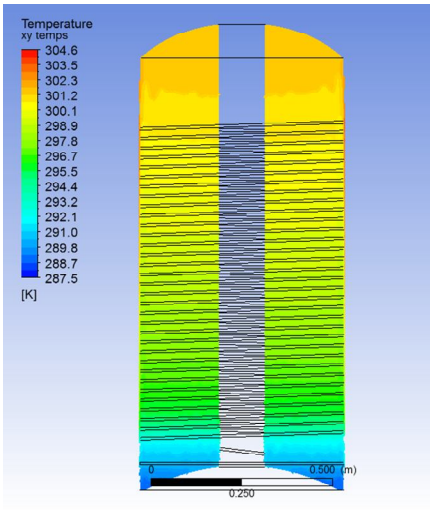

Figure 10: Simulation Results at t=5000 Seconds

Subsequent modeling was performed with boundary conditions (heat flux) that changed as a function of water volume temperature (based on the predicted output of the heat pump cycle as a function of return water temperature). Two heat sources were modeled; the primary heat source came from the heat pump through an external heat exchanger on the tank jacket, and the secondary input used the exhaust gas of the heat pump to heat through the tank flue. To apply the boundary conditions as a function of tank condition, the tank jacket surface was broken into ten segments in the area of the external coil, based on the external

heat exchanger design used in a current electric heat pump product (Figure 11). Similarly, the flue tube surface was cut into segments as shown in Figure 12.

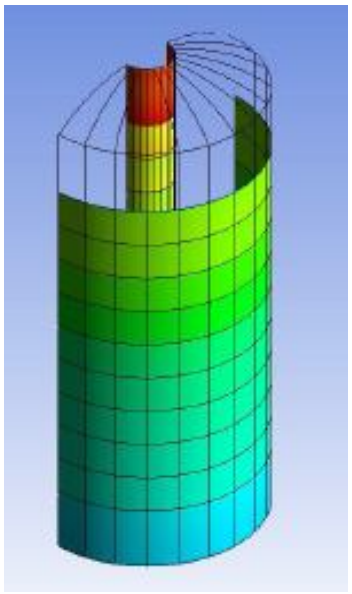

Figure 11: External Tank Coiled Heat Exchanger Surface Area

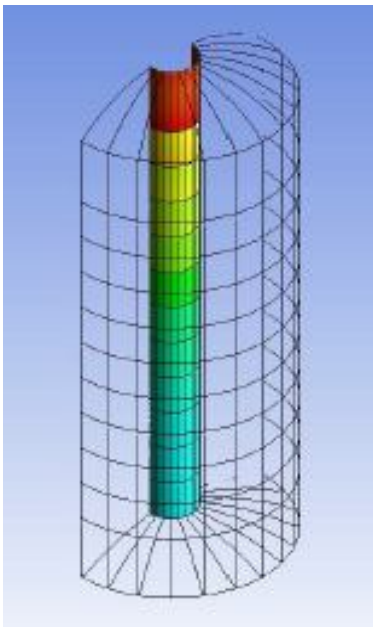

Figure 12: Flue Tube Surface Area

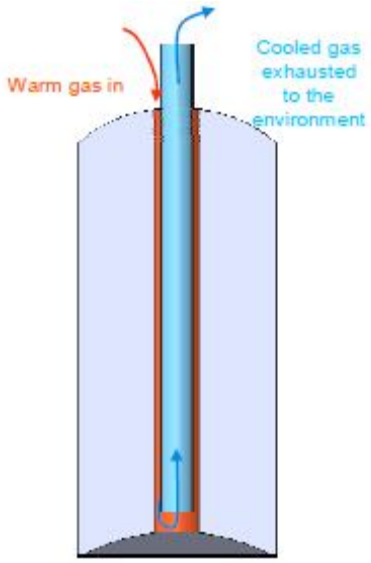

Figure 13: Flue Side Heat Exchanger

To reduce simulation time, one 18° segment of the tank volume was modeled, taking advantage of the axisymmetry of the tank. The initial simulation was based on laminar flow while the buoyant flow was developing, but moved to a k-epsilon turbulence model after the first 15 minutes.

A secondary method for heating the water is achieved by recovering energy of the heat pump exhaust through the center flue of the water heater. The heat exchanger for the exhaust gas will be designed to flow downward through the flue tube in the outer cylinder of two concentric cylinders, with the cooled gas returning through the inner cylinder and finally exhausting to the environment (Figure 13). The local water temperature, the velocity and heat transfer rate on the flue walls was modeled using an Engineering Equation Solver (EES) model. This model includes condensation of the exhaust gases in the flue tube.

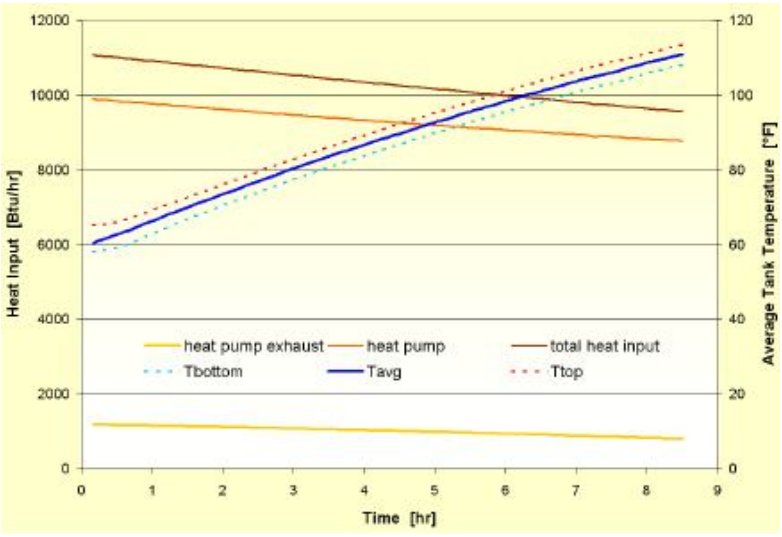

Figure 14: Tank Temperatures and Input Rates vs Time

Figure 14 shows the increase in tank temperature as a function of time for this analysis. Also shown are the heat input rates for both the heat pump and the flue gas heat exchangers as a function of time (water temperature) as the simulation progressed.

Small changes in flue side heat transfer are not expected to strongly affect the average water temperatures in the tank, so the results provided by this CFD analysis were used in the EES model to estimate the difference in heat transfer rates for varying inner tube dimensions as a first step toward optimizing the dimensions of the flue side heat exchanger. As the gap between the flue wall and the inner wall of the heat exchanger decreases, the velocity of the exhaust increases, resulting in higher heat transfer rates to the water. Unfortunately, reducing the space between the inner and outer flue surfaces also increases the pressure drop through the heat exchanger.

A parametric study compared heat exchanger performance vs the annular gap between the inner flue insert and the outer flue tube. In addition, CFD was used to analyze the pressure distribution in the flue gas heat exchanger for each configuration to compare performance with pressure drop. Figures 15 and 16 compares the performance of the heat exchanger for several gap widths as the tank is heated and the corresponding increase in pressure loss for the same conditions (note for all cases, the flue side pressure loss is negligible, less than 0.001 inches of water).

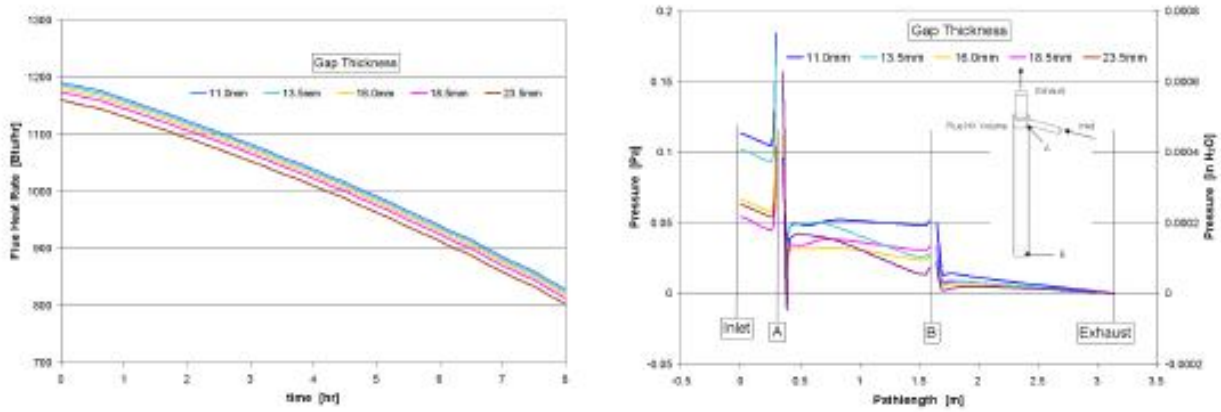

Figure 15: Flue Gas Heat Exchanger: Heat Rate and Pressure Loss

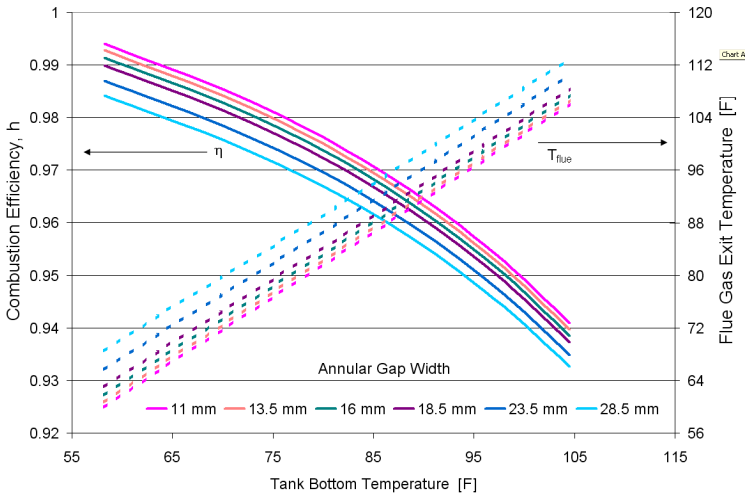

Figure 16: Flue Gas Heat Exchanger – Combustion Efficiency

When the tank bottom is very cold (long water draw scenario), the combustion efficiency approaches 99%. As the tank warms up, the combustion efficiency drops to the low 90's. Most of the heat pump operating hours will occur with the water in the bottom of the storage tank at 90 deg and above, so the typical combustion efficiency will be between 92 and 96%. This is satisfactory to meet our overall efficiency target.

A similar analysis was performed to analyze the pressure loss through the copper coil external heat exchanger. The resulting pressure loss given this tube (currently used to carry a refrigerant in an electric heat pump) at the targeted (water) flow

rate is very high, in excess of 20 psi. Therefore, the decision to move to an internal tank hydronic heat exchanger was made.

Nine potential concepts for internal heat exchangers to transfer heat from the hydronic loop of the heat pump to the storage tank were developed and evaluated for their strengths and weaknesses. Two with the strongest potential (Figure 17) were evaluated in detail for feasibility: (1) an Internal Coaxial Heat Exchanger, in which the hydronic fluid flows through the outer cylinder of a tube-in-tube type heat exchanger and back through the center tube to be returned to the heat pump, and (2) a wound coil mounted near the bottom of the storage tank, where the cold water resides. The advantage to a coaxial system is that it requires no tank modifications. The limitation is that since the heat exchanger is inserted into the top tank spud the maximum size of the tube is fixed, and may be inadequate for the heat load. The advantage to the wound coil is that most of the heat transfer occurs in the region of the tank with the coldest water, minimal tank modification is required, and because the coil also exits at the bottom of the tank, there is minimal heat loss from the tank to the hydronic return line. In addition, this design allows full flexibility in tube diameter, coil diameter and number of turns to optimize heat exchanger design for performance.

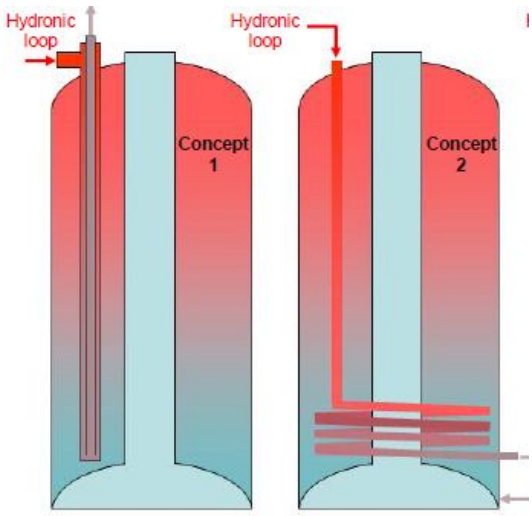

Figure 17: Internal Tank Heat Exchangers

An initial LMTD/UA analysis has showed that the coaxial heat exchanger does not have enough surface area for this application A model for an internal helical coil heat exchanger was completed and validated with experimental data. The model was used to evaluate required dimensions for the internal coil heat exchanger, with forced convection heat transfer inside the tube, with natural convection tube OD to the water in the tank.

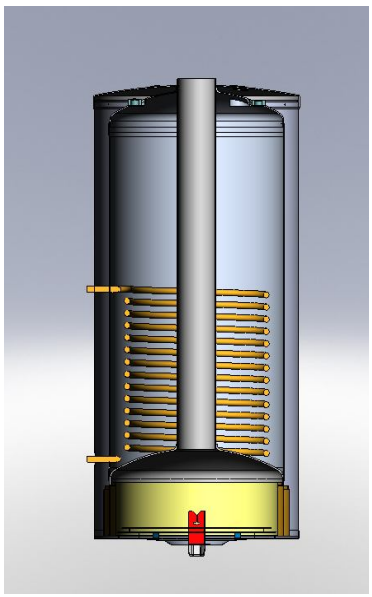

Fig 18: Alpha Storage Tank Assy

Initial analysis/testing was conducted using a fairly large tube diameter plain tube heat exchanger equivalent to that used in a current (solar tank) production model. The low heat transfer coefficient resulting from the large inside diameter combined with no external surface area enhancement, resulted in the prediction of a long required coil length, with a projected cost exceeding our target. Subsequent analysis resulting in two prototype coils selected, based on projected performance and cost, for testing. Both coils utilized plain ¾" OD steel tubing, one with approximately 1200 sqin of surface area, the other 1900.

Bench testing was completed on the larger coil prototype (Figure 18). Heated water was pumped through the heat exchanger coil to produce a heat exchanger exit temperature (heat pump inlet temperature) of 90°F. To achieve steady state performance, a small amount of heat was removed from the storage tank by continuously drawing a minimum amount of water from the tank. The system was tested at two input rates of 7,631 Btu/hr and 14,307 Btu/hr, bracketing the nominal input rate of 9,500 Btu/hr.

The LMTD difference measured at these two input rates was 4.5°F and 6°F (Figure 18).

For the transient testing, the tank was filled with cold water, and then allowed to heat up as heated water passed through the heat exchanger coil. A strong temperature gradient of 2.5°F per inch is seen at the bottom of the tank resulting in an 11°F difference between the coil outlet temperature and that measured at the bottom of the tank, but a difference of only 6°F at a location 2 inches above that.

The exhaust gas heat exchanger was bench tested using simulated flue gas, with and without a flow distribution feature in the flow annulus near the flue gas inlet location. Results indicated the distribution feature was necessary to achieve the desired performance (Figure 19).

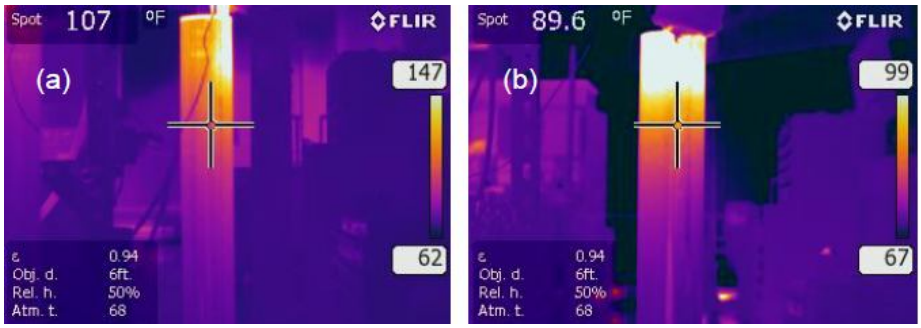

Figure 19: Flue Gas Temperature Distribution With and W/O Flow Distribution

5.0 Task 4: HEAT EXCHANGER DESIGN

SMTI developed detailed designs for the GAX cycle heat exchangers using conventional geometries, while Georgia Tech (GT) developed designs for the Single Effect (SE) cycle using microscale geometries (with the exception of the gas-fired Desorber and associated Rectifier, which were conventional geometries by SMTI). The GT microscale designs are not well suited for the gas-fired Desorber and Rectifier components.

SE Microscale: Heat exchanger design tools developed by GT were used to design the absorber, condenser, evaporator, solution heat exchanger and refrigerant precooler for the single-effect cycle. Segmented heat and mass transfer models for each component use appropriate correlations for heat transfer, pressure drop and phase change predictions. Individual component sizes and predicted pressure drops are presented in Table 4. The components were designed with the same number of shims so that they could be manufactured as individual units or as a monolithic block. Each component uses channels with a hydraulic diameter of 0.442 mm, which corresponds to a width and depth of 0.75 mm and 0.35 mm, respectively.

Microscale heat and mass exchangers provide very high heat transfer coefficients, excellent volume-to-performance ratios, and minimize the refrigerant charge. The potential for increased pressure drop is mitigated by implementing arrays of many parallel channels. For breadboard testing, each heat exchanger was fabricated individually to maintain design/test flexibility through the breadboard phase.

Table 4: SE Micro Chanel HX Envelope Size

HX	HX Width [in]	HX Length [in]	HX Depth [in]	Water-Side dP [psi]	Refrigerant dP [psi]	Total # Shims
Absorber	3.25	9.25	1.00	0.7	0.12	30
Condenser	3.25	8.75	1.00	1.1	0.03	30
Evaporator	3.25	7.00	1.00	2.6	0.03	30
SHX	1.00	4.50	1.00	-	0.038/0.015	30
RHX	1.75	6.50	1.00	-	0.06/0.007	30

GAX Conventional: Envelope sizes (including headers) and estimated pressure losses for the GAX cycle heat exchangers are shown in Table 5 and Figures 20 and 21. The designs utilize a general shell and tube geometry (with the exception of the RHX which is tube-in-tube), with specific features and dimensions specific to the needs to ammonia-water absorption heat exchangers. Where possible, the heat exchangers were specifically designed to share many of the same individual components in order to minimize the variety and maximize the manufacturing volume. Budgetary cost estimates of various tube diameter and wall thicknesses were compared to modeling results to arrive at an optimal size/cost ratio.

The SCAGAX absorber is preferably a counter-flow design (vapor and absorbing solution travel in opposite directions) and required careful evaluation of flooding (which can occur with the vapor velocity shear force on the solution causes the solution flow to stop and/or reverse. The Wallis flooding number was calculated vs HX length to arrive at appropriate tube and baffle spacing.

Table 5: GAX Conventional HX Envelope Size

HX	HX Dia [in]	HX Length [in]	Water-Side dP [psi]	Refrigerant dP [psi]
Absorber	1.75	18.00	< 0.1	< 0.1
SCAGAX	1.75	18.00	---	< 0.1
Condenser	1.50	18.00	0.5	< 0.1
Evaporator	1.50	18.00	2.0	< 0.1
RHX	0.50	60.00	---	< 0.25
Note: SHX is integrated into the Desorber				

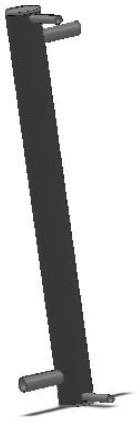

Figure 20: GAX Evaporator/Condenser

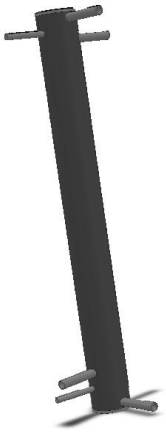

Figure 21: GAX HCA / SCAGAX Absorber

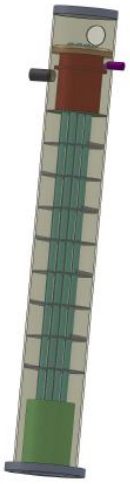

Figure 22: Gas-Fired Desorber

Gas-Fired Desorber: The gas-fired Desorber design is similar for both the SE and GAX cycles, with the primary difference being the GAX has a larger analyzer (refrigerant vapor purification) section and an internal SCA. Both desorbers are 2" OD, with the SE version 14" tall and the GAX 18" tall. Fourteen flue tubes collect flue gas from the combustion chamber and staggered flow distribution baffles are used to maintain the required temperature and concentration profiles (Figure 22). Tube and baffle spacing for both were determined in part by consideration of the Wallis flooding number, similar to the SCAGAX. Strong solution enters (and refrigerant vapor exits) an analyzer section near the top before the entering the fired section. Weak solution will be collected at the bottom of the combustion chamber through an external trap-leg. In the GAX version, the weak solution travels back up the assembly inside a small diameter coiled tube that functions as the SHX.

Rectifier: Two designs for the rectifier were developed and fabricated, one using a small coil of plan tubing and one using a segmented finned-tube. Both are integrated into a 2" OD chamber that doubled in function as a solution storage reservoir.

6.0 Task 8: SOLUTION PUMP DEVELOPMENT

Ammonia-water absorption heat pump cycles require a small positive pressure pump to move ammonia-water solution from the low pressure to the high pressure side of the cycle. Since the solution is often at or near saturation, slow moving diaphragm or piston pumps that can handle a two-phase mixture are typically used. Due to the unique requirements of this application (high head, low flow, ammonia-water solution near the saturation point) cost effective pumps are not commercially available for volume heat pump production. Low internal pressure losses and the ability to pull solution into the pump, especially at low ambients where the low side pressure may be close to, or below atmospheric, is also critical.

The solution pump must be compact, corrosion resistant, provide a pressure lift on the order of 300 psi, be able to pump liquid and vapor (or both), and have a long service life while using no normal lubricants.

Prior to designing a suitable solution pump for a residential heat pump water heater application, solution pump designs utilized on, or developed for, prior ammonia-water absorption systems were evaluated and critiqued. Based on the prior art analysis, a piston pump was developed for the residential water heater application. The design borrowed a few positive features from prior prototypes developed by Columbia Gas (1974) and Phillips Engineering (1990's).

Prior art designs evaluated included:

- Whirlpool Piston Pump, 1972
- Columbia Gas Piston Pump, 1974
- Phillips Engineering Piston Pump, 1990's
- Whirlpool Diaphragm Pump, 1968
- Servel/Robur Diaphragm Pump, 1968-Present
- Battelle Diaphragm Pump, 1990
- Wanner Engineering Diaphragm Pump, Commercially Available
- Norcold/GRI Diaphragm Pump, 1997
- Cooling Technologies Diaphragm Pump, 1999
- Rocky Research Diaphragm Pump, 2004
- Tuthill Gear Pump, Commercially Available
- UTRC/Carrier Solution Pump Evaluation Report, 1996

Approximate Performance Specifications, Residential Heat Pump Water Heater

- Flow Rate: 25 lbm/hr (0.336 lbm/min, 0.05 gpm, 2.9 gph, 191 cc/min)
- Solution Concentration: 0.4 – 0.85 lbm/lbm
- Solution Temperature: 65 – 145 F
- Solution Viscosity: 1.5 – 2.5 lbm/hr-ft (0.6 – 1.0 cp)
- Minimum Inlet Pressure: 40 psia
- Maximum Outlet Pressure: 370 psia
- Maximum Pressure Differential: 270 psi

A preliminary, compact design was completed (Figure 23). Piston diameter was slightly less than 0.5" and the total stroke less than 0.10 inches. The inlet check valve is a critical component of an ammonia water solution pump. It must provide for free flow of the solution into the piston chamber during the back stroke, with negligible pressure loss to prevent flashing of the near-saturated solution. It must also close quickly at the initiation of the down stroke and have near zero "dead volume" to maintain a high pressure

ratio necessary for pumping any vapor during periods of low solution flow to the pump. The very small geometry of this pump (piston is on the order of ½" diameter) provides additional design challenges.

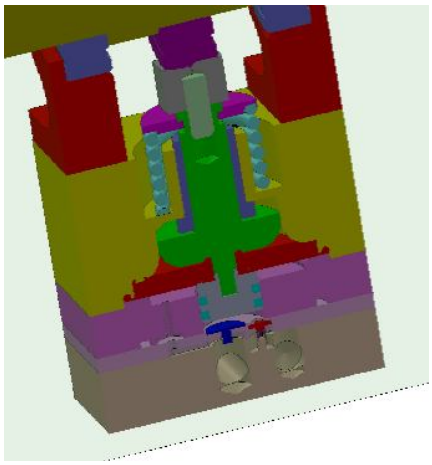

Figure 23: Preliminary Solution Pump

The outlet check valve design is not as critical, as pressure loss is not a big concern. However, the near zero dead volume provision also applies and it should be spring loaded to prevent solution flow through the pump during off periods.

The resulting inlet check valve design was a small flat (less than 3/8" diameter) disk attached to a short shaft with a snap-fit feature for retention. A tapered edge feature ensures inlet flow can start almost immediately after the piston begins the return stroke. Pressure loss calculations, in-conjunction with comparison of prior art designs, were used to determine the minimum flow area of the openings below the disk. Using suitably sized openings and the cycle operating pressures, an FEA analysis was conducted on the disk assuming stainless steel and engineering plastic at several disk thicknesses.

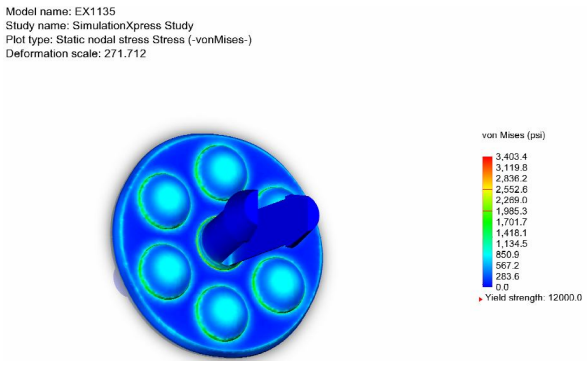

Figure 24: Inlet Check Valve FEA, FS = 3.5

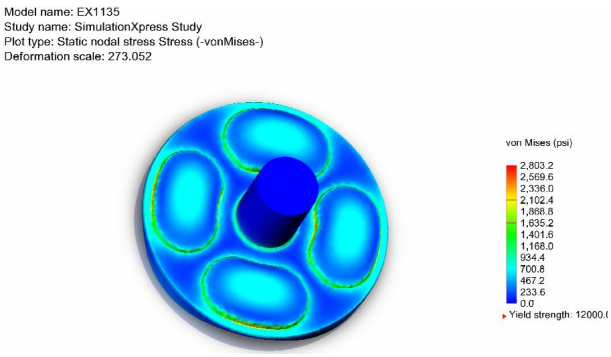

Figure 25: Inlet Check Valve FEA, FS = 2.9

Figure 26: Prototype Solution Pump

Results of the initial FEA analysis is shown in Figure 24 for 0.020" plastic (PEEK), indicating a factor of safety of 2.9. Peak stresses resulted from the un-supported area over the inlet openings. Based on this analysis, the shape of the openings were revised (while maintaining the same flow area) in order to reduce the peak stress. FEA results of the final design (again for 0.020" thick PEEK) are shown in Figure 25 (factor of safety = 3.5). The factor of safety assuming stainless steel was two times higher.

A prototype pump using a piston with two o-rings providing the seal to the cylinder wall was fabricated and tested using straight water (Figure 26). The test stand consisted of a small cylinder filled approximately ½ full of water, pressurized with air to set the inlet pressure. The pump pulled water from the tank, pushing it through a mass flow meter and needle valve before returning to the cylinder. The pump performed well, achieving the target flow rate and the target differential pressure. Testing was also

completed at higher differential pressures (350 psi) and performance was maintained (Figure 27). Outlet pressures as high as 500 psi were developed during testing with no detrimental results. A light spring added to the inlet check valve to reduce its closing time. The change improved measured performance (red line, Figure 27).

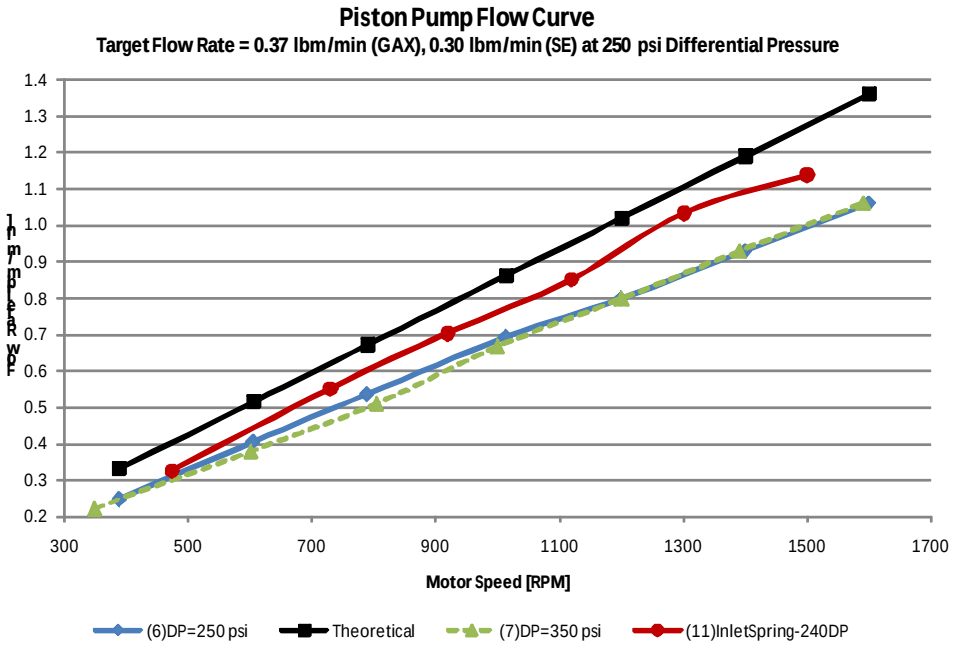

Figure 27: Initial Prototype Piston Pump Performance

Although not required for a this application, the pump was tested with the inlet pressure set to atmospheric and sub-atmospheric pressures. At atmospheric inlet pressure, measured flow rate was approximately 85% of theoretical below 1000 rpm. Above 1000 rpm, performance dropped appreciably with a cavitation type noise noted (due to the high velocity at low pressure through the inlet check valve). At 16 inHg (7.9 psia) inlet pressure, the push rod lost contact with the camshaft and intermittent flow was noted. The lost contact is due to fact that the piston return spring did not have enough force to pull the piston back up against the vacuum pressure in the piston chamber.

An alternate piston design, with an integrated “lip seal” replacing the o-rings was developed and tested with very good results. Measured flow rate was 95% of theoretical across a broad range of operating conditions, except at slow motor speeds (below 500 rpm), where the flow dropped to 90%. Although noise was not a concern with the alpha piston design, operating noise was reduced with the beta piston, believed to be a result of the larger bearing surface area which reduces the side loads on the piston/push rod bearing.

The beta piston design also performed exceedingly well with atmospheric and below atmospheric inlet pressures. Measured flow was maintained above 90% of theoretical at inlet pressures as low as 20 inHg vacuum, and performance was maintained at higher motor speeds. The return spring maintained the push rod in contact with the cam bearing at all times, believed due to the fact that the sealing performance of the lip seal differs between the down and reverse stroke, compared to the o-ring design which is direction neutral (lip seal relieves a bit of the vacuum during the reverse stroke, decreasing the pull force exerted on the return spring).

The pump was operated for 60 hours in the pump stand and then installed in the heat pump breadboard test facility (pumping NH_3-H_2O solution). Performance was inconsistent in the breadboard where a solution-vapor mix is often entering the pump. Inspection and off-line testing showed the inlet check valve (PEEK), fabricated initially with a slight domed surface to create a line seal at its OD, had taken a set, increasing leakage past the valve. A new check was installed and worked very well for about 16 hours, then exhibited the same problem.

The issue was solved by switching to a stainless steel valve disk and a PEEK valve seat (previous seat was steel). Performance using water on the pump test stand was equivalent to the PEEK valve performance and performance in the breadboard (NH_3-H_2O solution) was very good and did not degrade over time. A second prototype pump incorporating the improved design features was fabricated and sent to Georgia Tech to use in their breadboard.

Figure 28: Solution Pump & Drive

A review of possible speed reduction techniques between a standard 1750 RPM motor and the pump was completed, with the low cost option being a simple belt-pulley design (Figure 28). Sample 1/15 and 1/20 hp motors were obtained and evaluated on the Alpha and Beta packaged prototypes. The 1/20 hp motors provide very good performance at the lowest amp draw.

The original GT breadboard pump internals was modified to test a conceptual design that eliminated the inlet check valve (aka side inlet). The design tested well on the pump test stand and was operated for a short time in SMTI's breadboard facility with positive results. The side inlet design has a lower part count, *potentially* lower cost, and reduces the possibility of long-term reliability problems due to fouling of the inlet check valve seat. Design choice for the commercialization phase will depend on the results of a detailed cost-risk analysis that is beyond the scope of this R&D project.

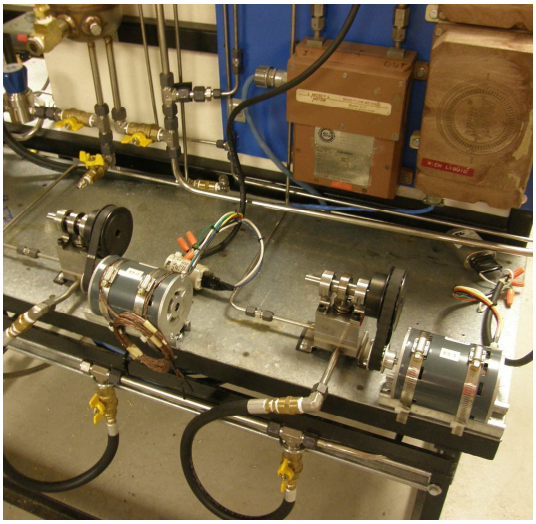

Figure 29: Solution Pump Life Test

Near the end of the project, two additional pumps were installed on the pump test stand to support continuous operation (Figure 29). These pumps will continue to run through subsequent design for commercialization phases, providing valuable life/reliability data. As of the writing of this report, the pumps had accrued over 400 hours of operation (17 million piston stokes).

7.0 Task 5: COMBUSTION SYSTEM DESIGN

The GTI project team supported the GHPWH combustion system development in two phases, to best support the overall development program.

1) **Specify components for a workable assembly –** Early in the project schedule, a working combustion system composed largely of off-the-shelf componentry was required to operate the breadboard heat pump systems at SMTI and GT.

2) **Component design and refinement –** As operating conditions and design requirements of the GHPWH are outside the norm for residential-sized gas fired equipment, several combustion system components required significant research and development. Following the specification of a workable combustion system, GTI supported the design and refinement of specific components, namely the burner and fuel/air mixer.

Testing and Specifying of Workable Assembly

GTI developed a list of candidate component suppliers and customized burner designs (Table 6). Beyond the evaluation of a workable combustion system, several components were not discovered or evaluated until the second phase of this effort, as indicated.

The challenge in specifying components lies in the unique requirements and application of this combustion system, which a small burner is directly fired into the desorber. The design of the desorber is

Table 6: Combustion System Candidate Suppliers/Components

Component	Manufacturer	Components of Interest	Off-the-shelf?	Evaluated at GTI?
Gas Valve	BASO	Dual Operating Gas Valve (w/o regulation)	Yes	Yes
	Maxitrol	Dual Operating Gas Valve, Zero Governor Valve	Yes	Yes
	Karl Dungs	Dual Operating Gas Valve	Yes	No, lower cost alternatives proved sufficient
Control Module	Capable Controls	Gas Ignition Control Module	Yes	Yes
	Honeywell	Gas Ignition Control Module	Yes	No
Ignition & Flame Sense	Precision Speed Equipment	Spark Igniters and Flame Sense Rods	Yes	Yes
	Norton	Hot Surface Igniter	Yes	No, at SMTI
Combustion Blower	Honeywell	Integrated Gas Train (Valve, Mixer, Blower)	Yes	No, oversized
	EBM Papst	Premix Blower	Yes	Yes
	Micronel	Micro-blower	Yes	Yes*
	Ametek	Micro-blower	Yes	Yes*
Fuel/Air Mixer	Pyronics	Mixer	Yes	Yes*
	Honeywell	Mixer	Yes	Yes
Burner Design	Bekaert	Burner	Yes	Yes
	Micron Fiber-Tech	Burner	No, custom built	Yes*
	Worgas	Burner	No, custom built	Yes*
	Selas	Burner	Yes	Yes*
	Solaronics	Burner	No, custom built	Yes*
	Russian Academy of Sciences**	Burner Design	No, custom built	Yes*

* Evaluated after specification of workable assembly
** Not a manufacturer.

an up-fired combustion chamber transitioning rapidly to a bank of 14 tubes with external baffling then back to a manifold at the desorber outlet. The combustion chamber is designed such that the boiling strong solution will fill an annular space surrounding the chamber. Depending on the temperature of the condenser heat sink and the cycle evaluated, the boiling strong solution will have a temperature of 250°F to 350°F. Rather than vent this high temperature flue gas, it is run through secondary condensing heat exchanger submerged in the storage tank to extract the latent heat of vaporization in the stream. As this extends the flue gas pathway considerably, the flue-side pressure drop becomes non-trivial. The initial critical design requirements of the combustion system were:

- *Firing rate*: 6.5 kBtu/hr, single stage
- *Turndown*: None, fixed firing rate
- *Emissions*: 10 ng/J NO_x (SCAQMD), no more than 50 ppm CO
- *Target Combustion Efficiency*: 95%
- *Estimated Flue Side Pressure Drop*: 5"-6" W.C. (leaving 2" W.C. available for venting)
- *Inlet Natural Gas Pressure*: 4.5"-10.5" W.C., testing at 3.5" W.C.
- *Combustion Chamber Size*: Cylinder of 1.4" diameter and 2.0" height (up-firing), need room for hot surface igniter and flame sense within chamber.
- *Burner setback*: Preferable that the flame bed is not flush with the combustion chamber inlet, being at 1/2" into the chamber would be best (prevent heating of stagnant ammonia-water solution in surrounding annulus)

Issue #1: Low-flow and High Pressurization: With a firing rate of 6,500 Btu/hr, the total gas flow through the desorber, assuming 20% excess air, is approximately 1.5 scfm. This is small even by residential gas product standards and presents a challenge to the gas train and blower. In order to push these flue gases through the desorber, submerged condensing heat exchanger, and the venting system, the combustion chamber must be pressurized as high as 6" W.C.

Gas Valve and Regulation – Gas valves and regulators that are designed for approximately 6 scfh of natural gas and below are typically seen in food service applications. Of the gas valve manufacturers met with, BASO and Maxitrol both marketed components for this sector. This appliance will be required to have a so-called "dual operating gas valve" which has a redundant shut-off. To save internal space, it is desirable for valves to have integrated regulation.

Combustion Air Blower – Blowers that operate efficiently in the range of low flow and high pressurization mentioned are few a far between, less than 2 scfm with a ΔP of greater than 5" W.C. It was decided initially that the system would be a premix combustion system. The primary reason that drove this decision was that draft inducers that can operate in the temperature range, flow, and pressurization required do not exist off-the-shelf, while premix blowers do exist. In other words, it is easier experimentally to operate an oversized premix blower with flow restrictions to achieve reduced flow at a desired pressure than it is to operate an oversized inducer similarly restricted and outside of its temperature limits.

To minimize unit cost and maintain system simplicity, a premix blower system that mixes in natural gas *downstream* of the blower is desirable, however residential manifold fuel pressures of 3.5" – 4.5" W.C. would be overwhelmed by the requirement of a combustion chamber pressurized to 6" W.C. Therefore fuel/air mixing was performed *upstream* of the blower using a Honeywell venture mixer. As an alternative, Honeywell has supplied GTI with its new "Premixengine™" gas train, which uses a specially designed orifice and venturi mixer to overcome this fuel-to-air mixing pressure disparity, greatly simplifying the blower construction. This new system is designed for much larger systems, up to 125,000

Btu/hr thermal input, so it is most certainly oversized, however such a concept scaled down to 6,500 Btu/hr would be ideal.

To facilitate testing of a workable combustion system with off-the-shelf components, EBM Papst provided GTI with samples of their NRG-118 blower, which was their smallest premix blower for high-pressurization applications at the time, primarily marketed overseas. While GTI was negotiating with EBM Papst and the samples were in transit, GTI performed initial testing with their similarly sized but slightly larger RG-130 premix blower, which was on-site from a prior project. In both cases, the premix blowers are able to function at the operating point of the desorber, however said operating point nears the bottom of the blower's operating range, thus control and flexibility were a challenge.

Issue #2: Small Combustion Chamber: The second challenge in approaching a workable combustion system is the design of the combustion chamber of the desorber, which with a 1.4" I.D. and 2" height is small for premix combustion. This introduces several challenges, specifically to the design of a burner and the ignition system. In order to have a low-flame profile and acceptable CO & NO_x emissions, a radiant-style metal fiber mesh burner was selected. The requirement of an ignition and flame rod within the chamber adds additional size constraints, as the fluid filled annulus surrounding the chamber prevents an approach from any direction besides the chamber bottom. Thus, a compromise must be struck between the space required for the ignition and flame rods (including spark gap) and the radiant heating surface area to meet the thermal input specification.

Combustion System Test Setup

A prototype Desorber provided by SMTI was installed in a flexible test stand in GTI's Residential/Commercial Laboratory. The stand is flexible in that each component (burner, blower, gas valve, etc.) may be swapped in and out, and warm water was used to remove heat of combustion. Test stand and instrumentation and flow diagram are shown in Figures 30 and 31. The flexible test stand was used to test and evaluate a series of burner designs under a variety of operating conditions (firing rate, excess air, back pressure, etc.)

Figure 30: Combustion System Test Stand (GTI)

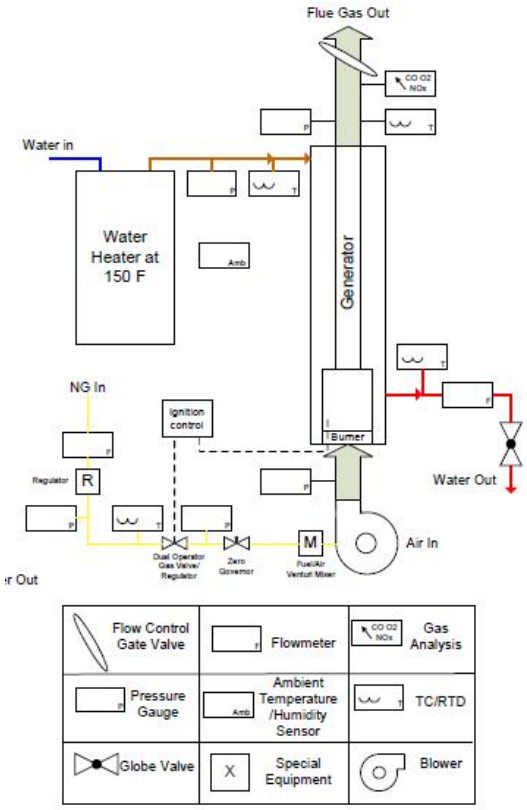

Figure 31: Combustion Test Stand Schematic

Note on NO_x Emissions - The South Coast Air Quality Management District (SCAQMD) requires that residential storage water heaters meet 10 ng NO_x/J output, to which the GHPWH has a distinct advantage over existing gas-fired water heating systems. As the estimated COP is anticipated to be 1.5 or above, this NO_x limit actually is less stringent due to an efficiency greater than 1.0. As a guide for this effort, the effect that COP has on this 10 ng/J NO_x limitation in ppm NO_x at 3% O_2 is given by: *NO_x Emission Limit (ppm dry at 3% O_2) = 19.14*COP*

Therefore, if the GHPWH has a COP of 1.5, the NO_x limitation in SCAQMD would be 28.7 ppm NO_x at 3% O_2. By contrast, typical storage water heaters have a recovery efficiency of 78%, leading to a NO_x requirement of 15 ppm at 3% O_2.

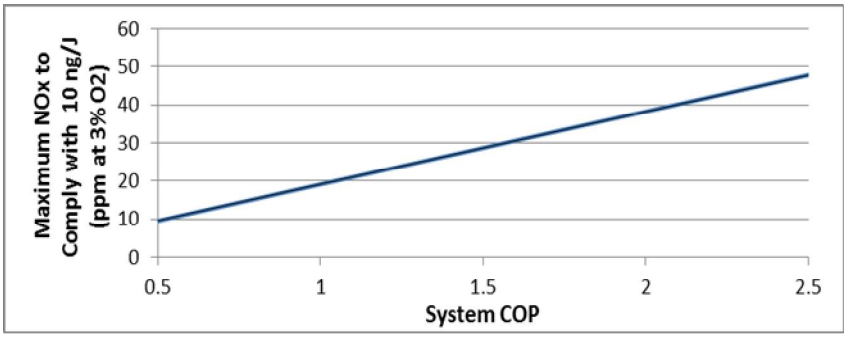

Figure 32: SCAQMD Rule 1121 NO_x Requirement vs. COP

Burner Development

The following sections describe the eight burners, categorized by their design, which were solicited or designed, and evaluated.

Up-Fired Designs - Three up-fired burner designs were evaluated, two custom designs and one off-the-shelf, the only such off-the-shelf burner tested in this effort (Figures 33 and 34). Micron Fiber-Tech provided a bowl-shaped design with sintered metal fibers; Selas provided an off-the-shelf porous ceramic design (PR2-1N); and Bekaert provided a woven-fiber version.

Figure 33: Selas Pilot Burner (Left); Micron-Fiber Burner (Right)

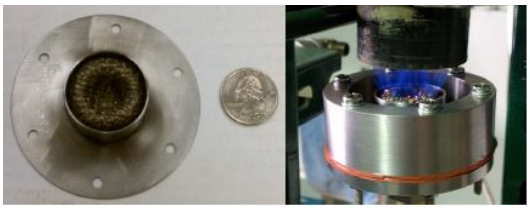

Figure 34: Bekaert Burner Provided during Initial Testing (Left) with Open Air Firing to Highlight Spacer (Right)

The **Bekaert** design provided mixed performance. The burner was able to perform at the required levels of pressurization/back pressure, meet heat transfer and NO_x requirements without issue at target firing rates. However, as the manufacturer was unable to tool below an O.D. of 25 mm, this burner required a setback from the desorber flange to accommodate the ignition/flame sense rod. It exceeded the CO requirements, though not by much, and *stable combustion was not achieved below 35% excess air* (5% Stack O_2, dry), with blow off observed at excess aerations above 45%.

The **Micron Fiber Tech** (MFT) burner was similar to the Bekaert 'bowl-shaped' design, however the burning surface was slightly larger at 2.5 in^2 and composed of a sintered metal fiber mat. While MFT was mindful of the space constraints for the igniter & flame rod, limiting the burner O.D. to 1.0", this narrower tube coupled with the tighter fiber mat density had a higher pressure drop, approximately twice that of the woven fiber mesh Bekaert burner. As such, this burner was unable to fire stably at the target firing rate of 6,500 Btu/hr.

The MFT burner exhibited similar stability issues with blow off/flashback bracketing a narrow range of combustion chamber pressurization for a given firing rate and net desorber pressure drop. As the firing rate was increased and excess aeration decreased, a low frequency oscillation was observed, marked by a slight buzzing sound which was speculated to be intermittent flame quenching at the tube bank transition. The burner was able to operate over a wide range of firing rate and excess aeration without blow off/flashback issues and NO_x emissions requirements were met without issue. However, the long flame at the target firing rate required significant excess aeration to have reasonable CO emissions. Similar to the Bekaert design, ignition point is wholly above the burner, providing logistical problems in small combustion chamber.

The **Selas** burner is the only off-the-shelf burner tested (model PR2-1N). The porous ceramic burner fits easily within the chamber, with critical dimensions of C = ¾" and F = 1-3/32", however the flame vertically extends well beyond the transition to the tube bank at 2.0". During open air testing, the ignition point of the fuel/air mixture was approximately ½" above the top of the burner, presenting ignition problems to be exacerbated within the chamber. For these reasons, the team was unable to stably fire this burner within

the desorber, thus no data was taken.

Radial Designs - As the desorber combustion chamber is cylindrical, a radially-fired design is a natural choice to maximize burner surface area within a confined space, thus the majority of burner designs tested were radially-fired. The designs evaluated varied by: height and outer diameter of burner; mesh material and hole pattern/weave style; and existence of and design of the hole pattern on the backing plate. Two examples are shown in Figure 35, a woven metal fiber mesh and a ceramic mesh. In general, these burners all out-performed the up-fired designs.

Figure 35: Radially-Fired Burners: SMTI "Short" (Left) and Solaronics (Right)

Solicited by SMTI and sent to GTI, **Solaronics** provided a ¾" O.D., 1-¼" tall burner with approximately 3.0 in^2 of burning surface area. The flame distributed evenly, ignition was rapid, and stable operation was observed over a wide range of firing rates. While this burner was used successfully by SMTI and GT for breadboard testing, the CO measured by both SMTI and GTI was unacceptably high (Figure 36). Solaronics provided an optimized prototype, however its performance did not surpass that of other burners.

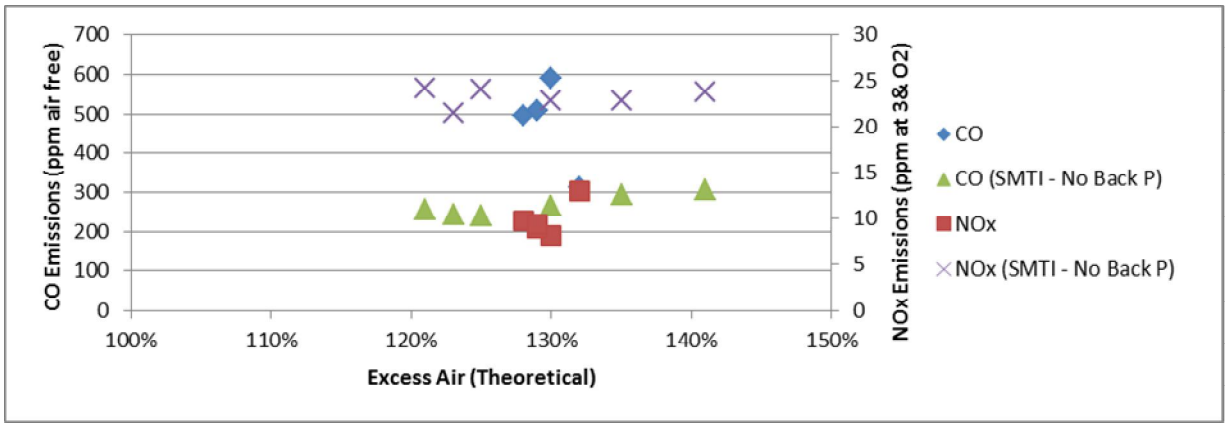

Figure 36: Solaronics Prototype Burner Emissions As Measured by SMTI and GTI

SMTI designed a prototype woven mesh burner **(SMTI Short)** with an inner distribution tube, based on popular designs used in condensing gas boilers. Since off-the-shelf versions are not available in a diameter small enough to fit inside the combustion chamber, the inner distribution tube and base plate were laser cut by a third party. Two sets of burners were produced, one using mesh provided by Bekaert (with GTI welding mesh to inner tube), and one using Worgas mesh and welding service (Figure 37).

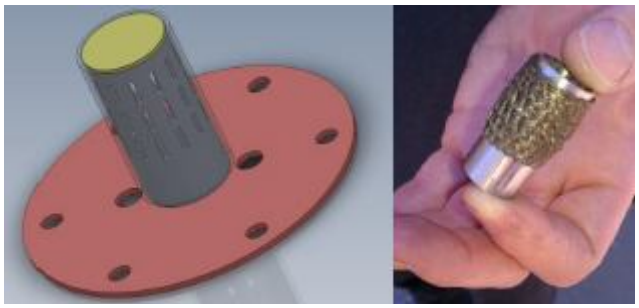

Figure 37: SMTI "Short" Prototype Burner

Testing at both GTI and SMTI confirmed stable operation and quick ignition. The flame length was shorter than the Solaronics (as expected). Overall, CO emissions were lower than the Solaronics design, while NOx remained low. Very little performance difference was noted between the two mesh manufacturers, although the Bekaert mesh exhibited slightly lower pressure drop which created some instability at higher firing rates.

GTI collected test data at firing rates ranging from 3,308 – 5,083 Btu/hr at an excess air of 114-133%. Ignition was smooth and the burner operated quietly and stably over the range of test conditions. Measured CO was 170 ppm at 133% excess air, while NOx was less than 10 ppm, compared to a CO of over 300 for the similarly sized ceramic mesh Solaronics prototype. SMTI's test results of the alpha SMTI burner during heat pump testing showed similar CO values and slightly higher NOx emissions, with the optimum operated point at about 125% excess air.

Based on the test results, Beta SMTI burners were fabricated **("SMTI Long")**. The Beta burners were taller than the Alpha, providing more flame holder surface area to reduce the flame height the amount flame quenching on the combustion chamber side-walls. SMTI's test results of a Beta SMTI burner (30% taller than the Alpha versions) with Worgas mesh showed a slight improvement in CO emissions compared to the Alpha, but less than anticipated. GTI's testing showed very similar results. In open air, the flame pattern was very stable and very short, although a "Christmas Tree" effect was noted (flame length longer near the top of the burner than the bottom). However, the CO emissions indicated the flame is still being slightly quenched by the combustion chamber walls.

In cooperation with researchers from the Russian Academy of Sciences (RAS), a burner was designed to maximize the burning surface area while limiting the pressure drop of fiber mesh burners. The so-called **Three Tower** burner has three radially-fired cylinders arranged in a triangular pattern with a metal screen replacing the combined slotted backing plate and metal mesh of previously tested burners. For the fraction of screen surfaces on the cylinders that have non-zero view factors to one another, a potential exists for super-adiabatic combustion, able to enhance heat transfer rates. While anticipated levels of excess air and heat sink temperatures will prevent true super-adiabatic combustion, this will nonetheless improve heat transfer.

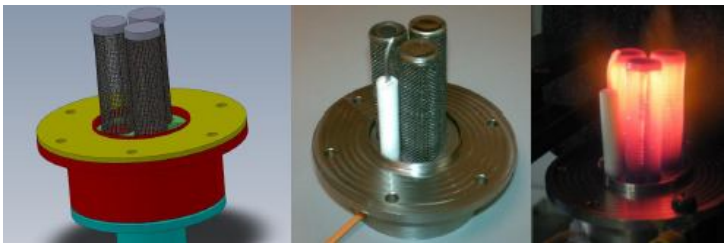

Figure 38: "Three Tower" Burner

The Three Tower burner showed ready ignition with a significantly lower pressure drop than all other burners, due to the coarser metal screen without a perforated backing plate. Vertical flame distribution was not complete, as the bottom ¼" was observed to be colder than the balance of the burner (Figure 38).

The results of the burner testing are shown Figure 39. Overall, the combustion chamber required a lower pressurization to achieve an outlet static pressure of 2" WC, compared to all previous burners. While able to ignite and fire stably over a wide range, the Three Tower metal screen design had unacceptably high CO emissions. Open air firing showed that the vertical flame distribution skewed slightly to the burner top, evening this distribution

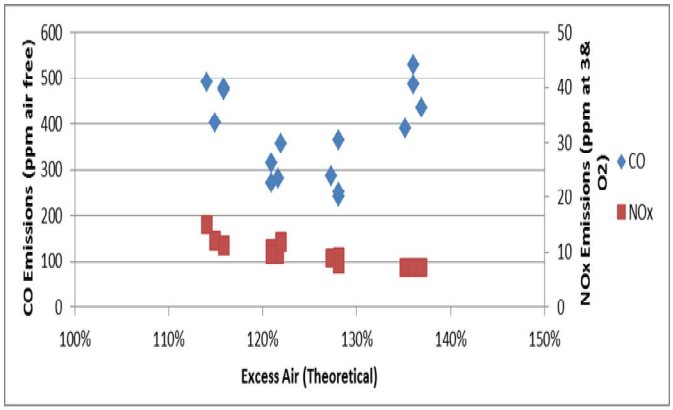

Figure 39: Three Tower Burner Emissions

could bring CO emissions down. Additionally, a shorter or lower profile ignition rod may improve CO emissions.

Although promising, further development of the Three Tower burner was suspended due to the performance of SMTI Long burner, the required effort to resolve the Three Tower CO emission issue, and the projected lower cost of the SMTI Long design.

Addressing CO Emission Issues – CFD Analysis

To investigate the impact of post-combustion quenching, generating the observed higher than target CO emissions, a CFD analysis of the SMTI Long burner firing into both 2D and 3D models of the desorber chamber, using the parametric modeling capabilities of ANSYS FLUENT 13.0 and Workbench™ was completed. The following assumptions were employed by the model:

- Mesh is modeled as a porous media
- Turbulence modeled with k-ω with shear stress transport modeling on walls
- Combustion is a 2-step global mechanism, partial CH_4 and CO oxidation (Eddy-Dissipation)
- Radiation is modeled with the Discrete Ordinates method.
- Absorption coefficient of flue gases is estimated using the weighted-sum-of-gray-gases method.
- Due to tube bank geometry, a quarter-slice was the best method to leverage symmetry
- Combustion was permitted to occur within the fiber mesh and all points downstream
- The viscous and pressure (momentum) losses within mesh section were empirically modeled using referenced pressure vs. flow curves.

Processing time (greater than 3 days) for the initial 3D cold flow model prompted a switch to a simpler 2D simulation. For 2D modeling, the following geometrical simplifications are made:

- The burner ports (3 rows of 12) were modeled as a porous media with its porosity equal to the percent open area and an assumed inertial resistance factor (viscous resistance is assumed to be negligible).
- The tube bank is approximated as a single opening, as an annular channel, with an open area equal to that of the 14 tubes, to minimize impact on the velocity field upstream of the bank.
- The burner mesh is modeled as porous jump of zero thickness using same parameters as with 3D, thus flames are assumed to be matrix-stabilized

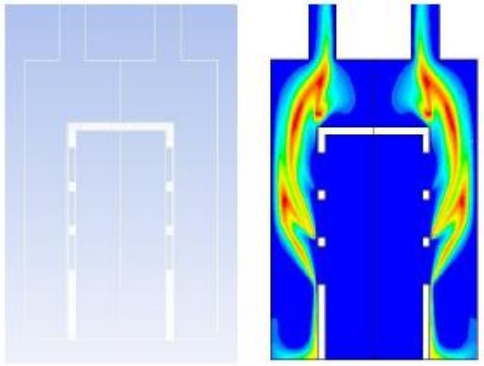

Figure 40: 2D Burner Geometry (Left); Example CO Mole Fraction Contour (Right)

The 2D workbench model was setup (Figure 40) such that the chamber diameter and height can be varied through automation of the process. With resistance fitting parameters

found and tuned to experimental data, an analysis was performed testing the sensitivity of CO emissions to these physical dimensions with automated geometry variation, meshing, and simulation. Target baseline conditions are from SMTI data during a standard breadboard run:

- **Burner:** SMTI Long with Worgas mesh
- **Input Rate:** 5,700 Btu/hr
- **Excess Aeration**: O_2: 5.3%; CO_2: 8.7%; CO: 273 ppm
- **Solution Temp At Combustion Chamber**: 220°F
- **Back Pressure on Desorber Outlet:** None
- **Blower Outlet Pressure**: 2.0" W.C.

Comparing CO emissions for various chamber geometries (Figure 41), it is apparent that the chamber radius has a larger impact on CO than the height, with the exception of the 3" tall chamber. Similarly in Figure 42, chamber radius has a larger impact on heat transferred than the height with the exception of the 3" height case. These effects are related, however it is clear that to achieve reduced CO emissions, a larger chamber radius is required. Note that this is the heat transferred to the truncated domain, thus heat flows are lower than that for a complete desorber.

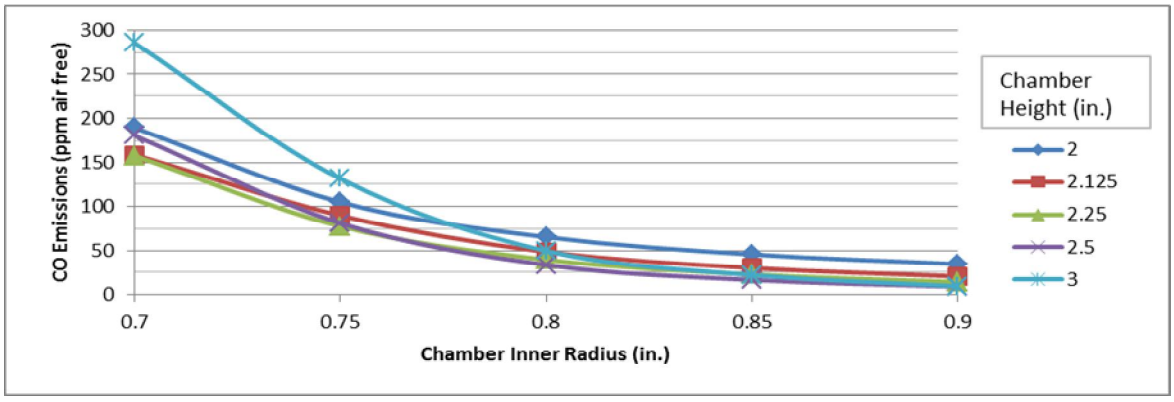

Figure 41: 2D CFD Results – CO Emissions vs. Chamber Radius & Height

Breaking down the distribution of heat transferred for the parametric cases (Figure 42), the fractions of available heat absorbed at the chamber wall and at the tubes is approximately invariant with the chamber radius. This is not the case for chamber height, which has a relatively large impact on the distribution of heat transferred. Note that in as the chamber height increase from 2.0" to 2.5", the fraction of heat transferred to the chamber walls increases and that to the tubes decreases, suggesting that while the increase in chamber wall surface area is beneficial, the residence time of post-flame gases does not proportionally increase, leading to a net decrease in total heat transferred for a taller chamber. Moving from a 2.5" to 3.0" tall chamber results in a sharp increase in net efficiency, where the fraction of heat transferred to the tubes and chamber walls both increase, suggesting that post-flame gases are hotter as they transition to the tube bank. This greater proportion of heat transferred at the tube bank, suggesting higher flue gas temperatures at this transition, is consistent with the quenching of CO oxidation, leading to higher emissions.

Investigating this "switch" in heat transfer between chamber heights of 2.5" and 3.0", the flow is visualized for the baseline radius of 0.7". Looking at an axisymmetric cut, of both path lines colored by

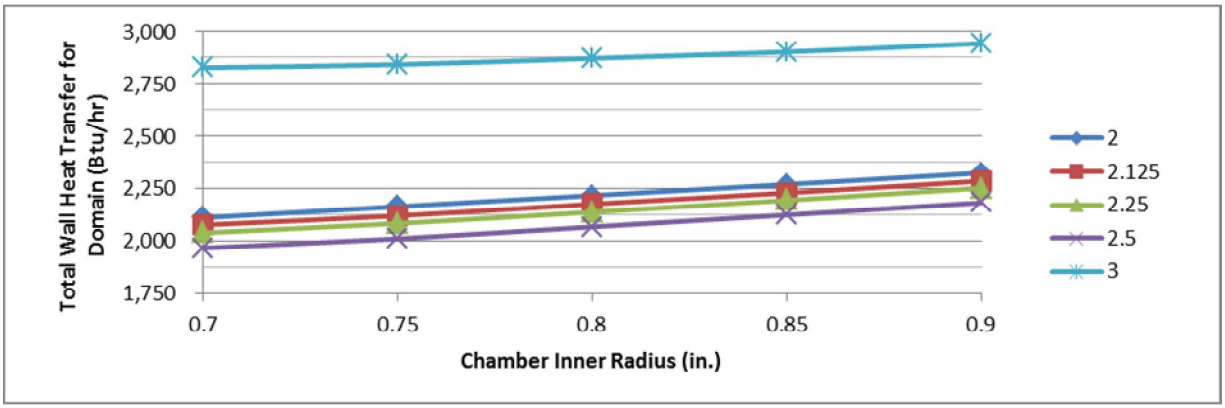

Figure 42: 2D CFD Results – Total Wall Heat Transfer for Domain vs. Chamber Radius & Height

temperature and contours of turbulent intensity, the local ratio of the fluctuating velocity to the bulk velocity, the basis for this flow "switch" is the destruction of a beneficial recirculation pattern between the 2.5" and 3.0" height. This recirculation leads to a high residence time for CO oxidation while limiting gas temperatures at the transition to the tube bank, thus preventing quenching of this slow and temperature dependent reaction. This recirculation zone, shown in Figure 43 by path lines, is also observed in Figure 44 as a highly turbulent shear boundary, whereby radial mixing is inhibited.

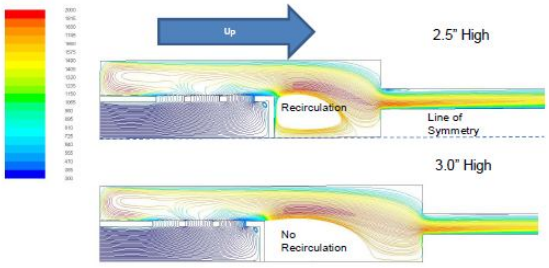

Figure 43: 2D CFD Results – Path lines of Temperature (K) for 2.5 and 3.0" Chamber Height

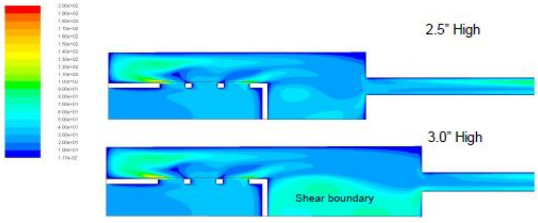

Figure 44: 2D CFD Results – Contours of Turbulent Intensity (%) for 2.5" and 3.0" Chamber Height

Burner Refinement

Based on the CFD results, smaller diameter versions of the "SMTI Long" burner, ½" and 5/8" O.D. versus the baseline ¾" O.D. burner, were fabricated and tested. These smaller burners effectively increased the chamber radius, and CO oxidation results were favorable, reducing CO below 100 ppm at the target excess air (Figures 45 and 46).

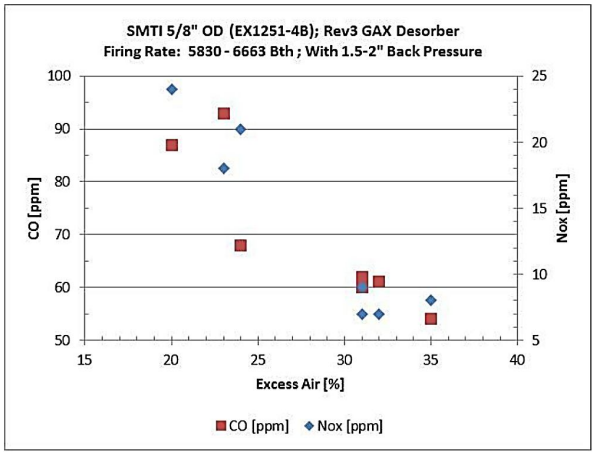

Figure 45: 5/8" OD "SMTI Long" Burner

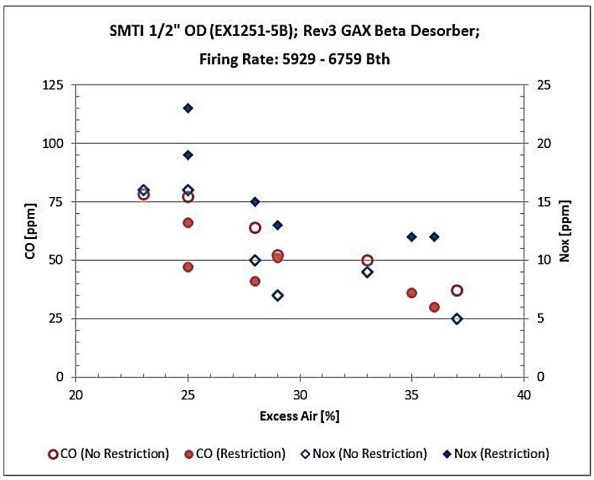

Figure 46: 1/2" OD "SMTI Long" Burner

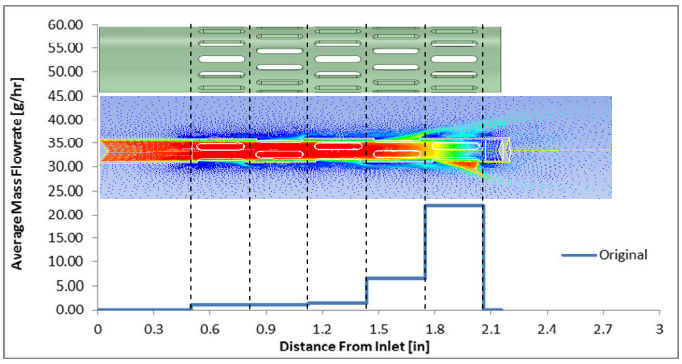

Figure 47: Baseline ½" OD Burner Flow Distribution

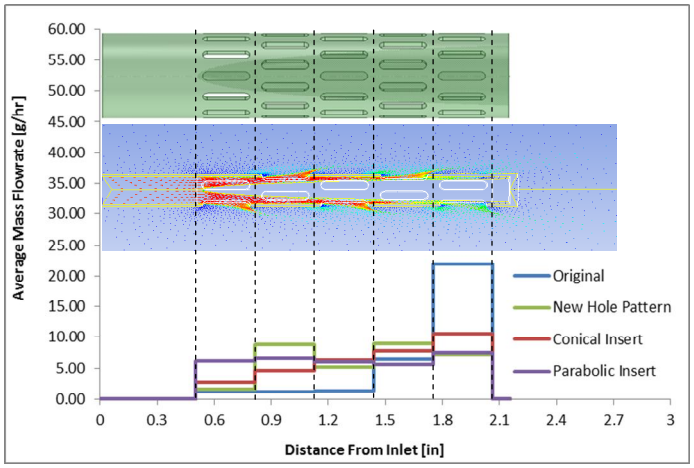

Figure 48: Effect of Distribution Methods

which showed the most effective distribution (Figure 48).

However, open-air firing of both small OD burners showed that the "Christmas Tree" effect was much more pronounced, due to the higher velocity of the fuel-air mixture entering the burner inlet. This creates an area of long flames near the top of the burner, which will be quenched by the combustion chamber wall, increasing CO emissions. If this effect can be eliminated, the CO emissions should fall well below target values.

GTI performed cold-flow (non-reacting) open-air CFD modeling to identify opportunities to optimize fuel/air distribution through the burner. Using the ½" OD burner design, this effect is clearly shown with the flow preferentially exiting the end (top) of the burner (Figure 47).

Multiple variations of hole patterns were evaluated, placing a greater concentration of open area at the base of the burner. While the axial distribution of flow was flattened somewhat, this created high velocity, low flow jets near the top of the burner, which may lead to the same quenching problem. Conical and parabolic inserts of various geometries were also evaluated with the original hole pattern,

Combustion Blower

Two candidate combustion blowers (Table 7) were identified to provide the low flow/high pressure air flow required for this application. Both blowers are commonly used in CPAP applications. Both blowers were tested by GTI and SMTI, with both finding satisfactory results at blower speeds near the bottom of their capability. Selection for production use will depend on cost and future reliability testing.

Fuel/Air Mixer

An off-the-shelf Pyronics Midget Mixer, utilized by GTI for burner testing and by SMTI for the Alpha packaged prototype, is both too costly for the prototype packaged GHPWH and designed for pressures higher than necessary. A more suitable gas/air mixer was designed and fabricated at GTI. This fuel/air mixer design (hereafter "lab mixer"), was a two-piece adjustable Venturi mixer intended be flexible for testing, whereby the orifice area letting fuel in peripherially into the venturi throat is variable (Figure 49).

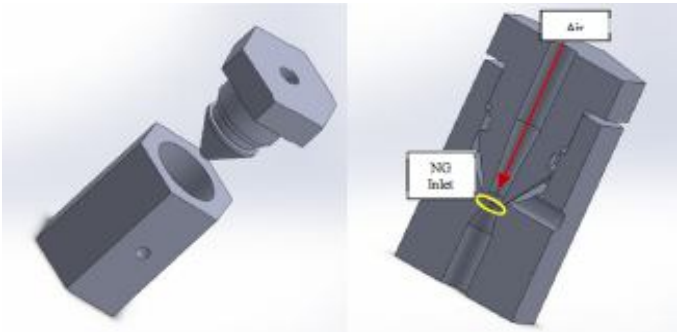

Figure 49: Adjustable Fuel-Air Mixer

Figure 50: Rapid Prototype Fuel-Air Mixer

Testing was completed using an "SMTI Long" burner and Micronel combustion blower. Optimum internal dimensions were identifed to provide the target excess air, at the target firing rate, with no more than 4" WC inlet gas pressure.

With dimensions determined, GTI developed CAD file of the mixer as a single part for rapid prototyping by A.O. Smith. Several prototypes were fabricated (Figure 50) with subsequent successful testing by SMTI on the breadboard test facility and then in the Alpha and Beta packaged prototypes.

Based on the successful testing of the rapid prototypes, SMTI designed a third version that could be produced inexpensively using aluminum castings, incorporated inlet and outlet features for quick assembly to the burner and combustion blower, and an integrated air pressure tap. A machined prototype was fabricated and successfully installed and tested on the "Beta 3" packaged prototype.

Table 7: Microblowers

Manufacturer	Model	Voltage (VDC)	Max. Power (W)	Max. RPM	Max. Flow (CFM)	Max. Pressure (" H_2O)	Outlet Outer Dia. (in.)
Micronel	U65MX	24	18.4	30,600	10.6	12.5	0.69
Ametek	150908-50	28	65.0	30,000	24.6	24.9	0.85

8.0 Task 6: BREADBOARD TESTING

Individual heat pump cycle components were initially tested in breadboard test facilities at SMTI and Georgia Tech. Breadboard testing allows detailed measurements (temperature, pressure and flow) to be recorded at each cycle state point, allowing detailed performance analysis of each individual component. Initial results fed design refinements, which were then tested and evaluated. This process allows overall performance to be refined before fabricating a packaged prototype where detailed measurements, and structural changes, are difficult to implement.

Breadboard Testing

Initial prototype heat exchangers for the GAX cycle were installed in SMTI's breadboard test facility (Figure 51). The hydronic evaporator was coupled to a copper fin-tube heat exchanger/fan assembly (ambient coupling). A second hydronic loop connected the absorber and condenser to an air handler to "dump" the heating load.

The breadboard system includes extensive instrumentation, creating the need for long lengths of connecting tubes and hoses that will not be required in the final design. Mass flow meters measured the strong solution, strong solution split, weak solution and ammonia flow rates. Magnetic flow meters measured the evaporator, condenser and absorber hydronic flow rates. Thermocouples or RTDs were installed at each heat exchanger inlet/outlet, along with pressure gauges and transducers at two high-side and two low-side locations. A lab-quality gas meter (with temperature and pressure correction) was used to measure the gas input rate, along with a combustion analyzer with O_2, CO, CO_2 and NOx measurement capability. Data was collected by a data acquisition system.

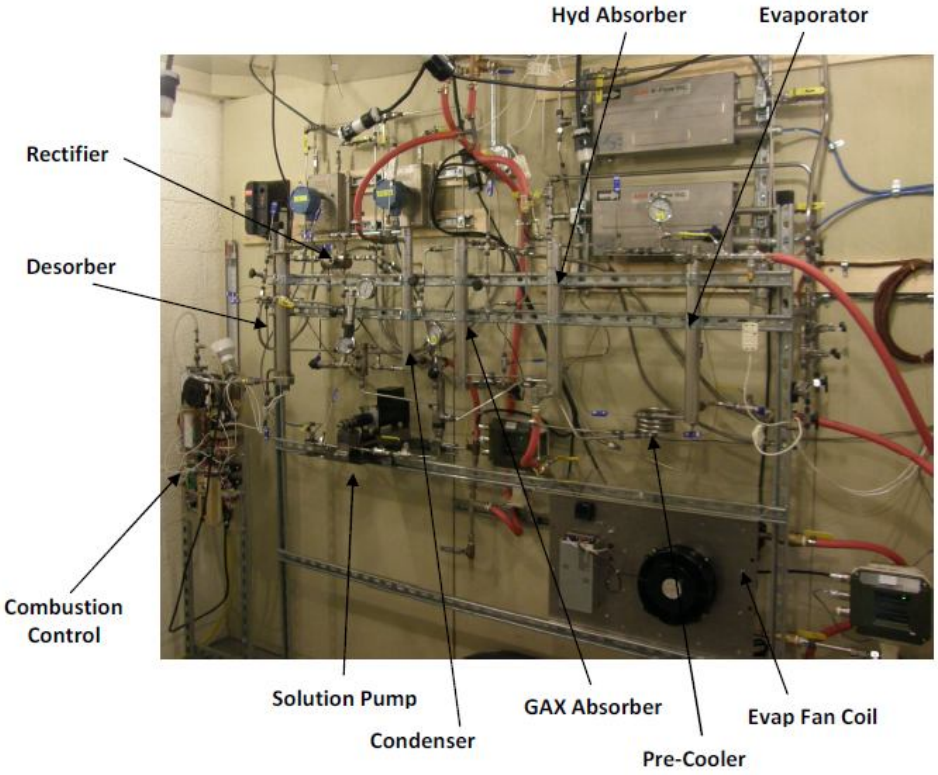

Figure 51: SMTI Breadboard Test Facility

SMTI GAX Phase 1: An initial round of testing was completed at the baseline conditions of 68°F ambient and 90/105°F return/supply water temperature, with stable operation and several sets of steady-state data collected. Five of the seven major heat exchangers performed as intended. Measured heating efficiency (cycle **COP**) with the first set of GAX cycle heat exchangers was 1.25 (2.0 target). Efficiency was limited primarily by the SCAGAX absorber and secondarily by the HCA Absorber (see below). Cycle COP is defined as the useful heating output (condenser + absorber), divided by the net gas energy input (gross gas input based on HHV less the measured combustion efficiency).

The alpha gas-fired **Desorber** performance was at or above target. At the target gas input rate, the flue gas exit temperature was 50-75 F lower than expected, suggesting a 2nd generation Desorber could be reduced in height. Gas-side pressure loss through the flue tubes equals the as-designed 2" wc.

The alpha coiled-tube **Rectifier** performed is at or above target. Ammonia vapor purity entering the condenser was 0.996 was higher. Testing was repeated using the alternate serrated fin-tube design. The serrated design worked well, but the measured UA was approximately 70% of design, compared to 90-100% for the coiled tube version, indicating the length of the serrated tube needed to be increased to meet design performance.

The alpha **Condenser, Evaporator and RHX** all performed as expected.

The alpha **HCA** (co-flow) provided close to target capacity, but a higher than target cooling flow rate (increasing the LMTD) was necessary. As a result, the low side pressure was higher than target, and the strong solution concentration was lower than target. Both have a significant (negative) impact on the cycle efficiency. Although not optimal for performance, the alpha HCA internal geometry was set identical to the alpha SCAGAX absorber geometry in an effort to utilize two identical heat exchangers (lower manufacturing cost). Breadboard test data was used to calibrate the original HCA design model, resulting in a revised beta HCA design.

The alpha **SCAGAX** (counter-flow) absorber performance was lower than target. The SCAGAX is a critical component regarding GAX cycle efficiency, as it recovers a portion of the heat of absorption back into the cycle (effectively reducing the amount of heat that must be added by the burner). Comparison of the alpha SCAGAX design with the test data indicated inadequate distribution of the weak solution over the heat transfer surface as the primary cause. A beta design was developed with revised internal geometry to improve the flow distribution.

Additionally, despite insulation, the long plumbing lines and instrumentation (flow meters) necessary to conduct breadboard testing, combined with the very low flow rates for this small system, resulted in a significant temperature reduction of the weak solution between the Desorber exit and SCAGAX inlet. The reduced weak solution inlet temperature limits the capacity of the SCAGAX.

SMTI GAX Phase 2: GAX cycle testing was repeated using new absorbers (HCA and SCAGAX) incorporating design changes based on the initial round of testing. Improved performance was obtained, with the measured cycle COP increasing by 20% to 1.5 when operating the SCAGAX absorber in counter-flow mode. Testing with the SCAGAX absorber operating in co-flow mode (theoretically increasing heat transfer coefficients while decreasing the LMTD) resulted in a steady-state cycle COP of 1.6. System energy balance consistently showed a 9-10% loss (heat lost to ambient due the extra length of lines and flow meters on the breadboard test cell), resulting in a probable packaged design COP of 1.6-1.7. A cycle COP of 1.7 – 1.8 is needed at baseline test conditions to achieve a water heater EF of 1.5.

The Beta HCA performed very well, meeting or exceeding the target performance. There may be opportunity to reduce the size of the HCA in future revisions. The Beta SCAGAX performance improved, but was still below target, both in counter-flow and co-flow modes. Performance is maximized using the co-flow mode.

The gas-fired Desorber continued to perform very well, with the flue gas exit temperature lower than target even at high firing rates. The difference between the weak solution exit temperature and the Desorber bottom temperature is 20-40 degrees lower than target (100 deg F), indicating the SHX inside the Desorber will need to be moved to a higher elevation in the Desorber. The lower weak solution exit temperature reduces the SCAGAX performance, lowering the COP. A beta version of the Desorber was designed and fabricated based on these results. The beta design incorporated changes to the internal SHX coil and a larger diameter combustion chamber (based on burner test results).

SMTI Single-Effect Cycle (conventional HX's) Phase 1: While waiting for the Beta GAX Desorber components to be fabricated and assembled, SMTI converted the breadboard test stand to run a single effect cycle using conventional components. The key difference between the two cycles is the replacement of the SCAGAX absorber with a much simpler solution heat exchanger (SHX).

Steady-state cycle COP's of 1.58 – 1.65 were obtained at the base conditions, compared to the cycle model prediction of 1.7. At the target gas input rate of 6,400 Btu/hr, the measured heating capacity was 9,018 Btu/hr (95% of theoretical target) with a cycle COP of 1.63.

A series of tests were conducted using a prototype (modified production model) electronic expansion valve (EEV) using a stepper motor control. After determination of the proper PID control parameters, the valve provided very stable control of the refrigerant superheat and allowed the cycle to operate without fluctuation. Several cold and hot starts were completed with the valve providing acceptable control. However, the valve in its current configuration was over-sized for this application. Fixed restriction had to be installed downstream of the EEV in order for it to operate between its full open and full closed position and it did not appear that the valve will allow operation over the wide range of water and ambient temperatures (pressure differentials) this product will need to operate under.

SMTI Single-Effect Cycle (conventional HX's) Phase 2: A direct air-refrigerant evaporator coil was designed and fabricated to replace the hydronically coupled evaporator and a water-air coil. This design potentially reduces the overall cost of the system and may provide increased efficiency due to the elimination of the hydronic loop temperature delta penalty (Figure 52).

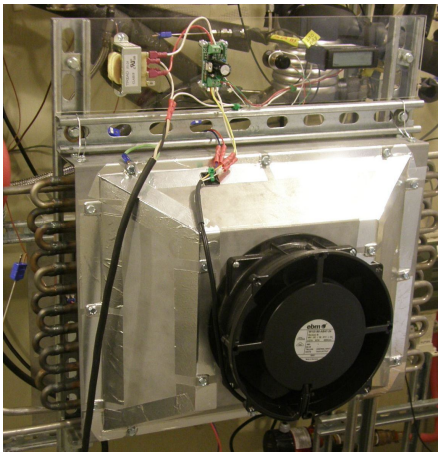

Figure 52: Prototype Evaporator Coil & Fan

The prototype evaporator coil was fabricated so that the refrigerant flow could be configured in two ways, down/down and down/up. A variable speed fan was utilized in order to measure the effect of air flow on performance. Additionally, since the tube diameter was larger than desired due to tooling availability from applicable vendors, extra return bends were supplied with the coil so inserts (to reduce the inside flow area) could be added if required.

Initial testing in the down/up configuration resulted in slugs of liquid refrigerant exiting the evaporator due to a slug/plug flow regime in the upward flowing pass.

Subsequent testing in the down/down configuration resulted in improved operation and performance. Target evaporator capacity was obtained with this configuration using an air flow rate 50% higher than desired.

Based on the test results, inserts were installed inside the tubes, sized to provide the optimum inside flow area (flow regime) for refrigerant boiling. Target evaporator performance at the target air flow rate was obtained using the first set of inserts. However, the ammonia-side pressure drop was twice the target value. Using a second set of smaller diameter inserts, performance was maintained while the pressure drop was reduced to acceptable values.

A proportional solenoid valve was tested (manual control) as an ammonia EEV. After testing with manual control demonstrated the revised valve was capable of controlling the ammonia flow to the evaporator over the range of heated water temperatures, PID control via a PLC was implemented. After optimizing the PID parameters, the valve provided acceptable control during start-up and through the progression of heating water from cold to hot temperatures. This valve was implemented in the Alpha packaged prototype.

SMTI GAX Phase 3: The breadboard was then switched back to the GAX cycle configuration in order to complete one more round of tests incorporating the beta Desorber and air-coupled evaporator. The changes to the Desorber improved the stability of the cycle, but the maximum cycle COP remained at 1.6. Target performance was obtained from all of the cycle heat exchangers except the SCAGAX absorber.

Measured test data and target cycle state points were compared to the SCAGAX design model, which indicated that a pinch point between the coolant and absorbing side at the coolant side saturation temperature was causing the poor performance. A 3rd generation design was completed based on a lower LMTD and more aggressive baffle spacing.

SMTI GAX Phase 4: A final round of GAX cycle testing was completed using a revised (Rev3) SCAGAX absorber. Repeatable, steady-state cycle COP was 1.68, compared to 1.6 using the beta SCAGAX absorber. Although the revised SCAGAX absorber provided improved performance compared to previous prototypes, but remained lower than target. The results compare favorably to the 1.55 - 1.60 COPs obtained with the single effect cycle, but remain lower than the 1.8-2.0 goal for the GAX cycle. Use of the GAX cycle increases estimated heat pump manufacturing cost by $50 (± $10), so the 1 point EF gain is probably not justified given the extra cost.

The Rev3 SCAGAX absorber utilized the same components, and is the same height (so maximum envelope size not increased) as the hydronically cooled absorber (HCA), with a slightly different internal arrangement reflective of differing flow conditions, in order to minimize manufacturing costs. The HCA in both the single-effect and GAX cycle performed very well, meeting or exceeding UA and LMTD goals, and the heat/mass transfer coefficients are theoretically higher in the SCAGAX due to higher vapor velocities. However, the temperature profile between the absorption side and the coolant side of the SCAGAX absorber contains a “pinch point” near the saturation temperature of the coolant, resulting in a much lower LMTD for the SCAGAX. The test results indicate that in order to hit cycle COPs of 1.8 to 1.9, the height of the SCAGAX will have increase by 4-5 inches, which may have a negative impact on market penetration due to the taller overall assembly height.

Georgia Tech Single Effect Phase 1: Georgia Tech completed the initial round of breadboard testing using micro channel heat exchangers for the evaporator, absorber, condenser, SHX and RHX, in a single-effect cycle. GT’s breadboard system is similar to SMTI’s, with thermocouples, mass and magnetic flow meters,

and pressure transducers recording all cycle state points (Figure 53). Gas energy was measured using a lab-quality volumetric gas flow meter (corrected for temperature and pressure), and a flue gas analyzer. Georgia Tech's evaporator was hydronically coupled.

Figure 53: Georgia Tech Breadboard Test Facility

Stable operation was obtained, with heating cycle COP's ranging from 1.2 – 1.3 (1.7 target). Component data analysis showed that the SHX (solution heat exchanger) and absorber performance were the primary factors limiting cycle COP. The SHX recuperates energy between the desorber and absorber, with the cycle COP highly dependent upon its performance. Evaporator performance was also below target, and higher hydronic temperatures (simulating an ambient higher than 68°F) were used to achieve the noted COP.

Georgia Tech Single-Effect Phase 2: GT replaced the SHX with a larger Beta prototype and modified the lines connecting the HCA to the solution pump in an effort to reduce the low side pressure. With the larger SHX, cycle COP increased by 12% to 1.4, with the HCA absorber remaining the primary factor limiting performance. Although SHX performance was improved, it was still below target. The Desorber, Rectifier, Condenser and RHX performed at or near target. Evaporator performance remianed below target, as higher than target hydronic temperatures had to be used to achieve the reported results.

Georgia Tech Single-Effect Phase 3: A beta HCA absorber incorporating internal mixing features was installed and breadboard testing repeated. Performance of the Beta absorber was improved compared to the original version, but it's performance, combined with the SHX, still limited the cycle COP to under 1.5. Analysis indicated that channel to channel distribution and vapor-solution mass transfer within the channels needs to be improved to hit target performance.

9.0 Task 7: COMPONENT AND CYCLE EVALUATION

Two candidate cycles (single effect and GAX) were modeled and breadboard tested using micro channel and "conventional" heat exchanger geometries. Single effect cycle modeling provided a theoretical cycle COP of 1.7 at the design conditions (68°F, 90/105°F return/supply water temperature), while the GAX cycle model predicted cycle COP's greater than 2.0. The GAX is a more complicated cycle to fabricate and operate, with higher anticipated manufacturing cost. Accounting for storage tank standby losses, and parasitic power use, a cycle COP close to 1.8 was thought to be needed to achieve an EF rating of 1.5.

Conventional heat exchangers, with envelop sizes small enough to practically fit on top of a residential water storage tank performed very well in both the single effect and GAX cycles. At the design condition, cycle COP's greater than 1.6 were measured using the single effect cycle, and near 1.7 using the GAX.

Micro channel heat exchangers were tested using a single effect cycle. Channel to channel distribution issues limited the performance of the absorber, evaporator and SHX, resulting in measured cycle COP's just under 1.5

Preliminary manufacturing cost estimation assuming conventional geometries and the GAX cycle, for the Desorber, Rectifier, Evaporator, HCA, SCAGAX, RHX and Condenser was $524 per RT, compared to the original target of $452 per RT (+16%). Eliminating the SCAGAX and adding a SHX (for a single effect cycle) reduced the cost estimation by $25-$35.

Since the micro channel geometries did not perform as well as the conventional, and it was unclear what design changes were required to improve performance, a detailed costing of the micro channel system was not completed.

Based on the simplicity and projected lower cost of the single effect cycle, combined with measured performance very close to what was obtained using the GAX cycle, the decision was made to use the single effect cycle and conventional geometry heat exchangers for the Alpha and Beta packaged prototypes. Based on the single effect cycle COP of 1.6+, the target EF for a packaged system was reduced from 1.5 to 1.3.

10.0 Tasks 9 & 10: ALPHA PACKAGED PROTOTYPE

Components and controls for the single effect sealed system were arranged on a mounting plate matching the diameter of the prototype storage tank (Figure 54). With the exception of solution and ammonia storage chambers, the heat exchangers utilized were those previously tested on the SMTI breadboard. The arrangement accounted for storage tank features such as the center flue tube, water inlet/outlet spuds and anode rod. Connections between the heat exchangers consisted of welded and compression fittings depending on the space available. Isolation valves were installed between the EEV, weak solution restrictor pack and solution pump so that maintenance/replacement could be performed if required, and the restrictor pack could be sized correctly after initial testing.

Controls for the prototype (Figure 55) consisted of a PLC programmed to turn ON/OFF the combustion system, solution and hydronic pumps, evaporator fan and provide PID control of the EEV. The PLC also monitored several safety conditions (desorber temperature, high side pressure). Variable speed controllers were incorporated for the combustion blower (to obtain the target excess air) and evaporator fan (to optimize evaporator air flow).

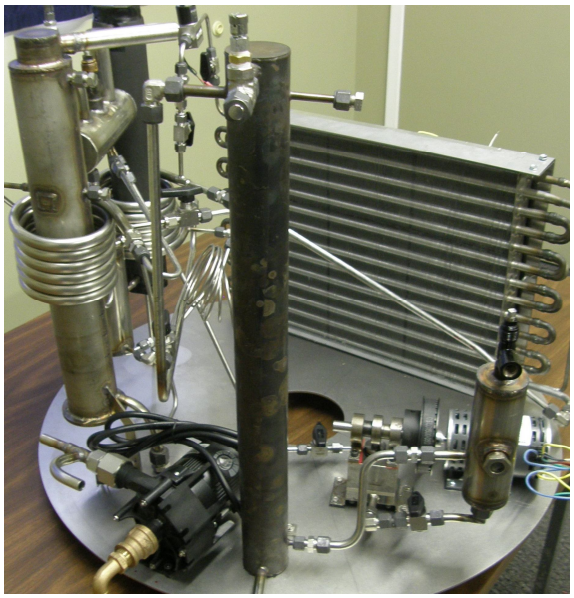

Figure 54: Alpha Prototype Heat Pump Sealed System

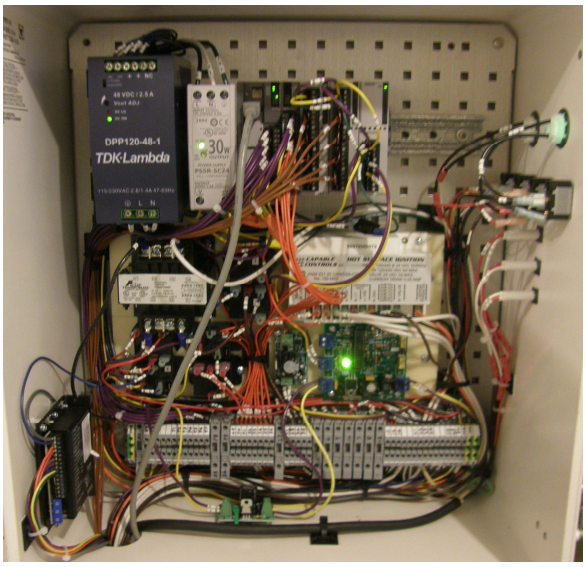

Figure 55: Alpha Prototype Controls

The alpha heat pump sealed system was installed on top of the (A.O. Smith) prototype storage tank (Figures 56 and 57). The Alpha storage tank was insulated with 2 layers of 1 inch fiberglass (in place of shot-in-place foam used for production tanks). Connections for the hydronic heat exchanger were located on the side of the Alpha tank (this was changed to top connections for the Beta prototypes). Hose was used to connect the hydronic heat exchanger to the hydronic pump inlet and absorber-condenser outlet. A turbine flow meter was installed in the leg to the hydronic pump to measure the total hydronic flow rate, which combined with RTD's installed at the hydronic heat exchanger inlet and outlet, allowed for direct measurement of the heat pump heating capacity. Pressure transducers were installed to measure the high and low heat pump cycle pressures, as well as taped-on thermocouples at key cycle state points.

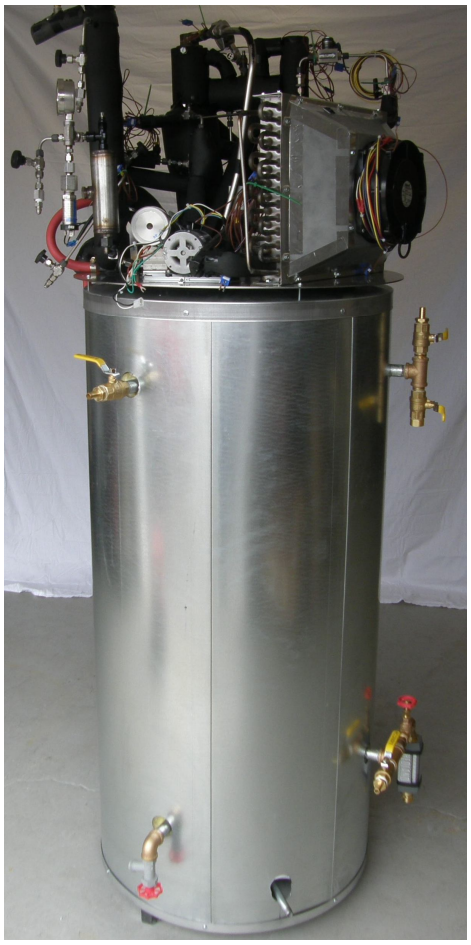

Figure 56: Alpha Heat Pump Water Heater

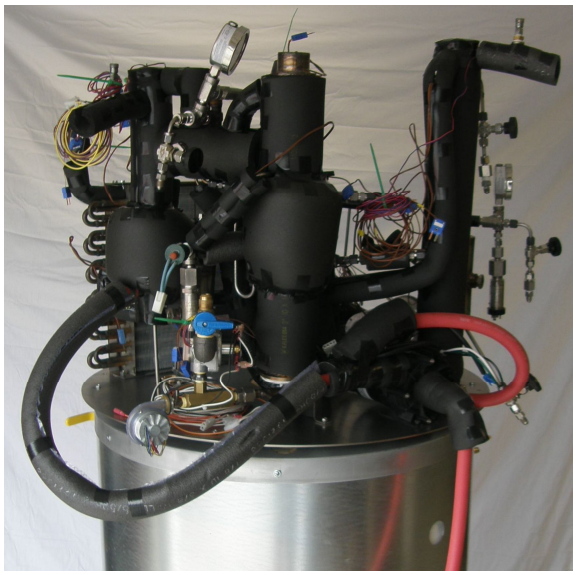

Figure 57: Alpha Heat Pump Water Heater

With water in the storage tank pre-heated and actively cooled to hold the heat pump hydronic inlet temperature at 90 F (base cycle state point), the ammonia-water charge and flow controls were configured to achieve steady-state operation. The total charge for the sealed system was only 3 lbm (approximate 50-50 mix of ammonia-water). Full condensing combustion was readily obtained at a firing rate of 6,500 Btu/hr. Total pressure loss through the burner, desorber and condensing heat exchanger was about 2.5" water (excellent result and below target).

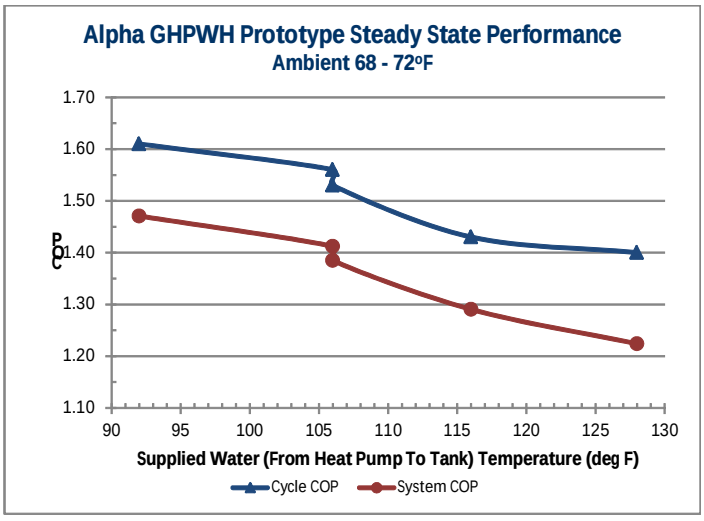

Figure 58: Alpha Steady-State COP

Testing was then completed at high (125 – 135° F) and low (50 – 60° F) storage tank temperatures to trim ammonia charge at the extremes (the cycle stores ammonia out at high temperatures, "soaks" it up at low temperatures), and verify operation and control methodologies.

Heat pump performance was measured at steady-state conditions at several supply water temperatures (temperature of hydronic supplied to the storage tank from the heat pump – Figures 58 and 59).

Cycle COP ranged from 1.61 at 92°F to 1.40 at 128°F. System COP (total heating capacity (heat pump + condensing flue gas) divided by gross gas input) ranged from 1.47 to 1.23. Heat pump heating capacity ranged from 9,039 to 7,430 Btu/hr, while the system heating capacity ranged from 9,891 to 7,968 Btu/hr.

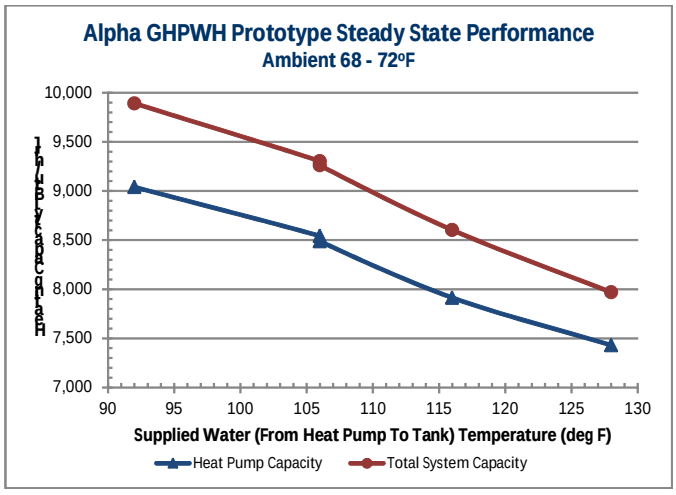

Figure 59: Alpha Steady-State Heating Capacity

The temperature difference (pinch) between the hydronic heat exchanger and the water in the storage tank ranged from 6-7°F at the bottom (return temperature to the heat pump), and 13-14°F at the top. Higher than desired, this represented an opportunity for improvement for the Beta prototypes.

Testing then focused on system (cold) start-up at various storage tank water temperatures. Starting with cold water in the storage tank (less than 60° F), when the strong solution concentration is very high (greater than 60% ammonia) and its temperature low, two issues were identified. The low solution temperature entering the desorber created condensation of the flue gas inside the desorber. The increase pressure loss decreased the firing rate and the condensate created problems with the flame rod.

Figure 60 shows a heating cycle from a tank temperature of 55 to 126° F. The heat pump ran without interference except for a superheat set-point change at 110 and 200 minute marks. COP varied widely initially as the high side pressure struggled to reach an operating level, then fell sharply during the period of condensation in the desorber and improper ammonia flow to the evaporator. A change in the superheat set-point (increase) was made at the 110 minute mark and the condensation stopped, the evaporator was satisfied, and COP returned to normal levels. As the water temperature increased, the superheat set-point was manually returned to the original level.

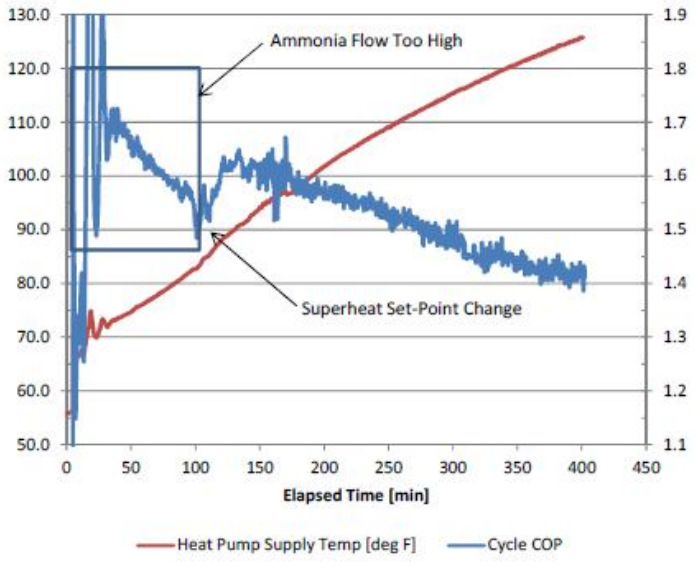

Figure 60: Cold Water Start, Alpha Prototype

Subsequent testing using different control strategies at low water temperatures involving the superheat set-point and hydronic flow were evaluated. Ultimately, a strategy was obtained that provided a smooth start-up at cold water temperatures, with the cycle COP starting at 1.75-1.8 and slowly falling to 1.4 as the tank temperature increased above 125°F. Cold start testing revealed several issues regarding the proportional valve EEV, most of which we were able to create "work-arounds" using control algorithms. The opening point, closing point, and flow characteristics of the valve (flow vs voltage) are a function of the differential pressure across the valve.

These issues will need to be resolved prior to production in order to achieve reliable start-up and operation over the infinite number of operating conditions present in "real life" installations.

Remaining tests included:

- Heating the tank to 125-130°F and performing hot water draws of varying volume, with and without the heat pump running at the time of the draw.

- Starting the heat pump with the tank full of cold water (nominally 60°F) and running until the top of the tank reached 125°F.

- Starting with a hot tank, drawing hot water out in 10 gallon increments (simulating the DOE EF test) to determine the profile temperature in the tank vs the draws and in relation to the internal heat exchanger. The heat pump was turned ON at different temperatures (as indicated by the middle tank side wall thermocouple) to determine the optimum "thermostat" temperature (for both hot water availability and heating efficiency).

- A simulated EF test in which 10 gallon draws were conducted and the heat pump turned ON and OFF automatically by the PLC based on the "thermostat" temperature.

Alpha Prototype EF Testing: The Alpha prototype was installed in A.O. Smith's certified test lab and two back-to-back Energy Factor (EF) tests were completed. The EF test covers a 24 hour period with six 10.6 gallon draws initiated on the hour for the first six hours, followed by a stand-by period. The recovery efficiency is determined during the draw portion of the test, with the remainder determining the heat losses to the ambient from the storage tank (stand-by loss). Energy Factor (EF) is a (complicated) calculated value from these two results. The tests were conducted at 125°F stored water temperature and 68°F ambient.

Note: For prototyping purposes, Tank 2 was insulated with a fiberglass blanket between the tank and the outer jacket, instead of the usual foam insulation, and there were a variety of valves, fittings and a flow meter in the hydronic loop connecting the tank to the heat pump. Therefore we expected the stand-by losses to be much higher than an equivalent production model. Additionally, the Alpha prototype parasitic power was much higher than anticipated for a production model given the PLC and the use of low efficiency variable speed motors/fans.

The prototype completed the full sequence of tests in automatic mode, without issue or operator interference (a significant milestone at this point of development). The heat pump turned ON after the 3rd (Test 1) or 4th (Test 2) draw and ran continuously until the thermostat was satisfied. The recovery time was approximately 4 hours (equal to if not shorter than most electric heat pump models when the auxiliary elements are not used). In addition to the standard EF test measurements, SMTI monitored several key heat pump cycle and hydronic temperatures using a portable data acquisition unit.

Although the heat pump performed well during the EF tests, the raw calculated EF was on the order of 1.0 due to very high stand-by and parasitic power losses. The measured UA (stand-by loss coefficient) was 5.16/4.85, significantly higher than a production unit (fiberglass insulation was used in place of foam for the Alpha tank). Due to the PLC, variable speed control boards and low evaporator fan efficiency, the parasitic power during heat pump operation/stand-by was on the order of 140/20 watts.

Therefore, the measured test data was adjusted accordingly, to values anticipated in a production model (UA of 3.5 and parasitic power 105/5 watts). Summary results are shown in Table 8. Recovery efficiency, neglecting the parasitic electrical load averaged 1.425 for the two tests. Recovery efficiency, defined by the DOE EF test procedure, is essentially equivalent to the heat pump COP, based on the higher heating value of the natural gas. Recovery efficiency, including the anticipated 100 watt heat pump and 5 watt control parasitic loads, averaged 1.345. Correcting the data for a UA of 3.5, the EF averaged 1.23 (neglecting parasitic power) and 1.145 (including parasitic power).

Starting with a COP (recovery efficiency) of 1.425, stand-by losses reduce the resulting Energy Factor (EF) by 0.2, while parasitic power results in another 0.085 reduction.

Table 8: Cold Water Start, Alpha Prototype

	Test 1		Test 2	
	Without Parasitic Power	**Including Parasitic Power**	**Without Parasitic Power**	**Including Parasitic Power**
Recovery Efficiency	1.42	1.34	1.43	1.35
EF	1.22	1.14	1.24	1.15
T_o1	127.7		127.4	
T_o2	127.3		127	
T_o3	126.8		126.5	
T_o4	127.3		125.8	
T_o5	126.1		125.4	
T_o6	122.9		117.2	
Parasitic Power Assumption: Heat Pump = 100 watts; Control = 5 watts				
Data Assumes Standby Loss Coefficient = 3.5				

The average outlet water temperature for the six draws is shown in Table 8 as T_i. Note that the outlet water temperature during the 6th draw was lower for Test 2 than Test 1. This is due to the heat pump being turned ON after the 3rd draw for Test 1, and after the 4th draw for Test 2 (start was delayed manually to determine the impact of the delayed start). By delaying the start, a larger volume of cold water accumulated in the bottom of the tank, allowing the heat pump to operate for a longer period of time with "cold" return water temperatures (maximizing cycle COP). However, this allowed the cool water to start decreasing the temperature of the water at the top of the tank prior to the last draw. Since the EF calculation penalizes for reduced outlet temperatures, the average cycle COP improvement was essentially offset by the calculation penalty.

Given a target EF is 1.3 using the Single Effect cycle, the average recovery efficiency (COP) needed to be increased by 0.15 to achieve an EF of 1.3 in the Beta units. Areas or improvement include:

1) Increasing the effectiveness of the storage tank heat exchanger to reduce the temperature pinch points at the inlet and outlet. This will allow the heat pump to operate at higher COP's given the same tank temperature.

2) Decreasing the standby loss.

3) Detailed cycle data suggests some room for improvement is available for the evaporator (achieving a higher pinch between the ammonia and ambient temperature) and Rectifier (increasing the ammonia purity, especially as the water temperatures approach 125°F and higher.

11.0 Task 11: BETA PACKAGED PROTOTYPES

Three "Beta" packaged prototypes were designed and fabricated, incorporating several minor design changes and "lessons learned" from the Alpha prototype (Figures 61-63). The prototypes consisted of a single-effect ammonia-water heat pump sitting atop a modified 75T75 gas storage tank with PLC automatic control.

Steady-state and "simulated DOE draw" heat pump performance was measured at SMTI's laboratory for all three prototypes. Energy Factor (EF) testing per the DOE test procedure was conducted at AO Smith (Beta 2) and at Gas Technology Institute (Beta 1).

Significant changes from the Alpha prototype included:

1. The storage tanks incorporated a hydronic heat exchanger with more surface area (to reduce the temperature differential between the hydronic and the stored water), and input/output locations through the top of the tank instead of the side. The tanks were insulated with 2 inches of foam.

2. The length of the Rectifier coil was increased by one turn in order to improve ammonia purity as the stored water temperature increases above 120^{o}F.

3. The evaporator coil was increased in size by "one tube" in order to bring the inlet and outlet on the same side, simplifying assembly and reducing cost.

4. Off-the-shelf (low cost) single-speed evaporator fan motor and blade replaced the variable speed DC fan. The evaporator and fan was incorporated into a shrouded sub-assembly with a matching venturi (rapid prototype).

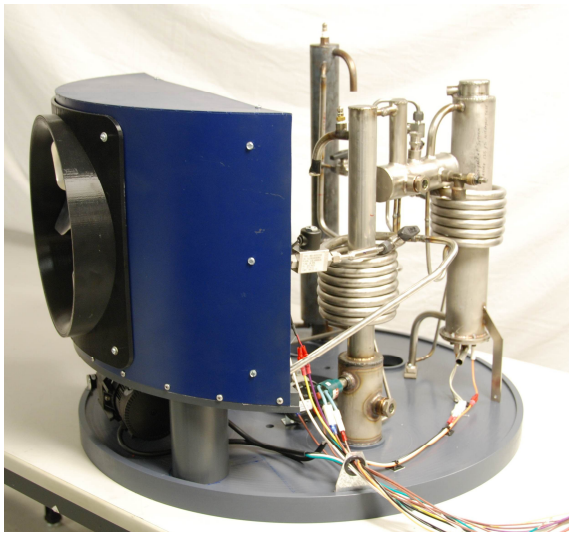

Figure 61: Beta1 Sealed System

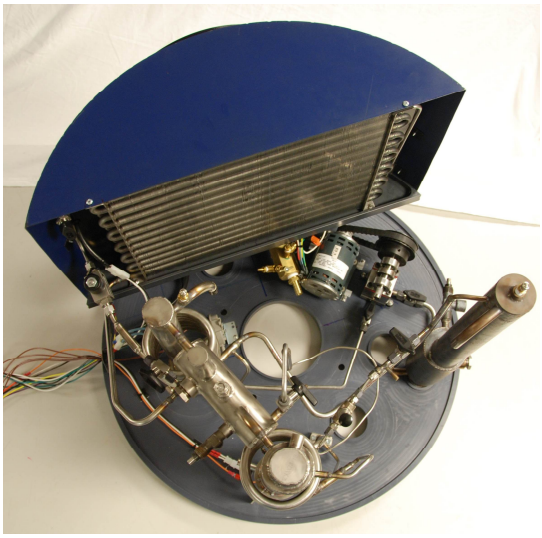

Figure 62: Beta1 Sealed System

Figure 63: Beta2 GHPWH Prototype

SMTI's testing consisted of trimming the ammonia-water charge, sizing the weak solution capillary tube, tailoring the start-up algorithm to the EEV characteristics, recording steady-state heat pump cycle performance, and conducting simulated EF tests by imposing the draw pattern from the DOE test procedure. A small venturi-type flow meter was installed in the hydronic loop, which combined with thermocouples installed at the hydronic heat exchanger inlet and outlet, provided for calculation of the heat pump heating capacity.

Well into the testing phase, it was found that all three tanks were undershot with foam (creates large areas of voids and/or reduced foam thickness). A tank assembly without the proper amount of foam will increase standby losses and decrease the resulting EF when DOE testing. Undershooting prototype tank assemblies is not uncommon due to the bit of guesswork involved in determining the foam volume required for a complete fill.

Beta 1 and 2 were tested at GTI and AO Smith with the "as-received" tanks. Beta 3 heat pump was steady-state tested using the Alpha tank (providing a good comparison). Tanks 2 and 3 were re-foamed (successfully) and the Beta 2 heat pump was re-tested at SMTI with the re-foamed tank, but we were not able to get it back to A.O. Smith for repeat EF testing.

Steady State Performance: Steady state heat pump performance was measured by SMTI by flowing a small amount of water through the tank, at a controlled inlet temperature, until a steady-state condition was obtained. Cycle COP was calculated based on the hydronic flow rate and inlet/outlet temperatures and the net gas input (gross input x combustion efficiency at the desorber outlet). Steady state cycle COP vs. return water temperature (hydronic temperature returning from the tank heat exchanger to the heat pump) is shown in Figure 64 for the three Beta and single Alpha prototypes. The small difference between the Beta units is considered to be measurement error. Tests were conducted at a nominal 68 F ambient.

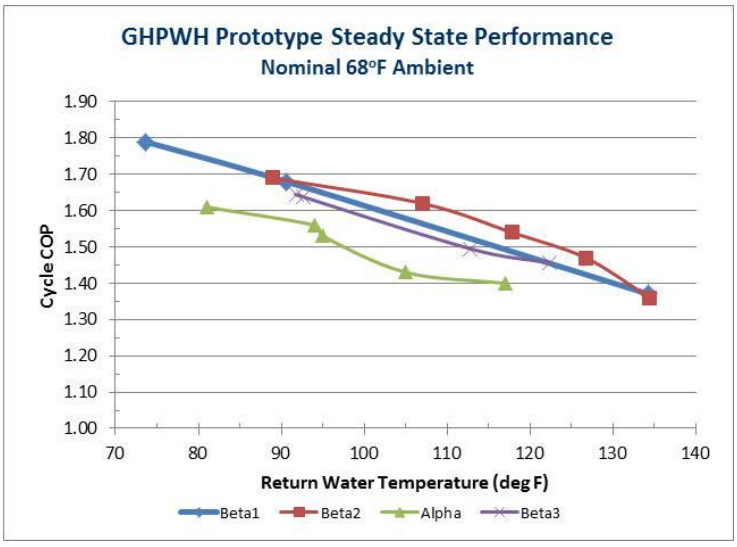

Figure 64: Cycle COP vs. Return Water Temperature

Average ***cycle COP*** from 75 to 125°F hydronic temperature was approximately 1.61 (1.65 target for an EF of 1.3). Improvement from the Alpha prototype is due primarily to the design changes made to the Rectifier and Evaporator, as well as slightly lower ambient heat losses due to the more

compact construction. Figure 64 shows the importance of keeping the bottom of the tank initially as close to the inlet water temperature as possible (to take advantage of the high COPs at those temperatures), and maintaining tank stratification so that the return water temperature does not have to increase all the way up to the mean tank temperature before recovery end.

Figure 65 shows the ***gas-fired COP*** for the same tests, calculated by adding the energy input to the tank in the flue gas heat exchanger to the heat pump heating load and dividing by the gross gas input. The average gas-fired COP from 75 to 125°F hydronic temperature is approximately 1.45 (target 1.49 to achieve and EF of 1.3). However, since the water in the tank during these steady-state tests was almost completely uniform top to bottom, and equal to the return water temperature, the resulting flue gas exit temperature was higher when operating "normally", so the resulting gas-fired COPs are slightly understated.

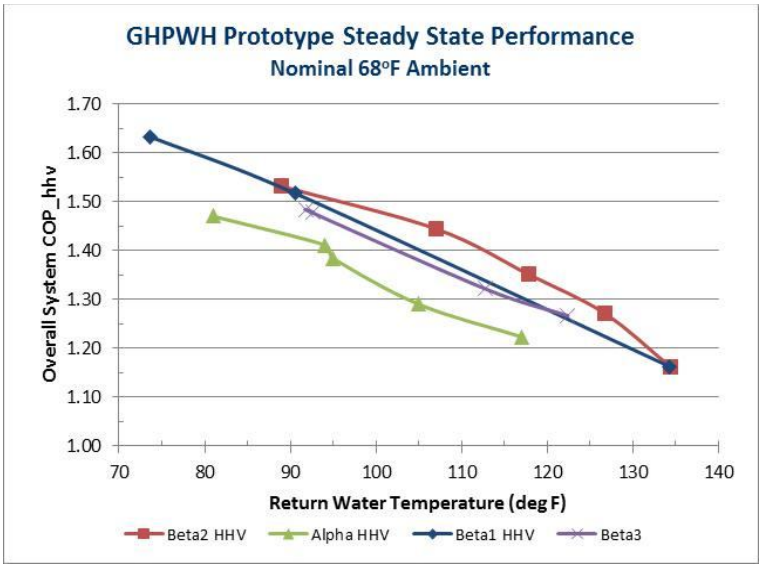

Figure 65: Overall COP vs. Return Water Temperature

In order to hit our targets, the average combustion efficiency needs to be close to 95%. Therefore, the average flue gas exit temperature must be about 90 F.

Start-Up and Control: Deficiencies with the proportional solenoid EEV, noted during the Alpha prototype testing, became more problematic on the Beta prototypes. Although Beta 1 operation was very stable after the initial start-up sequence (first 15 minutes after heat pump turns ON), consistently achieving a smooth start proved challenging. During the first 15 minutes, system flow rates and differential pressure quickly increase from zero to steady-state values. Since the flow rate through the EEV is a function of the differential pressure and control voltage, and the valve characteristics change with differential pressure, the start-up control algorithm is very "active" during the first 15 minutes to keep the system balanced. The first two (brand new) EEV valves used in Beta 1 were very inconsistent from one start to another. After installing the valve from the Alpha prototype, consistent start-ups were obtained. However, observation of the starts indicated that the current valve/control algorithm is not robust enough for field use, where the water and ambient temperatures will vary much more than the test lab conditions.

This opinion was verified during testing at GTI, which conducted a few tests at "non-standard" water and ambient temperatures. Similar inconstancies were observed in the Beta 2 and 3 prototypes. Subsequent discussions with the valve manufacturer (we are using this valve in an application for which it was not intended) have identified a few simple design changes that can be incorporated to resolve the start-up issues.

Implementation of these changes must be completed during the next phase of development, prior to field testing.

EF Test Results – AOS Beta 2: Three DOE Energy Factor (EF) tests were conducted by AO Smith using the Beta 2 prototype. Tests 1 and 2 were conducted at a stored water temperature of 125°F, while Test 3 was 135°F. The heat pump turned ON (recovery start) during the 3rd draw for Test 1 and during the 4th draw for Tests 2 and 3 (thermostat set-point was changed to achieve this result). The prototype started and operated very well during these tests, in full automatic mode.

Raw unmodified data for the five EF tests conducted by AO Smith (the original two for Alpha prototype, three for Beta 2) is shown in Table 9. Since the parasitic power drawn by the prototype units is much higher than for production models, the electrical power was not measured for two of the tests in order to quantify the effect of parasitic power on the EF. For all tests, the standby heat loss was very high. The Alpha tank was not foamed (two one inch layers of fiberglass) and the foam shot in the Beta 2 tank was incomplete.

Table 9: AO Smith EF Tests, Raw Data

AOS EF Test Results: Raw Data						
		Alpha EF1	**Alpha EF2**	**Beta2-EF1**	**Beta2-EF2**	**Beta2-EF3**
Thermostat	deg F	125	125	125	125	135
Avg Ambient	deg F	68.9	67.4	66.5	67.0	67.1
Recovery Start, Draw #		3	4	3	4	4
Tank Capacity	gallon	70.0	70.0	68.5	68.5	68.5
Gas Used	cuft	24.9	25.2	26.9	25.9	31.0
Gas Input	btu/hr	25,403	24,542	25,989	25,050	30,131
Total Parasitic Power (1)	watt-hours	1030	0	1037	1025	0
Qt	btu	28,921	25,541	29,619	28,687	30,131
Qstby	btu	1037	0	857	869	0.0
Qr, Standby Loss Rate	btu/hr	362	259	362	358	348
UA		7.08	4.89	6.93	6.84	5.68
EF		0.99	1.16	0.93	0.94	1.03
Recovery Efficiency		1.28	1.41	1.18	1.19	1.26
T_outlet - Draw 1	deg F	127.7	127.4	125.2	124.9	135.2
T_outlet - Draw 2	deg F	127.3	127.0	124.8	124.5	134.8
T_outlet - Draw 3	deg F	126.8	126.5	124.2	123.8	134.0
T_outlet - Draw 4	deg F	127.3	125.8	124.1	122.8	132.9
T_outlet - Draw 5	deg F	126.1	125.4	121.6	120.1	128.7
T_outlet - Draw 6	deg F	122.9	117.2	118.6	109.9	116.9
T_outlet - Average	deg F	**126.3**	**124.9**	**123.1**	**121.0**	**130.4**
T_mean - Initial	deg F	126.0	125.7	125.1	124.8	135.2
T_mean - End of 24hr Test	deg F	114.1	115.0	113.7	114.4	122.8
T_mean Standby Loss	deg F	11.9	10.7	11.4	10.4	12.4
Gas-Fired COP, calc (2)		1.41	1.39	1.36	1.40	1.36
Note (1): Parasitic Power was not measured for tests showing zero value						
Note (2): Estimate, based on energy of heated water divided by total gas input						

Given that the measured steady-state COP of the Beta heat pumps was much improved compared to the Alpha, the results were somewhat surprising. One major difference between the data sets is the average outlet water temperature, which was 3 to 4 °F lower than Alpha prototype, suggesting more mixing and less stratification inside the Beta storage tank. As discussed previously, the average outlet temperature has a large effect on the EF calculation (negative if it drops below the thermostat set-point). Additionally, the average hydronic inlet temperature (to the heat pump) was slightly higher for the Beta prototype (despite the larger heat exchanger), and the average flue exit temperature was slightly higher, resulting in

Recovery Efficiencies about 10 points lower. These findings are discussed in more detail in the sections below.

Similar to the Alpha EF test data, adjustments were made to the raw data to account for the high standby loss and parasitic power. For the Beta test results, an additional adjustment was made to the average outlet water temperature to determine its effect on the calculated EF (Table 10). The last column for each test shows predicted EF after adjustments for standby loss, parasitic power and outlet water temperature were made. The predicted EFs (1.13/1.15/1.14) were essentially identical to the Alpha corrected EFs. Curiously, the 135^{o}F thermostat test was not significantly different than the 125^{o}F tests.

Table 10: Adjusted Beta 2 EF Test Results

	Test 1			Test 2			Test 3		
	Without Parasitic Power	Including Parasitic Power	Higher Outlet w/Parasitic	Without Parasitic Power	Including Parasitic Power	Higher Outlet w/Parasitic	Without Parasitic Power	Including Parasitic Power	Higher Outlet w/Parasitic
Recovery Efficiency	1.34	1.27	1.31	1.32	1.25	1.33	1.27	1.21	1.28
EF	1.17	1.10	1.13	1.16	1.08	1.15	1.14	1.07	1.14
T_o1	125.2			124.9			135.2		
T_o2	124.8			124.5			134.8		
T_o3	124.2			123.8			134.0		
T_o4	124.1			122.8			132.9		
T_o5	121.6			120.1			128.7		
T_o6	118.6			109.9			116.9		
Parasitic Power Assumption: Heat Pump = 100 watts; Control = 5 watts *Data Assumes Tmean Standby Loss = 7 deg F*									

Subsequent data analysis and testing identified 3 major reasons for the lower than anticipated Beta prototype EF test results, despite the higher heat pump steady state COP:

1. The average hydronic return temperature (to the heat pump) was higher than obtained with the Alpha prototype, despite the larger heat exchanger. A higher average return temperature equates to a lower average cycle COP. This result suggests more mixing of the cold and hot water occurred in the Beta tanks compared to the Alpha.

2. The average delivered hot water (outlet) temperature was lower than obtained with the Alpha prototype, despite roughly equivalent tank capacities. A lower average outlet water temperature negatively impacts the EF calculation and lowers the calculated Recovery Efficiency. This result also suggests more mixing (less stratification) in the Beta tanks.

3. The average flue gas exit temperature from the condensing heat exchanger was higher than obtained with the Alpha prototype, despite no changes to the design. A lower average flue gas temperature results in a lower combustion efficiency, calculated Recovery Efficiency and EF. It is unclear whether this result is due to the mixing or to an unintended geometry difference during fabrication.

Flue gas exit temperature during the recovery portion of the EF test for the Alpha and Beta 2 prototypes is shown in Figure 66. Although the flue gas exit temperatures are roughly equivalent at the end of the recovery, the temperature at the beginning was much lower for the Alpha. Also, the average exit

temperature varied by 6 degrees for the Alpha dependent upon whether recovery started on the 3rd (Test 1) or 4th (Test 2) draw. However, the draw start changed the Beta average temperature by only 1 degree.

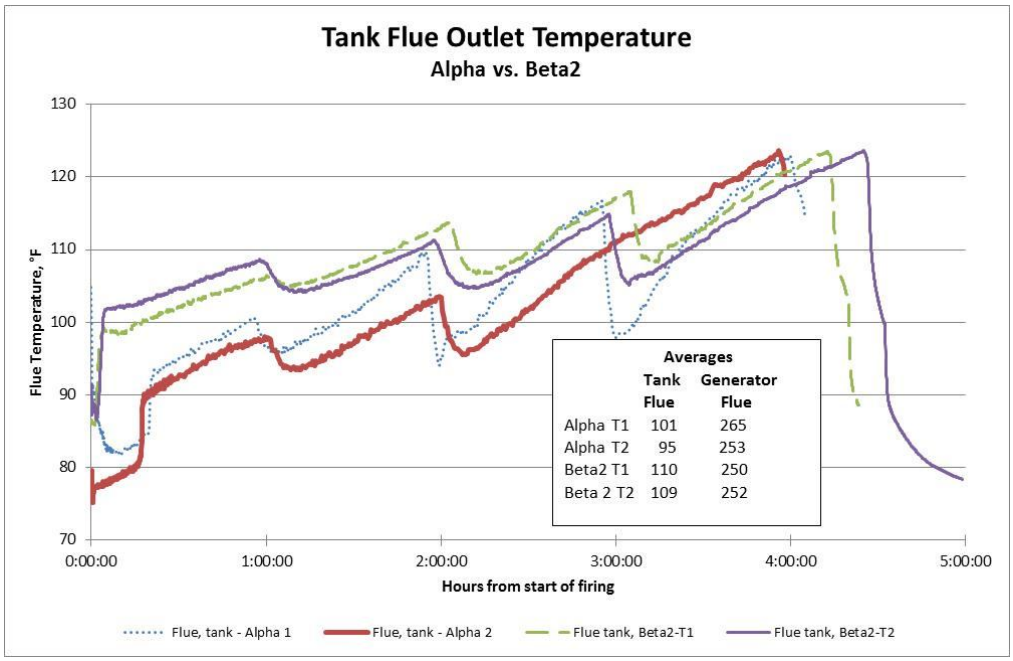

Figure 66: Alpha vs. Beta2 Flue Gas Exit Temperatures

Following the A.O. Smith Beta 2 EF testing, SMTI conducted additional tests, focusing on the mixing issue. Since the cold water inlet spud was roughly located at the same elevation as the bottom of the hydronic heat exchanger, we theorized that the cold inlet water could be striking the heat exchanger and deflecting upwards, inducing mixing currents. A short inlet tube assembly was fabricated (Figure 67), designed so that the cold water entered the tank tangentially to the tank side wall, instead of straight in towards the center.

Figure 67: Inlet Tube Prototype

The impact on the hydronic return temperature during the first 75 minutes of recovery were dramatic, 10 degrees lower initially compared to testing without the inlet tube (Figure 68). The impact on the flue exit temperature was negligible, possibly due to the fact that the cold water entering radially does not make it all the way to the center flue tube.

Although not shown in Figure 68, the use of the inlet tube also increased the average outlet water temperature several degrees, further indication that it reduces mixing and improves tank stratification. We anticipate this combined improvement (lower average hydronic return temperature and higher average outlet temperature) to have a dramatic (positive) impact on the measured EF.

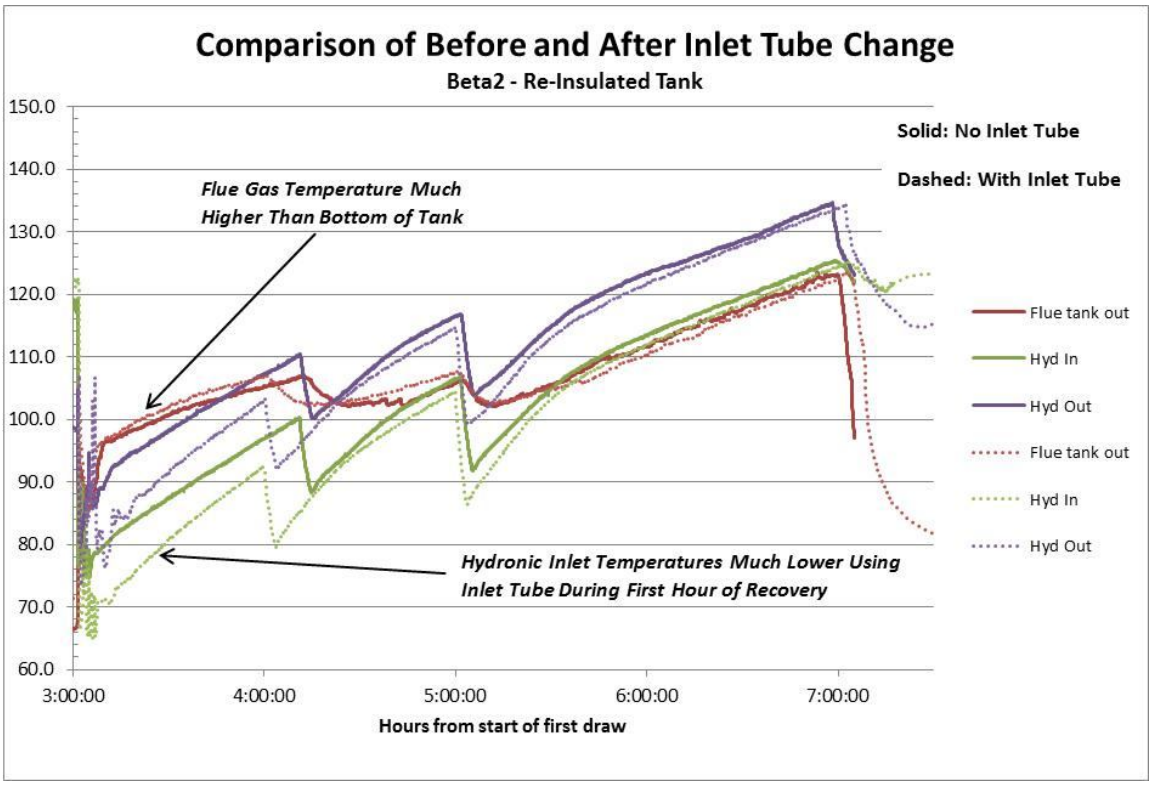

Figure 68: Beta2, With and Without Inlet Tube

EF Test Results – GTI Beta 1: Gas Technologies Institute (GTI) completed 7 Energy Factor tests using the Beta 1 prototype, over a variety of test conditions (Table 11). In addition to the standard DOE conditions of 67.5°F ambient and 58°F inlet water (at both 125 and 135°F set point), GTI conducted tests at cooler and warmer ambients and colder and warmer inlet water. A final test was conducted using a non-standard draw pattern. For the standard DOE draw tests (1-6) the heat pump turned ON (recovery start) during the 3rd draw.

Table 11: GTI Energy Factor Test Conditions

Test Number	Name	Ambient Condition			Water Condition		Draw Pattern
		Dry Bulb (F)	Dew Point (F)	RH (%)	Main Temp. (F)	Set Point (F)	
1	Hot/Humid	75	60.2	60	72	125	DOE
2	Warm/Mild	71.3	51.8	50	65	125	DOE
3	Standard	67.5	48.3	50	58	125	DOE
4	Standard	67.5	48.3	50	58	135	DOE
5	Cool/Mild	63.8	44.9	50	56	125	DOE
6	Cold/Dry	60	35.6	40	54	125	DOE
7	Standard	67.5	48.3	50	58	125	GTI – Mid

During installation (Figure 69) and initial start-up testing, three unfortunate events occurred that negatively impacted the testing:

1. The storage tank was initially filled prior to the installation of the thermocouple tree, causing water to flood the top of the heater and flow into the foam insulation surrounding the tank. Wet foam has very poor insulating properties, further aggravating the standby heat loss issue already present due to the incomplete foam fill.

2. SMTI connected a charging manifold gauge to the high and low service valves, so that the high and low side pressure could be monitored during the initial heating cycle. The high side service valve was left open over a weekend (SMTI mistake), resulting in an unknown amount of ammonia charge leakage due to a small leak at the manifold hose connection. This issue was apparent due to the low system pressure present upon returning Monday morning.

   GTI purchased a small cylinder of ammonia and added ammonia per SMTI's instructions. However, based on how the prototype operated (especially during the first 20-60 minutes after heat pump start) and the recorded test data, the ammonia charge was low for all seven tests. The low ammonia charge negatively impacted the test results, especially at the lower ambient/water temperature tests.

3. During the initial heat-up cycle, the hydronic loop pressure exceeded the hydronic pump seal rating, causing the seal to fail and the need for a replacement pump. Other than the hydronic flow rate may not have been exactly the same as during SMTI's testing, this did not have an impact on the test results.

Figure 69: GTI Environmental Test Chamber

Overall, GTI's test results were similar to those at A.O. Smith. The raw EF calculation was penalized heavily by the very high measured parasitic power (170 watts operating, 19 watts standby) vs production target (100/5), very high standby loss (incomplete and wet foam), and the decreased outlet water temperature during the 6th draw (tank mixing). Additionally, evaporator and desorber temperature plots show the heat pump did not start up smoothly for most of the tests, a product of the low ammonia charge which aggravated the sensitive EEV control algorithm.

GTI completed a similar, but independent analysis of the test data, correcting for the parasitic power, standby loss, and outlet temperature (heat pump start-up problems could not be corrected for). Tabulated results are shown in Tables 12 and 13.

Table 12: GTI Modified EF Test Results: Reduced Standby and Measured Parasitic Reduced 33%

Test No.	Gas Consumption (Btu)	Electrical Input (Btu)	T_{24} (°F)	UA (Btu/hr-°F)	Recovery Efficiency (%)	EF_{adj}
1	17,120	2,040	120.3	3.07	1.40	1.22
2	22,700	2,290	120.5	2.67	1.23	1.11
3	25,340	2,510	120.4	2.68	1.20	1.09
4	29,380	2,730	129.7	2.65	1.16	1.06
5	26,830	2,540	120.2	2.66	1.15	1.05
6	28,300	2,590	120.0	2.82	1.07	0.98

Table 13: GTI Modified EF Test Results: Reduced Standby, Parasitic Reduced 33%, Higher Outlet Temperature

Test No.	Gas Consumption (Btu)	Electrical Input (Btu)	T_{24} (°F)	UA (Btu/hr-°F)	Recovery Efficiency (%)	EF_{adj}
1	17,120	2,040	120.3	3.07	1.44	1.28
2	22,700	2,290	120.5	2.67	1.27	1.16
3	25,340	2,510	120.4	2.68	1.25	1.16
4	29,380	2,730	129.7	2.65	1.24	1.16
5	26,830	2,540	120.2	2.66	1.21	1.13
6	28,300	2,590	120.0	2.82	1.16	1.08

GTI's adjusted EF for the two "standard" tests (3 and 4) was 1.16, very similar to the A.O. Smith adjusted values of 1.15 and 1.14. As expected, adjusted EF's were higher at higher ambients and lower at lower ambients.

GTI estimated the cycle COP during heat pump operation using changes to the stored water energy (via six thermocouples inserted into the tank per the DOE test procedure) and the net gas input to the desorber. Curve fits of the raw data for Tests 1-5 are shown in Figure 70 as a function of the hydronic return temperature. At the lower hydronic temperatures, GTI's cycle COPs closely match SMTI's steady-state measurements (Figure 64), but are lower at higher temperatures.

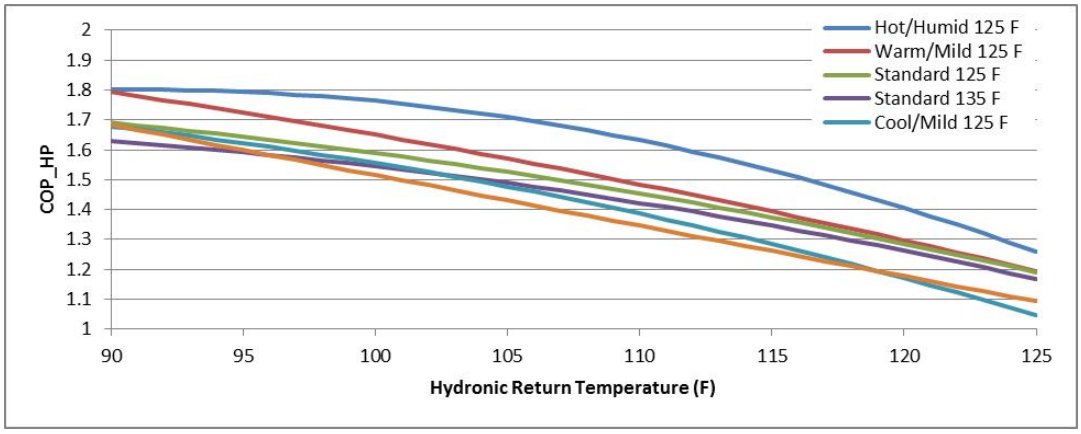

Figure 70: Trend lines of Cycle COP vs. Hydronic Return Temperature

The effect of poor tank temperature stratification (mixing) is apparent in Figure 71, which shows the average hot water outlet temperature for each of the six draws. Since the heating capacity decreases with decreasing ambient, the effect is more pronounced for the cool/cold ambient tests. As previously stated, the EF calculation heavily penalizes any reduction in the outlet water temperature, so this is an issue that must be resolved during product development. The prototype inlet tube that appears to improve this issue (Figure 67) was not developed until after GTI completed their testing.

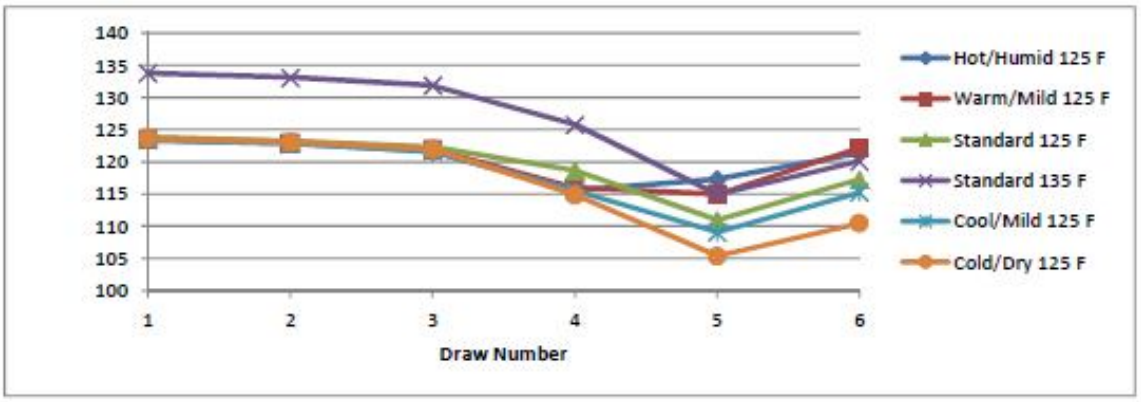

Figure 71: Average Hot Water Outlet Temperature vs. Draw Number

GTI continuously monitored flue gas emissions while the heat pump was operating (Beta 1 utilized one of the "SMTI Long" ¾" OD burner prototypes). Average results are shown in Table 14. Measured CO was very close to slightly lower than measured at SMTI for this burner. Measured NOx was slightly higher than SMTI measurements, but very close to that required to pass SCAQMD regulations. As noted in Section 7, additional burner refinements were completed after fabrication of the burner used in Beta 1.

Table 14: Average Flue Gas Analysis Results

Test No.	O_2 (%, dry)	CO (ppm, as measured)	CO_2 (%, dry)	NO (ppm, as measured)	NO_2 (ppm, as measured)	NO_x (ppm, as measured)
1	5.0	84.9	8.8	13.6	6.9	20.5
2	5.1	87.4	8.8	15.1	6.8	21.9
4	5.0	88.7	8.9	7.9	3.3	11.2
5	5.1	87.8	8.8	15.6	6.1	21.7
6	5.0	100.4	8.7	10.1	3.8	13.8

As discussed above, the low ammonia charge resulting from the accidental loss and replacement, combined with the sensitive EEV control algorithm at heat pump start, caused Beta 1 to start sluggishly during all of the GTI tests except Test 2 (Warm and Mild). A fast start (off to full capacity and efficiency) is critical to ultimately achieving the target EF, especially since the hydronic temperature is the lowest when the heat pump initially turns ON, representing the highest operating COP condition.

Heat pump temperatures during the first 55 minutes after the heat pump turned on for Test 2 (a good start) is shown in Figure 72. The evaporator outlet air temperature fell quickly during the first 5 minutes, indicating that the evaporator load came up quickly, required for high COPs. The small "bounce" at the 128-129 minute mark is normal as the EEV PID algorithm adjusts to the rapidly changing conditions.

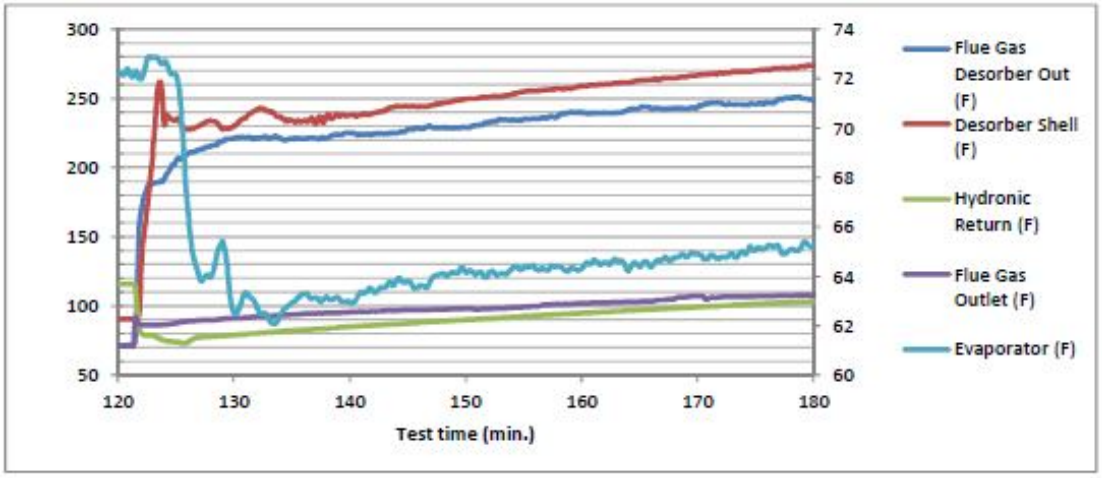

Figure 72: Initial Startup During Test 2 (Warm and Mild)

A similar plot is shown in Figure 73 for Test 3 (a poor start). The evaporator outlet air temperature initially fell, then rose to a level indicative of almost zero evaporator load for a period of 45 minutes, before falling briefly and then rising for another 1.5 hours. This pattern is typically caused by the EEV opening too far, dropping the high side pressure to the point where the differential pressure between the high and low side is too low to allow the valve to achieve the correct ammonia flow rate. The high side pressure is much more likely to fall to this point when the ammonia charge is low.

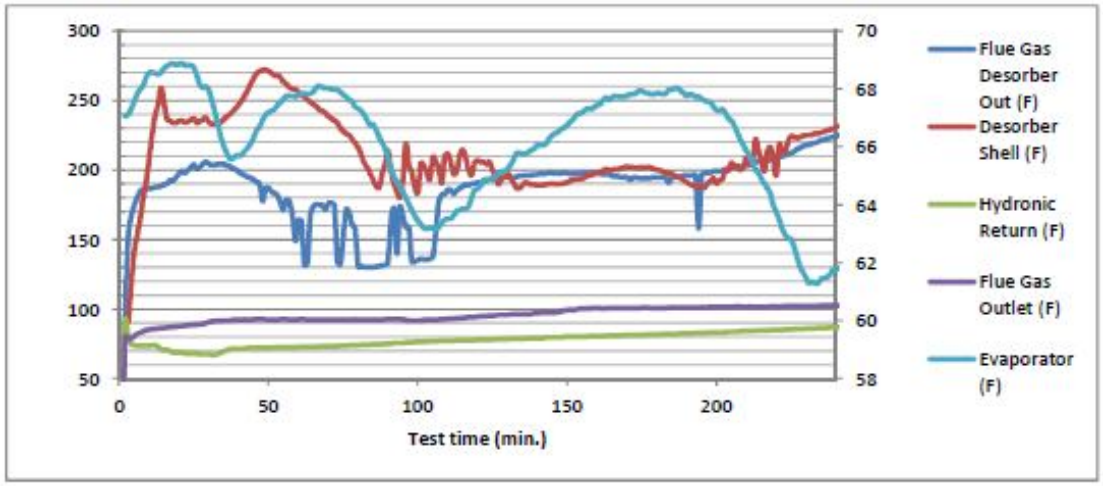

Figure 73: Initial Startup During Test 3 (Standard 125)

Achieving an EF of 1.3: Using the Energy Factor (EF) calculation from the DOE test procedure, the key performance targets to reach an EF of 1.3 can be identified:

- The average (from recovery start to stop) heat pump cycle COP must be at least 1.65
- The average system COP must be at least 1.49
- The average combustion efficiency must be at least 95%
- The average hot water outlet temperature must at least equal the starting average tank temperature
- The standby loss coefficient (UA) must be about 2.5
- Parasitic power use during recovery must be on the order of 110-120 watts
- Parasitic power use during standby must be on the order of 5 watts

Based on steady state testing, the cycle COP of the Beta prototypes average 1.61 (Figure 64) over hydronic return temperatures of 75 to 125^{o}F, very close to the target 1.65. Incremental improvements in evaporator capacity, lower heat losses to the ambient from the heat pump heat exchangers, and improved tank stratification (less mixing) so that the starting hydronic temperature is 70^{o}F or below (the inlet water temperature for EF testing is 58^{o}F), should result in average cycle COPs of 1.65 or higher.

Based on steady state testing, the system COP of the Beta prototypes average 1.45 (Figure 65) over hydronic return temperatures of 75 to 125^{o}F, very close to the target 1.49. The incremental improvements noted above plus improvements to the average combustion efficiency should result in average system COPs of 1.49 or higher.

In order to achieve an average combustion efficiency of 95%, the flue gas exit temperature from the condensing heat exchanger must average about 90^{o}F. The Alpha prototype average flue gas exit temperature was 95^{o}F (Figure 66), while the Beta prototypes back-tracked to about 110^{o}F. An incremental improvement in condensing heat exchanger performance, combined with improved tank stratification so the water temperature at the bottom of the tank is lower, should result in average combustion efficiencies close to, if not equal to 95%.

Starting with a mean tank temperature of 125^{o}F, the Alpha prototype achieved an average hot water outlet temperature of 126^{o}F (starting on 3rd draw) and 125^{o}F (starting on 4th draw), indicating low mixing and decent tank stratification. Beta performance went backwards due to increased tank mixing, with average outlet water temperatures of 123/121^{o}F (3rd/4th draw).

A storage tank with 2" of good quality foam should be able to meet the target UA of 2.5. GTI has suggested that their test data implys that part of the high standby loss measured on the Beta prototypes may be due to natural circulation in the hydronic loop during standby. This has not be determined as true or false at this point. But if true, it can be eliminated through the use of inexpensive plastic flappers.

Use of higher efficiency (and commercially available) solution pump and evaporator fan motors will provide a parasitic power use of about 120 during operation. Typical standby power use of electric heat pump water heaters is 5 watts.

Summary: ***Efficiencies necessary to reach an EF of 1.3 have essentially been achieved from the heat pump cycle point of view. Better integration of the heat pump to the storage tank and reduced parasitic power and standby losses is required and subject of further work.***

12.0 Task 12: WATER HEATING SYSTEM APPLICATION MODELING

Through three interested parties: DOE, Air Conditioning, Heating, and Refrigeration Institute (AHRI), and ASHRAE, the method of defining and rating residential water heaters is currently under revision. As a wholly cofunded task from the *Residential Water Heating* project (California Energy Commission Contract 500-08-060, 2009-2012), a comprehensive market transformation program for high-efficiency natural gas-fired residential water heating in California, this section focuses on: (a) how data generated during this GHPWH development can to inform this revision process, through the ASHRAE Standard Projects Committee (SPC) 118.2, (b) using data generated from laboratory testing under both programs to develop a comparative analysis of operating economics for GHPWH versus other gas water heating options, and (c) a summary of developing modeling tools for gas storage water heaters and challenges for extending capabilities to GHPWHs.

Developments Concerning a Revised Method of Test

Under the National Appliance Energy Conservation Act (NAECA), residential water heaters are rated for efficiency by the U.S. Department of Energy (DOE)[1,] whereby the performance of an established MOT results in an Energy Factor (EF) rating for efficiency and a First Hour Rating (FHR)/Maximum Flow (gpm) for capacity. If a water heater is considered a commercial product, it is instead rated by through the Energy Policy Act (EPAct), whereby a Thermal Efficiency (TE) and Standby Loss (SL) are defined[2]. For gas-fired water heaters, the distinction between residential and commercial water heaters is significant, summarized for gas-fired water heaters in Table 15, as the recently passed U.S. bill *HR 6582* seeks to bridge this regulatory gap with a universal descriptor. This is important, as:

(a) At the time of writing only residential water heaters are eligible for the Energy Star® designation, a recognized market driver for high-efficiency water heating.
(b) The Federal Trade Commission prevents water heater manufacturers from publishing an EF for commercial products, thus limiting the consumer from comparing products.

Table 15: Characterization of Gas-fired Water Heaters

Water Heater Characteristics		Applicable Test Procedures	Eligible for Energy Star?
Firing Rate > 75,000 Btu/hr	Storage ≥ 2 gallons	Commercial Storage Water Heater - EPAct applies (TE)	Not at time of writing[3]
	Storage < 2 gallons & Firing Rate < 200,000 Btu/hr	Residential Tankless Water Heater - NAECA applies (EF)	Yes
	Storage < 2 gallons & Firing Rate > 200,000 Btu/hr	Commercial Tankless Water Heater - EPAct applies (TE)	Not at time of writing[12]

1 Dept. of Energy. *Energy Conservation Program for Consumer Products: test Procedure for Water Heaters.* 10 CFR Part 430, 1998.
2 Dept. of Energy *Uniform test method for the measurement of energy efficiency of commercial water heaters and hot water supply boilers (other than commercial heat pump water heaters)*, 10 CFR 431.106, 2012.
3 The U.S. EPA & DOE are in the process of including commercial water heating in the Energy Star Program, http://energystar.gov/products/specs/sites/products/files/Commercial%20Water%20Heaters%20V1.0%20Draft%201%20Webinar%20Final%20Slides.pdf

Firing rate **< 75,000 Btu/hr**	Storage ≥ 20 gallons and ≤ 100 gallons	Residential Storage Water Heater - NAECA applies (EF)	Yes
	Storage < 20 gallons and > 2 gallons	*Hybrid water heater*: "Reserved" DOE classification	No

Whereas the determination of a commercial water heater's (CWH) TE & SL are straightforward, determining the EF and FHR of a residential water heater (RWH) are as follows:

- **First-Hour Rating** – This is a measure of the hot water capacity. The test procedure determines the volume and average temperature of hot water delivered by a water heater during an hour of operation. A draw of 3.0 gallons per minute (gpm) is sustained until the draw temperature drops more than 25°F below the maximum delivered temperature for that draw. At this point, the draw ceased and the water heater recovers to its set point temperature. Subsequent draws are initiated following satisfaction of the thermostat(s). The First-Hour Rating (FHR) is the total volume of hot water delivered over an hour.
- **Energy Factor** – The Energy Factor (EF) is determined by the performance of the DOE *24 Hour Simulated Use Test*, which estimates the aggregate energy efficiency over a representative daily hot water draw pattern. The test sequence consists of six hourly hot water draws at 3.0 gpm that sum to 64.3 gallons, visualized in Figure 74. Following these six draws, the water heater idles in standby for the remainder of the 24 hour period. From this test, an EF is calculated representing the transient efficiency of the water heater, following numerical adjustments for variations in ambient conditions, inlet and outlet water temperatures, and the estimated recovery efficiency. This recovery efficiency, akin to a steady state thermal efficiency, is determined between the initiation of the test to the first "cut-out", or satisfaction of the thermostat(s).

Drawbacks of the Current MOT and Proposed Revisions

Ending on November 28th, 2011, DOE opened a Request for Information (RFI) concerning a modification to the current MOT for the rating of residential water heaters[4]. This RFI comes at the beginning of a concerted effort to revise a test method that has been in place for over 15 years in its current form, and which is used as the primary metric for determining compliance with minimum energy efficiency standards[5] and acceptance into the EnergyStar® program. The revised DOE MOT must be finalized by Q4 2013, due to the passed bill HR 6582. This RFI and recently passed bill come after several years of work performed by the following primary organizations and entities:

- **ASHRAE** – Through the SPC 118.2, this group has reopened this standard for review and evaluated modifications and alternatives to the current MOT, with significant activity over the past 3½ years. As a consensus building organization, with committee members from industry, academia/research, and government, progress has been slow. That said, the previous ASHRAE Standard 118.2 served as the primary basis for the current DOE MOT.
- **AHRI** – In support of, and in parallel to, the ASHRAE efforts, AHRI has convened a working group of water heater manufacturers[6] to develop an alternative MOT with initial focus on the opportunity for a so-called "Discrete Performance" replacement to the current SUT. Lately, focus has shifted to new hot

4 www.gpo.gov/fdsys/pkg/FR-2011-10-12/pdf/2011-25815.pdf
5 Via the National Appliance Energy Conservation Act (NAECA)
6 Recent meetings have had representation from the DOE (via NIST) and the ASHRAE SPC 118.2 chair

water draw profiles for the current SUT. To date, their meetings have been closed and the alternative MOT being developed has not been shared with ASHRAE.

- **DOE/NIST** – As compelled by the abovementioned legislative initiatives, researchers within the National Institute of Standards and Technology (NIST) are evaluating proposed alternative MOTs and changes to test conditions (e.g. groundwater temperature, ambient temperature, etc.) (Healy 2008, Healy 2011). Including input from ASHRAE, AHRI, and other stakeholders (via the RFI), ultimately DOE will likely look to NIST as the primary technical support authority concerning the revised MOT.

As outlined in the RFI, revisions to the MOT are gathered into four primary categories: Scope, Draw Patterns, Discrete Performance Tests, and Test Conditions. Issues concerning the Scope relate to residential equipment type and sizing that will be subject to this revised MOT. Concerns with test conditions, namely the uniform inlet water temperature of 58°F as a representative water temperature, will be similarly voiced by manufacturers, primarily tankless manufacturers in this case. The impact of Draw Patterns and Discrete Performance Tests on the rating of residential water heaters as two separate options for a replacement MOT are not trivial matters, which concern all high-efficiency gas water heating technologies including GHPWH. These impacts are summarized as follows:

- **Discrete Performance Tests** – If a "Discrete Performance" test is selected as the revised MOT, much uncertainty remains in the analytical methodology for generating rating metrics, its comparability across equipment categories, and if the development outcome would actually yield a simpler more repeatable alternative to the current MOT. DOE even expresses doubts about this test approach in the RFI itself, stating that "*DOE is uncertain of the feasibility of characterizing water heaters and developing an energy factor algorithm based on empirical data because it is not aware of any such algorithms that have been thoroughly proven to be effective at estimating the energy factor*."
- **Draw Patterns –** If an SUT is retained for the revised MOT, the current draw pattern will likely be replaced by a pattern that distributes the hot water volume in a greater number of draws over the 24 hour test (possibly several patterns that vary in total daily hot water draw volume may be used). Deviations from current Simulated Use MOT Energy Factor (EF) rating will differ across equipment categories. Tankless water heaters will see across the board EF reductions as a result of the increased thermal cycling losses with a more distributed 24 hour hot water draw pattern. In general, storage water heaters will have a more muted impact, as a change in the daily hot water draw will likely result in EF reductions however as standby losses increase while hot water deliveries decrease, however draw pattern intermittency and distribution have a reduced impact, particularly for large volume storage water heaters like GHPWHs.

Discrete Performance MOT: Based on discussions had with groups involved, the authors believe that outstanding issues with the development of a Discrete Performance test as a replacement for the current Simulated Use MOT will prevent it from being selected as the preferred revised MOT. While extensive work has been performed by members of ASHRAE SPC 118.2, GTI included, in the development of a particular Discrete Performance test – the "Input/Output Method", it has not been successfully demonstrated as a simpler, more accurate MOT applicable across equipment categories. The intent is attractive, use a series of short focused laboratory tests (e.g. Low/High use, Standby/Steady State/Recovery) and through a series of calculations, arrive at a performance curve that is sufficiently descriptive over a range of hot water use, equipment size, and type. Using the Input/Output method as an example (Butcher, 2011), the two primary unresolved issues with this MOT approach preventing its further development are:

- **As transient devices, water heater use is not path-independent –** In other words, it has been demonstrated that for a given hot water demand, 20 gallons/hour for example, the hot water can be delivered with a wide range of efficiencies. In Figure 74, several ways of delivering 20 gallons/hour are shown, where one could imagine that a tankless water heater would be more efficient for Draw #1 than Draw #3, with a greater potential for cyclic losses. Similarly, Draw #4 may see lower efficiencies due to reheating of the heat exchanger.

  Using these patterns, GTI tested a tankless water heater and found that a linear Input/Output relationship was not sufficient to capture the "flywheel" effect of the hot heat exchanger, with the results presented in Figure 75. A range of 4.4 efficiency percentage points are observed, where a 1 percentage point difference can determine compliance or non-compliance with minimum efficiency and acceptance to EnergyStar. Similar impacts have been observed for electric storage heat pump water heaters due to the control strategy of utilizing auxiliary electric resistance heat (Davis, 2010). Unless these effects of thermal capacitance and other issues are accurately incorporated into a model, the range in error will be prohibitive.

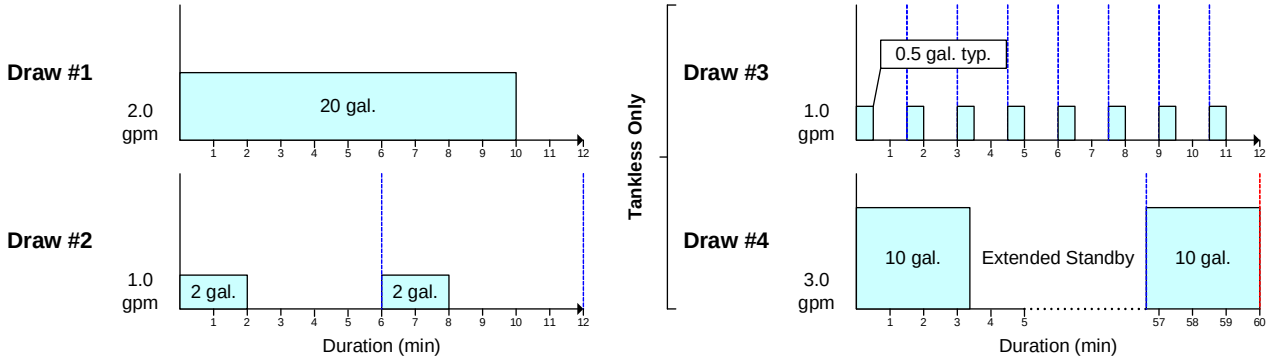

Figure 74: Examples of Differing 20 Gallon/Hour Draw Patterns Over an Hour

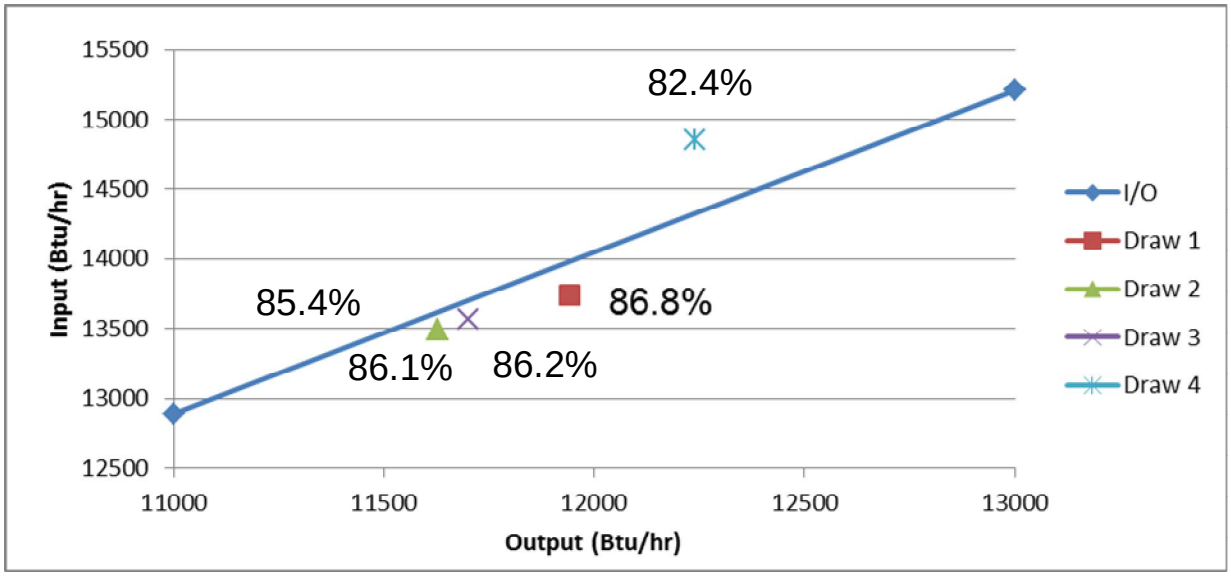

Figure 75: Variation in Delivered Efficiency for 20 gallons/day Delivered (Glanville, 2010)

- **Simplicity –** As including the thermal capacitance as a modeling parameter requires additional knowledge of the water heater (e.g. heat exchanger weight, materials, fin spacing), this does not simplify the test procedure. GTI also found that in defining the linear Input/Output performance curve, specifying the "Low Use" point proved problematic. For storage water heaters, the low use point is a small draw followed by an extended standby period of arbitrary duration. Depending on the standby heat loss, the water heater may or may not initiate a recovery to satisfy the thermostat during this period, introducing considerable error (Glanville, 2010).

  To simplify the current MOT, there is hope that a revised test would alleviate the need for the submerged temperature probes that must be inserted within storage water heaters. It was found that a vertical storage tank temperature distribution was necessary to account for a change in stored energy, with a gas storage water heater delivering 20 gallons of hot water/hour using Draw #1 vs. Draw #2 (3) had 72.5% vs. 66.3% efficiency. If the change in stored energy was accounted for, as Draw #2 caused temperature stacking, the two draws agreed at 75.0% (Glanville, 2010). The proposed Discrete Performance tests evaluated have not proved any simpler than the current MOT.

Simulated Use MOT: The authors believe that there is a high likelihood that multiple draw patterns will be selected as an alternative to the single draw pattern currently used. The multiple draw patterns will be categorized by daily total hot water usage, a low, medium, and high usage with the potential for the addition of a point-of-use draw pattern. The hot water draw pattern used in the current MOT has been criticized for:

- **Favoring Tankless Water Heaters –** One reason the current MOT favors tankless water heaters is that they have minimal standby losses during the extended standby period. Additionally the six hot water draws are large volume draws, 10.7 gallons, which allow the tankless units to reach efficient steady state operation readily. Recent research suggests that both (a) actual hot water use consists of numerous, small volume, short duration draws – estimates are an average of 79 draws/day at 0.7 gallons/draw (Thomas, 2011), and (b) that intermittent draw patterns, like those observed in the field, can contribute to a substantial degradation of tankless water heater efficiency (Davis Energy Group, 2006 & Schoenbauer et al., 2011).
- **Overestimating total daily usage** – Residential hot water consumption differs from space heating loads, in that it is primarily affected by household size rather than building type or climate (i.e. groundwater temperature). Recent research from the Natural Resources Canada, whose original field research over 25 years ago provided a basis for the current benchmark (Perlman & Mills, 1985), found that over a 74 house field study the average total usage has dropped to 49 gallons/day (Thomas, 2011). This has an important effect on daily efficiency, as the proportional relationship of Delivered Efficiency/EF to daily hot water usage has been demonstrated repeatedly (Davis, 2010 & Glanville, 2011).

Projected Impact to GHPWHs: The hot water draw pattern can have an impact on the estimated daily efficiency. As recent research suggests that the average U.S. household requires less than 64.3 gallons of hot water per day prescribed in the current standard, invariably a revised MOT will focus on smaller daily draw patterns. Additionally, as research simultaneously shows that the average household has numerous short duration, small volume hot water draws as opposed to six regular sustained draws, the revised draw patterns will capture this through increased draw number and intermittency. These two factors in a revised SUT will contribute to a likely reduction in the estimated efficiency of GHPWHs versus current

estimates for 64 gallons/day. This will impact all water heaters in comparison to current ratings, with disproportionate impacts on tankless units for reasons discussed previously.

To illustrate this, the following in Figure 76 through 78 (with data point tabulated and sources identified in Appendix A) summarize the impact of more "realistic" draw patterns from numerous laboratory studies within the past several years. Field studies are not included due to variability of test conditions, data collection, and equipment age. The draw patterns used from study to study are not identical, however they represent a potential spread for what impact future revised SUTs may have.

- "Estimated Energy Factor (EF)" is referenced as the efficiency metric, as the EF refers to a specific draw pattern and test conditions.
- "NAECA" refers to units at the minimum efficiency required, current and in 2015.
- "Standard" refers to data for the tests performing the currently required SUT.

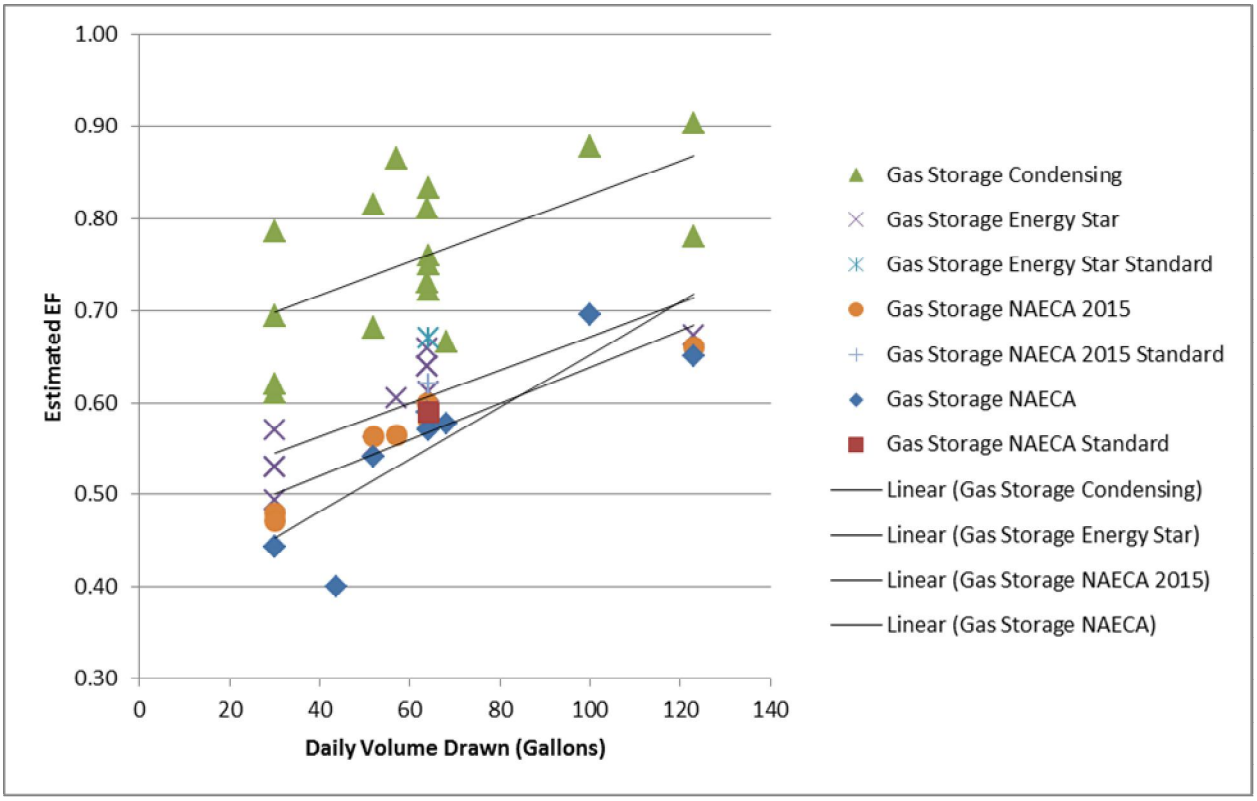

Figure 76: Delivered Efficiency vs. Daily Draw Volume for Gas Storage Water Heaters

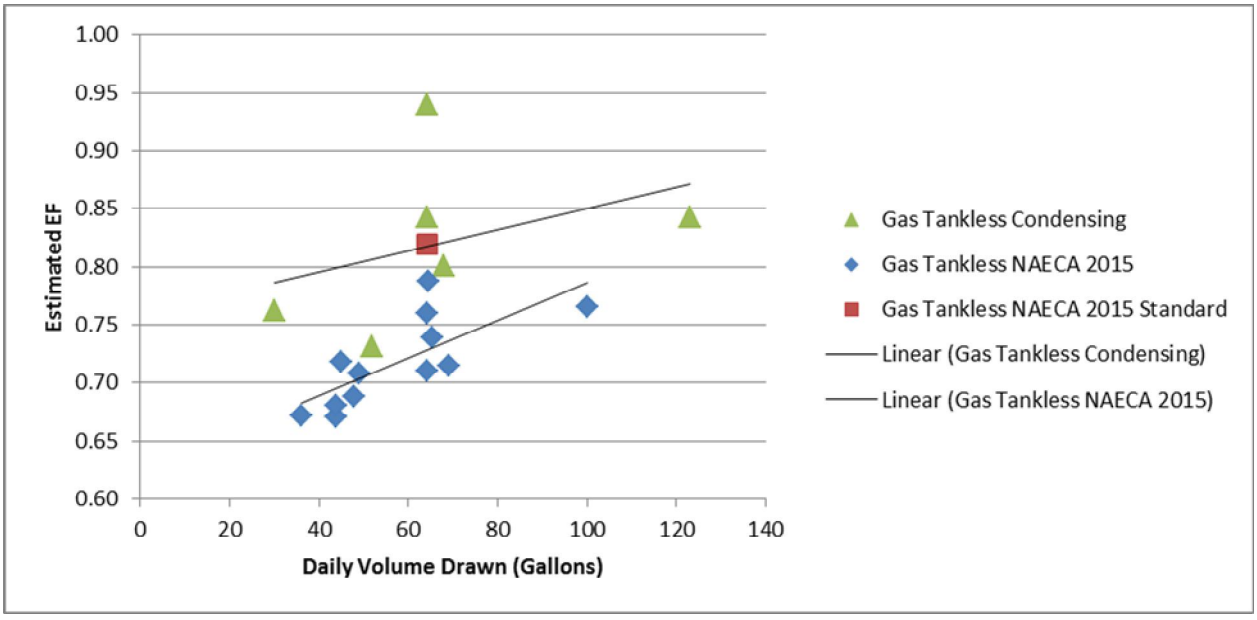

Figure 77: Delivered Efficiency vs. Daily Draw Volume for Gas Tankless Water Heaters

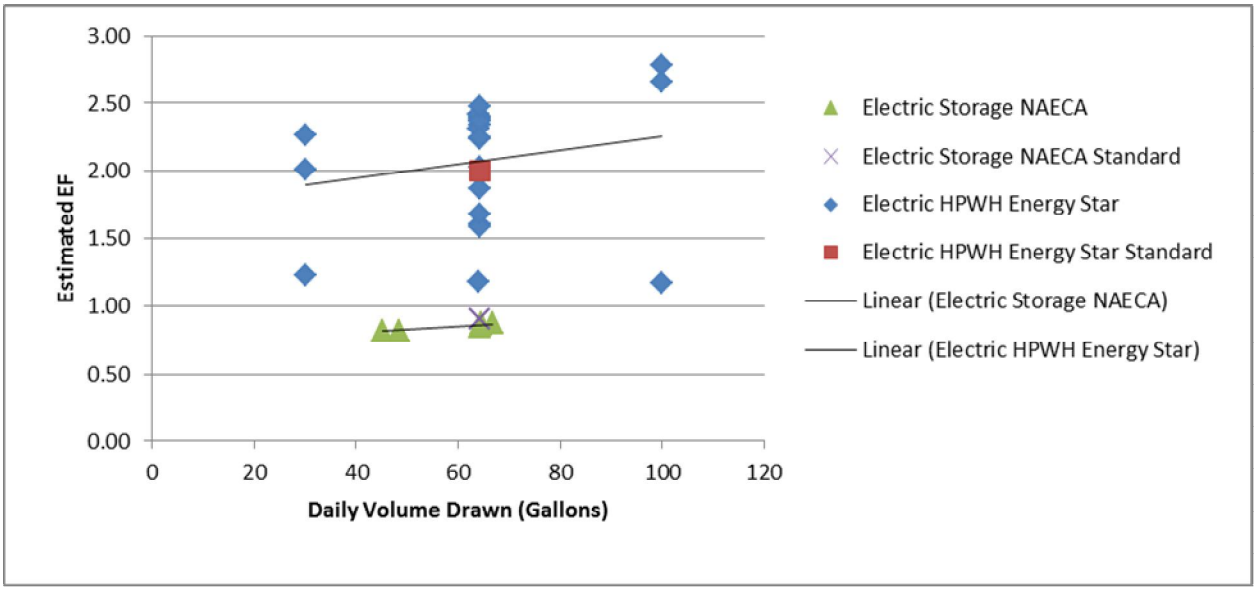

Figure 78: Delivered Efficiency vs. Daily Draw Volume for Electric Storage Water Heaters

Gas Storage Water Heater Testing and Model Development: Major Findings of Laboratory Testing

Under the cofunded CA Energy Commission program, the Gas Technology Institute (GTI) and Pacific Gas & Electric (PG&E) Applied Technology Services (ATS) conducted laboratory testing of a wide range of water heaters to foster a better understanding of results from water heater field testing being conducted by Davis Energy Group (DEG), and provide input for water heater modeling algorithm development being conducted by both DEG and Lawrence Berkeley National Laboratory (LBNL). GTI and PG&E generated and analyzed laboratory datasets for these two classes of water heater products:

- **High-Efficiency Storage Water Heaters** (PG&E) – Driven by both the change in EnergyStar® requirements, increasing the initial minimum EF from 0.62 to 0.67 in late 2010, and the coming change in the federal minimum efficiency standards, from an EF of 0.59 up to 0.62 in 2015[7], manufacturers have filled out their gas-fired storage water heater product families to meet these efficiency requirements. In addition to new condensing, power/direct vent, and hybrid gas-fired product offerings, many new products are compatible with Category I venting, including features such as small combustion air blowers & inducers and powered vent damper. Unlike the most common minimum efficiency products, these products with EFs > 0.62 are powered and the impact and cost of this added electricity consumption has not been adequately quantified. In addition to providing datasets to update the most current software for simulating residential gas-fired SWHs, TANK (Paul et al., 1993), analysis of testing will focus on electricity consumption.
- **Tankless Water Heaters** (GTI) – Gaining popularity over the past decade, tankless water heaters have enjoyed increasing market share due to their high-efficiency relative to standard gas-fired storage water heaters, marketing of "endless hot water", and incentive programs. Deficiencies in the delivered versus rated efficiency of tankless water heaters are a known issue (Bohac, 2010 & Butcher, 2011), due to the minimum draw rate requirements and startup sequence delays, however they remain a challenge to characterize analytically. To simulate the performance of tankless water heaters, researchers have developed a robust single node model (Burch, 2008), which while complete in describing the steady state and transient heat transfer behavior of the tankless unit as a heat exchanger, implementing the model required an initial laboratory investigation. Some inputs may have sensitivity to test conditions (e.g. thermal capacitance) and some impacts of tankless controls are not captured (e.g. startup heating delays). While startup issues with GHPWHs are unique to the absorption process and do not impact delivered efficiency in the same manner as tankless products, only the results of 24 hour SUTs will be included, where this study focused on short-term impacts.

Gas Storage Water Heater Results: The purpose of testing storage water heaters was to compare how different styles of water heaters with varying energy efficiency features performed. The tests performed were the DOE First Hour Rating, DOE Standard Draw 24-Hour EF Test, GTI Medium Draw Profile, and GTI Low Draw Profile. With the exception of the 0.67 EF water heater, the intent was to test the spectrum of efficiency in a product line from a manufacturer selected due to their availability of both gas hybrid and condensing storage products.

7 Example is for a 40 gallon storage water heater

Table 16: Storage Water Heaters Description and Model Number

Unit Name	Description
15 Year Old Water Heater	**Atmospheric combustion with pilot light that has been in the field since its manufacture**
0.62 EF Atmos	**Atmospheric combustion with pilot light**
0.67 EF Atmos/Vent Damper	**Atmospheric combustion with electronic ignition. Standby losses are mitigated with powered vent damper, activated during off-cycles**
0.67 EF Power Vent	**Powered combustion (induced) with combustion air drawn from indoors, with electronic ignition and PVC venting**
0.67 EF Direct Vent	**Powered combustion (induced) with combustion air drawn from outdoors, with electronic ignition and PVC venting/air intake**
0.70 EF Atmos/Fan Boost	**Slightly pressurized combustion (small blower), compatible with standard atmospheric venting, with highly restrictive flue baffle and electronic ignition**
Hybrid	**Powered combustion (blower) with electronic ignition, has high thermal input, small storage volume, condenses with secondary heat exchanger**
Condensing Storage	**Powered combustion (blower) for condensing unit with submerged helical coil flue, with electronic ignition**

The testing and analysis for the storage water heaters was performed by PG&E, supervised by Robert Davis. For each unit listed in Table 16, a First Hour Rating (FHR) short term test is performed and three 24 hour tests are performed using the standard Dept. of Energy *24 Hour Simulated Use Test* procedure followed by the "Mid" and "Low" patterns (Davis, 2012). Table 17 shows a summary of results from the daily simulated use testing for the DOE Standard EF, GTI Mid, and GTI Low draw patterns.

This linearity of results is also highlighted in Figure 79, whereby an "Input/Output" approach is used as an analytical technique. For smaller outputs, a single draw/recovery cycle or collection of cycles, a proportional thermal input is required, yielding the efficiency versus gallons drawn per day as shown in Figure 80, with the trend identified in Table 17 clearly presented.

Table 17: EF Results for Storage Water Heaters

Description	DOE First Hour Rating		DOE Std Draw[8]		GTI Mid Draw	GTI Low Draw
	Mnfr.	Test	Mnfr.	Test	Test	**Test**
"15 Year Old" Water Heater	63	80	0.64	0.59	0.60	**0.44**
0.62 EF Atmos	71	70	0.62	0.60	0.60	**0.48**
0.67 EF Atmos/Vent Damper	67	70	0.67	0.66	0.66	**0.57**
0.67 EF Power Vent	70	89	0.67	0.64	0.64	**0.53**
0.67 EF Direct Vent	73	76	0.67	0.64	0.64	**0.53**
0.70 EF AtmosFan Boost	70	77	0.70	0.66	0.66	**0.54**
Hybrid	189	130[9]	90%[10]	0.68	0.68	**0.56**
Condensing Storage	**123**	**148**	**90%**	**0.74**	**0.73**	**0.62**

8 The EF results for the DOE standard draw have been adjusted according to the DOE standard procedures for operational offsets from the standard test conditions and the change in stored energy between the start and the end of the test. The GTI profile tests have only been adjusted for the change in stored energy.

9 In manufacturer's test, First Hour Rating test was continuous, although it settles out at a temperature below the initial set point. In our tests, the delivery temperature did drop by over 25°F from the initial starting point, which resulted in two draw events. The test was incomplete since a third draw should have been started at the 60 minute mark, so this number is low. The manufacturer was consulted and it was suggested that an unwanted blockage existed in the recirculation loop, thus the results are not representative of a properly working product.

10 Both the Hybrid (100,000 Btuh) and the Condensing (76,000 Btuh) are rated with burner inputs above 75,000 Btuh, and thus are classified as commercial units and have a thermal efficiency rating.

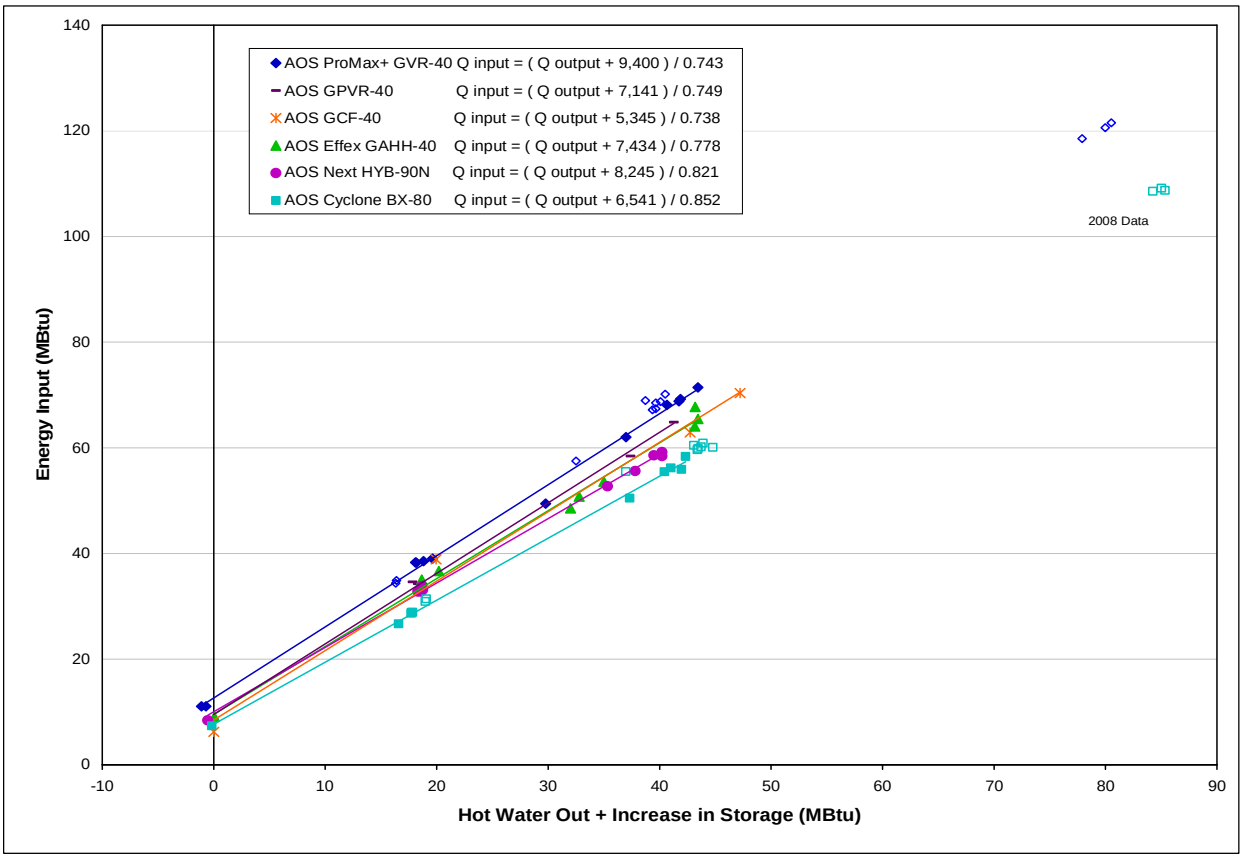

Figure79: Storage Water Heater Energy Input v Output Comparison[11]

11 Additional data included from 2008 PG&E study of gas water heaters as indicated

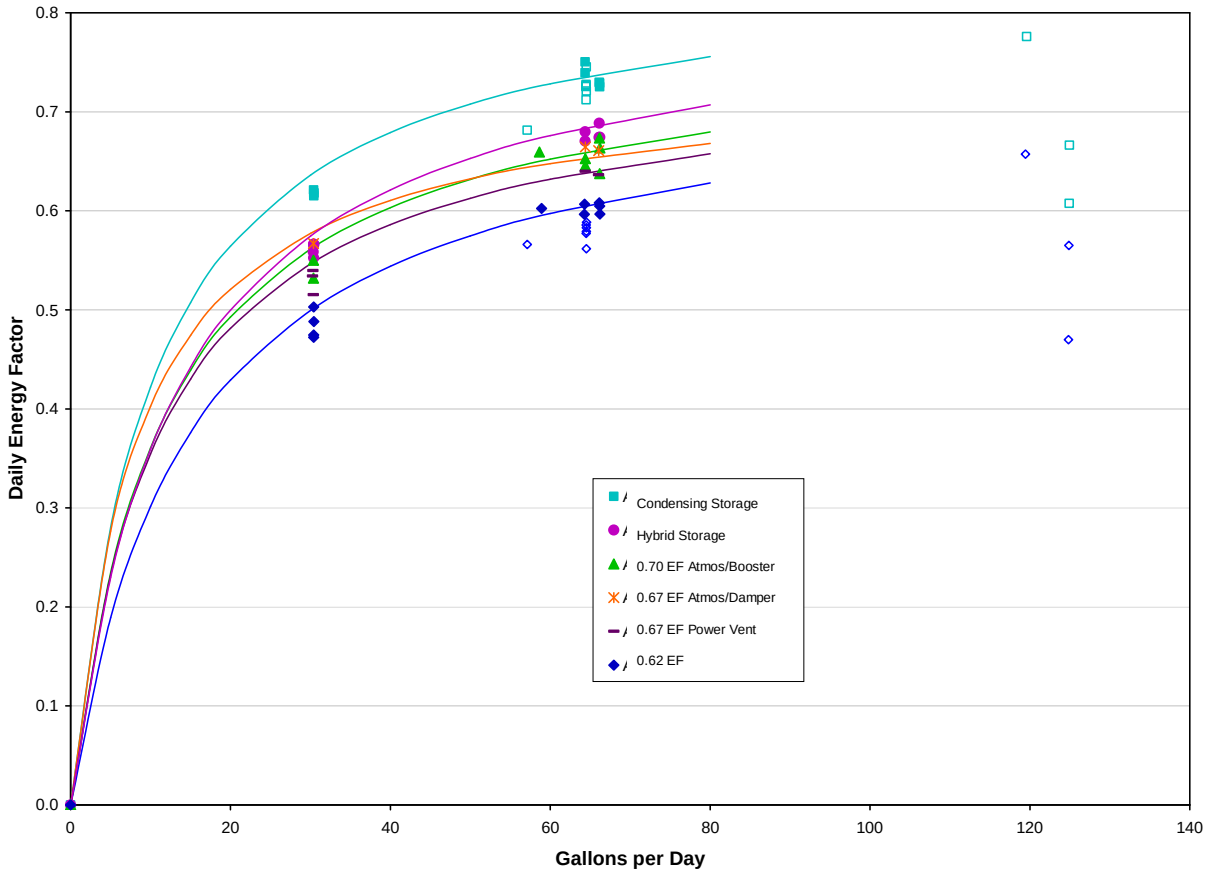

Figure 80: Storage Water Heater Daily Energy Factor v. Gallons per Day Comparison

Tankless: Tankless water heater testing was intended to (a) provided datasets for the validation of modeling tools and (b) investigate the nature of startup delays and other performance phenomena related to controls. Representative products were selected for testing, all whole-house water heaters, including a non-condensing, two standard condensing, and a condensing heater with a small onboard buffer tank, with details shown in Table 18.

Table 18: Tankless Water Heater Description and Model Numbers

Description	Firing Rate (Btu/hr)		Certified Performance			Unit Weight (lbs)	Water side volume (L, measured)
	Min	Max	EF	Max GPM	at ΔT (°F)		
Non-condensing	11,000	199,900	0.82	4.3	77	54	**0.875**
Condensing 1	9,500	199,000	0.93	4.4	77	70.5	**1.7**
Condensing 2	19,900	199,000	0.91	6.7	55	74	**0.92**
Condensing with small 2 L buffer tank	**17,000**	**199,000**	**0.95**	**5.1**	**77**	**86**	**3.7**

Reviewing the results in Table 19, first the trend observed with storage water heaters can be found whereby a lower daily hot water draw, in this case increasing the degree of intermittency, results in lower estimated EFs. To investigate the impact of the tankless product with a 2 L buffer tank and a pumped recirculation loop, two GTI-Mid tests compare the impact of active (24 hr/day) or inactive maintenance of this hot water store. While active, the unit has 50 recirculation events which act to decrease the overall efficiency, but reduce the time to deliver hot water and increase the average delivered temperature. It is worth mentioning that with an inactive buffer tank in the water pathway, a 2 L tank with a dip tube outlet 90% of the height, the average delivered temperature is lower and the delay longer than other tankless water heaters.

Table 19: Summary of 24 Simulator Use Test Data

	EF	Estimated EF		Average Delivered T (°F)		
	DOE	Mid	Low	DOE	Mid	Low
Non-condensing	0.77	0.75	0.73	129.6	125.3	129.9
Condensing	0.92	0.90	0.87	127.5	123.7	123.8
Condensing with BT (Active)		0.67			126.4	
Condensing with BT (Inactive)		0.85			119.8	

Comparing Operating Costs from Gas-fired Water Heater Lab Data

Using the energy cost assumptions shown in Table 20 and data from GHPWH and cofunded gas water heater testing, operating cost savings are estimated using representative California prices. These are summarized in Figures 81 and 82.

Table20: Energy Prices Used in Comparison (CA Focused)

Utility	Price	Reference
Electricity	15.32 ¢/kWh	**2011 PG&E Average**[12]
Natural Gas	**$0.9697/therm**	**2011 California Average**[13]

- Due to lower efficiencies and in some cases significant electric parasitic loads, gas storage water heaters have the highest operating cost. The condensing storage water heater has the lowest operating cost as it is the most efficient and at the other end of the efficiency spectrum are the 15 year old and 0.62 EF atmospheric water heaters which may be more cost effective than 0.67 EF storage water heaters for the non-standard draw patterns. Certainly these two have the lowest installed cost, thus they are overall more cost effective. Considering operating cost only, the difference in the cost of electricity eliminates savings from reduced fuel usage for some of the 0.67 EF SWHs. Keeping things in perspective, these differences in annual operating cost are no more than $45.
- Compared to gas storage water heaters, tankless water heaters offer operating cost savings for most or all cases, with non-condensing and condensing units respectively. The one exception is the

12 http://www.eia.gov/electricity/sales_revenue_price/pdf/table6.pdf
13 http://www.eia.gov/dnav/ng/ng_pri_sum_a_EPG0_PRS_DMcf_a.htm

condensing tankless unit with a continuously maintained buffer storage tank, where standby energy requirement greatly outweighs the efficiency benefit of such an arrangement. It is feasible that a properly scheduled circulation pump would result in higher efficiency than storage water heating options.

- With the results of the Beta GHPWH used with the assumed 33% reduction in the parasitic electricity load, in all cases operating savings are shown relative to tankless and storage options. In some cases, the operating savings are comparable to the condensing tankless water heaters, which is due to the lower than optimal efficiencies observed in Beta GHPWH testing, discussed in the prior section. As the estimated GHPWH EF is increased to 1.3, these savings will likely increase proportionally.

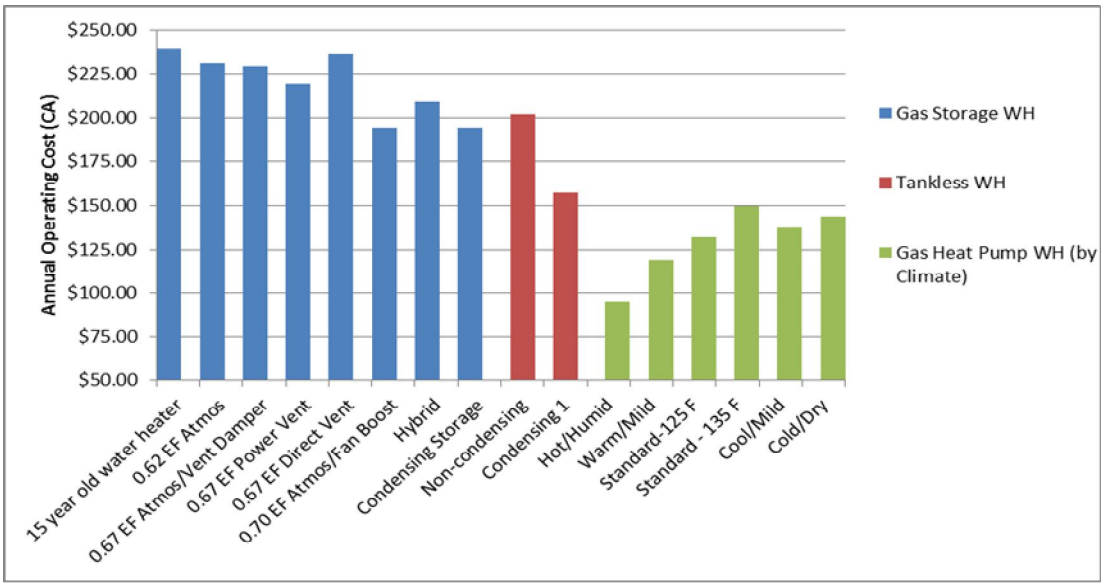

Figure 81: Annual Operating Cost Estimate for DOE Standard Draw Pattern (CA-Prices)

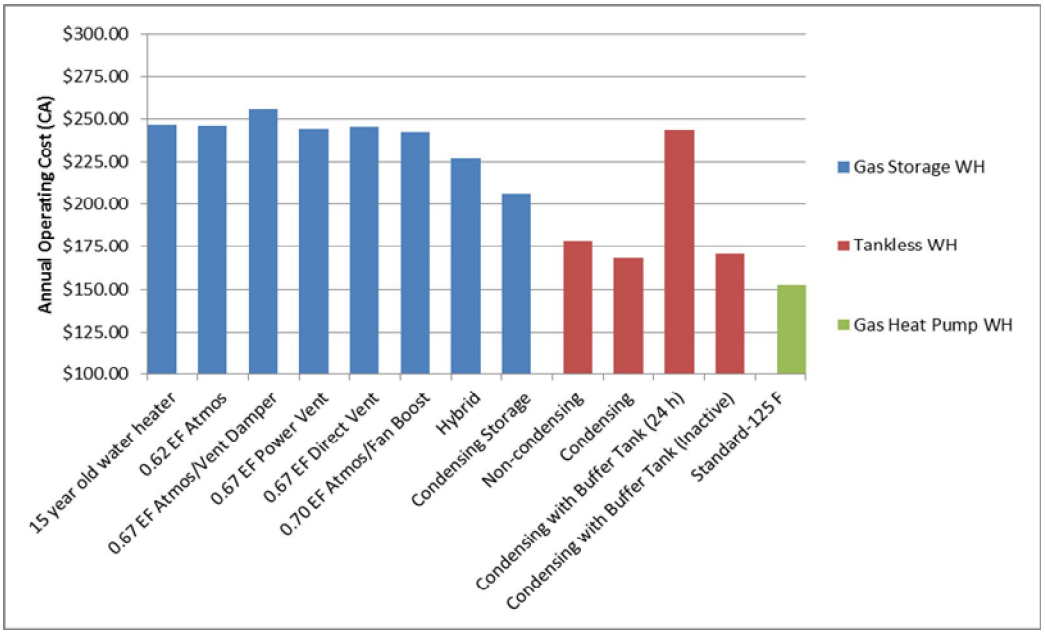

Figure 82: Annual Operating Cost Estimate for GTI Mid (Approx. 64 gal/day) Pattern (CA-Prices)

While in general electric parasitic loads increase with higher efficiency water heating options, the operating savings are heavily dependent on the price of natural gas. Using Florida as a comparative example, where the electricity-to-gas price ratio is much different than California as shown in Table 21, the operating cost savings are significantly greater for GHPWHs, by over a factor of 2 in most cases (Figure 83).

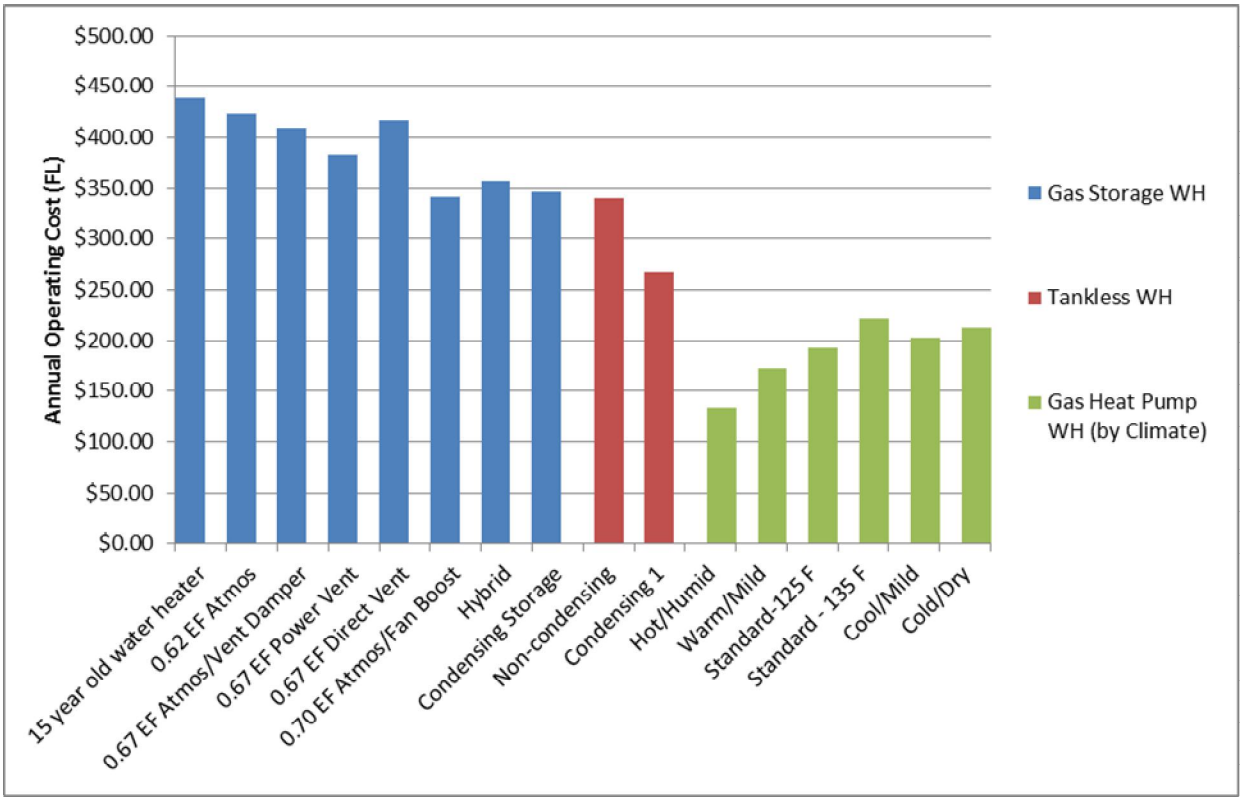

Figure 83: Annual Operating Cost Estimate for DOE Standard Draw Pattern (FL-Prices)

Table 21: Energy Prices Used in Comparison (CA Focused)

Utility	Price	Reference
Electricity	10.64 ¢/kWh	**2011 Florida Power & Light Average**[14]
Natural Gas	**$1.7734/therm**	**2011 Florida Average**[15]

Development of GSWH Analytical Model

A numerical model of typical gas storage water heaters, unpowered with center flue design, was developed for inclusion with whole-building models by the cofunded CEC project partner Lawrence Berkeley National Laboratory (LBNL) with validation data generated in GTI's laboratories. The intent for

14 http://www.eia.gov/electricity/sales_revenue_price/pdf/table6.pdf
15 http://www.eia.gov/dnav/ng/ng_pri_sum_a_EPG0_PRS_DMcf_a.htm

this component level sub-model, built in Modelica, is to be incorporated into the entire water heating system of a building, which will be maintained within the LBNL Buildings Library[16] for whole building simulations. The code is based on two simulation codes developed previously to model typical gas-fired storage water heaters, TANK developed by Battelle and primarily on HEATER developed by Arthur D. Little. GTI supplied high-resolution data within the storage tank, with submerged thermocouple assemblies at several elevations and radial distances from the center flue. Data was generated from the testing of a GE-branded Rheem gas storage water heater, 40 gallons, 36 kBtu/hr, and a 0.59 EF. In short, the LBNL effort was to (a) translate the original HEATER code into a Modelica-compatible format and (b) include validation of laboratory data generated by GTI. Full details of this effort are included with the forthcoming final reporting of CEC program 500-08-060.

With three rounds of testing, validation, and revision, the model produces reasonable agreement with experimental data. At the conclusion of this program, LBNL lists the following issues that remain to be addressed:

- A uniform heat transfer coefficient on the flue wall is used, there will need to be separate coefficients when firing and idle.
- The effect of numerical errors resulting from smoothing algorithms will need to be assessed and potential addressed.
- The model assumes the tank is well-mixed regardless of draw rates, future developments will consider the presence of stagnant zones with large volumes and/or low draw rates.
- The algorithms adopted from HEATER appear to release a noticeable quantity of heat from the flue side to the stored water after the burner cuts out. This will be investigated to determine its significance and, if any, physical reasoning.

Next Steps

Two aspects of the cofunded *Residential Water Heating* program experienced delays that impacted their integration with this GHPWH development effort. Concerning the development and revision of the MOT for rating residential water heaters, this process will continue to be unresolved beyond the close of these two programs in the end of 2012, thus it was not possible to consider the direct impact of a revised MOT on prototype GHPWHs. Concerning the development of a component level computer model of gas-fired storage water heaters and extending these results to GHPWHs, programming challenges resulted in significant delays such that a working model integrated with the hot water distribution model HWSIM was not achieved. These two efforts are ongoing, and as the GHPWH development effort continues the project team will (a) inform the continued regulatory effort for a revised MOT and (b) as a "production" level GHPWH is developed, consider methods to model GHPWH performance as part of an integrated hot water distribution model, using appropriate formatting (e.g. Modelica, etc.).

16 http://simulationresearch.lbl.gov/modelica/FrontPage

13.0 SUMMARY & TECHNOLOGY STATUS

Two candidate thermodynamic cycles were modeled and optimized for a residential gas-fired heat pump application. Breadboard testing was completed for a single-effect cycle using micro channel and conventional heat exchanger geometries, and for a GAX cycle using conventional. Based on obtained performance and projected manufacturing cost, the single-effect cycle using conventional heat exchangers was selected for packaged prototype development, with a target Energy Factor (EF) of 1.3.

Four packaged prototypes were designed, fabricated and tested: one "Alpha" and three "Beta" versions. The Alpha prototype was performance tested by SMTI, and Energy Factor (EF) tested by AO Smith. Beta 1 was EF tested by Gas Technology Institute (GTI), Beta 2 was EF tested by AO Smith and SMTI conducted optimization testing on Beta 3. All four Beta prototypes were capable of running autonomously, within certain ambient and water temperature regimes, and able to heat the stored water to 135^{o}F. The overall footprint of the gas heat pump is small enough to fit atop a standard residential storage tank, with overall dimensions very similar to electric heat pump water heaters currently in the market.

Measured heat pump efficiency (based on steady state measurements) is near maximum for a single-effect cycle. Incremental improvement is available by increasing the evaporator capacity and reducing ambient heat loss from the heat pump heat exchangers. Heating capacity ranges from near 10,000 Btu/hr at recovery start, to near 7,500 Btu/hr as the water is heated to 135^{o}F.

Raw EF test results were negatively impacted by:

- high energy losses from the storage tank (standby loss)
- high parasitic power use due to prototype controls and non-optimized motors
- lower than desired hot water outlet temperature during the 5th and 6th draws
- lower than target combustion efficiency
- higher than target hydronic return temperature during the first hour of recovery

Adjusting for standby, parasitic power and hot water outlet temperature, which can be corrected in production versions, resulted in an estimated EF of 1.15. Further work is required to increase the average combustion efficiency to 95% and reduce mixing in the storage tank to decrease the hydronic return temperature (allowing the heat pump to operate at higher COPs during the first hour of recovery). Based on the measured steady-state efficiency of the heat pump, if this two items can be corrected, an EF of 1.3 can be achieved on production models.

SMTI is currently negotiating a commercialization agreement, initiating a 24-30 month product development phase to bring this technology to the market by 2015.

14.0 REFERENCES

Bell, K. J. and M. A. Ghaly (1972), "Approximate Generalized Design Method for Multicomponent/Partial Condensers," *American Institute of Chemical Engineers, Papers* Vol. (24) pp. 72-79.

Bohac, D. et. al. "Actual Savings and Performance of Natural Gas Tankless Water Heaters". Minnesota Center for Energy and Environment (2010).

Brillant, S. et al. "Metal Fibre Particulate Filter: Function and Technology". 2005 SAE World Congress, Detroit, MI, paper 2005-01-0580.

Burch, J., Thornton, J., Hoeschele, M., Springer, D., and Rudd, A. "Preliminary Modeling, Testing, and Analysis of a Gas Tankless Water Heater". National Renewable Energy Laboratory paper NREL/CP=550-42917, presented at SOLAR Conference (2008).

Butcher. T et al. "Application of Linear Input/Output Model to Tankless Water Heaters", Brookhaven National Laboratory. Presented at ASHRAE Winter Meeting, Las Vegas, NV, 2011.

Carey, V. P. (1992). *Liquid-Vapor Phase-Change Phenomena : An Introduction to the Thermophysics of Vaporization and Condensation Processes in Heat Transfer Equipment*. Washington, D.C., Taylor & Francis Series, Hemisphere Pub. Corp.

Chen, J. C. (1966), "Correlation for Boiling Heat Transfer to Saturated Fluids in Convective Flow," *Industrial & Engineering Chemistry Process Design and Development* Vol. 5(3) pp. 322-329.

Colburn, A. P. and T. B. Drew (1937), "The Condensation of Mixed Vapours," *AIChE Transactions* Vol. 33 pp. 197-212.

Colon, C. and Parker, D."Side-by-Side Testing of Water Heating Systems: results from the 2009-2010 Evaluation" Rpt. No. FSEC-CR-1856-10.pdf, Florida Solar Energy Center, Cocoa, FL (2010).

Davis Energy Group (DEG), 2008 California Building Energy Efficiency Standards: Tankless Gas Water Heaters (2006).

Davis, R and Leni-Konig, K. "Laboratory Testing of Residential Gas Water Heaters" PG&E ATS (2008).

Davis, R. "Laboratory Evaluation and Field Testing of Residential Heat Pump Water Heaters" PG&E ATS (2010).

Davis, R. (2012) *Laboratory Testing of Advanced Storage Water Heaters*, presented at the ACEEE Hot Water Forum, Berkeley, CA.

Department of Energy (DOE), **10 *CFR Part 430*** *Energy Conservation Program for Consumer Products: test Procedure for Water Heaters*, Federal Register Vol. 63, No. 90 *(1998).*

Determan, M. (2005). *Experimental and Analytical Investigation of Ammonia-Water Desorption in Microchannel Geometries*. Mechanical Engineering. Atlanta, Georgia Institute of Technology, Vol. M.S. p. 104.

Garimella, S. (1999), "Miniaturized Heat and Mass Transfer Technology for Absorption Heat Pumps," *Proceedings of the International Sorption Heat Pump Conference*, Munich, Germany, pp. 661-670.

Garrabrant, M. A. and R. N. Christensen (1997), "Modeling and Experimental Verification of a Perforated Plate-Fin Absorber for Aqua-Ammonia Absorption Systems," *Proceedings of the ASME International Mechanical Engineering Congress and Exposition* Dallas, TX, USA, ASME, Fairfield, NJ, USA, pp. 337-347.

Garrabrant, M. (2012) *Gas-Fired Heat Pump Water Heater for Residential Applications*, presented at the ACEEE Hot Water Forum, Berkeley, CA.

Glanville, P. "Modified Simulated Use with Input/Output Method". Gas Technology Institute, presented at the ASHRAE Summer Meeting (2010).

Glanville, P., Kosar, D., and Suchorabski, D. (2012) , *Parametric Laboratory Evaluation of Residential Heat Pump Water Heaters,* Trans. of ASHRAE v. 118 pt. 1, Chicago, IL.

Glanville, P. (2012) *Lab Testing of Advanced Gas Storage and Tankless Water Heaters*, presented at Building America Expert Meeting on Water Heating, Golden, CO.

Glatt, E. et al. "Structure and pressure drop of real and virtual metal wire meshes". Frounhofer, ITWM, 2009. www.itwm.fraunhofer.de/fileadmin/ITWM-Media/Abteilungen/SMS/Pdf/bericht157.pdf

Healy, W, et al. "Input-Output Approach to Predicting the Energy Efficiency of Residential Water Heaters – Testing of Gas Tankless and Electric Storage Water Heaters". ASHRAE Transactions 117 (2011).

Healy, W.M. "Effect of Temperature Stratification Near Heating Elements on the Measured Energy Factors of Electric Water Heaters". ASHRAE Transactions 114 (2) (2008).

Hewitt, G. F., G. L. Shires and T. R. Bott (1994). *Process Heat Transfer*. Boca Raton, CRC Press; Begell House.

Hudon, K., Sparn, B., Christensen, D., and Maguire, J. "Heat Pump Water Heater Technology Assessment Based on Laboratory Research and Energy Simulation Models". NREL/CP-5500-51433 Presented at ASHRAE Winter Conference, Chicago, IL (2012). http://www.nrel.gov/docs/fy12osti/51433.pdf

Kakaç, S., R. K. Shah and W. Aung (1987). *Handbook of Single-Phase Convective Heat Transfer*. New York, NY, Wiley.

Kalensky, D. and Scott, S. GRI-06/0014, GTI Combo System Field Test Final Report, Gas Research Institute, December 2006.

Kang, Y. T., W. Chen and R. N. Christensen (1997), "Generalized Component Design Model by Combined Heat and Mass Transfer Analysis in Nh_3/H_2O Absorption Heat Pump Systems," *Proceedings of the ASHRAE Winter Meeting* Philadelphia, PA, USA, ASHRAE, Atlanta, GA, USA, pp. 444-453.

Kang, Y. T. and R. N. Christensen (1994), "Development of a Counter-Current Model for a Vertical Fluted Tube Gax Absorber, New Orleans, LA, USA, Publ by ASME, pp. 7-16.

Kang, Y. T. and R. N. Christensen (1995), "Combined Heat and Mass Transfer Analysis for Absorption in a Fluted Tube with a Porous Medium in Confined Cross Flow," *Proceedings of the ASME/JSME Thermal Engineering Joint Conference* Maui, HI, USA, ASME, New York, NY, USA, pp. 251-260.

Kang, Y. T., T. Kashiwagi and R. N. Christensen (1998), "Ammonia-Water Bubble Absorber with a Plate Heat Exchanger," *Proceedings of the 1998 ASHRAE Winter Meeting. Part 2 (of 2)*, San Francisco, CA, USA, ASHRAE, Atlanta, GA, USA, pp. 1565-1575.

Khir, T. et al. *Experimental Study on Forced Convective Boiling of Ammonia-Water Mixtures in Vertical Smooth Tube*, Arabian Journal for Science & Engineering, **30**, 1B pp. 47-63.

Klein, S. A. (2010). *Engineering Equation Solver*, F-Chart Software.

Khir, T. et al. *Experimental Study on Forced Convective Boiling of Ammonia-Water Mixtures in Vertical Smooth Tube*, Arabian Journal for Science & Engineering, **30**, 1B pp. 47-63.

Kwon, K. and S. Jeong (2004), "Effect of Vapor Flow on the Falling-Film Heat and Mass Transfer of the Ammonia/Water Absorber," *International Journal of Refrigeration* Vol. 27(8) pp. 955-964.

Lockhart, R. W. and R. C. Martinelli (1949), "Proposed Correlation of Data for Isothermal Two-Phase, Two-Component Flow in Pipes," *Chemical Engineering Progress* Vol. 45(1) pp. 39-45.

Nagavarapu, A. K. and S. Garimella (2011), "Design of Microscale Heat and Mass Exchangers for Absorption Space Conditioning Applications," *Journal of Thermal Science and Engineering Applications* Vol. 3(2) pp. 021005-021009.

Paul, D.D, Whitacre, G.R., Crisafullli, J. J., Fischer, R. D, Rutz, A. L., Murray, J. G., and Holderbaum, G. S. "TANK Computer Program User's Manual", Prepared by Battelle, July 1993, GRI-93/0186.

Price, B. C. and K. J. Bell (1974), "Design of Binary Vapor Condensers Using the Colburn-Drew Equations," *AIChE Symposium Series - Heat Transfer - Research and Design* Vol. 70(138) pp. 163-171.

RESNET. Results of Electronic Ballot of RESNET Board of Directors on Adopting Proposed Standard Amendment on Adjusting Instantaneous Water Heater Efficiency. April 4, 2012. http://resnet.us/board/Results_of_Electronic_Ballot_of_RESNET_Board_on_Adopting_Inst_Water_Amendment.pdf

Schoenbauer, B. et al. "Actual Savings and Performance of Gas Tankless Water Heaters" Minnesota Center for Energy and Environment. Presented at ASHRAE Winter Meeting, Las Vegas, NV (2011).

Silver, L. (1947), "Gas Cooling with Aqueous Condensation," *Industrial Chemist and Chemical Manufacturer* Vol. 23(269) pp. 380-386.

Sparn, B. et al. "Laboratory Performance Evaluation of Residential Integrated Heat Pump Water Heaters". National Renewable Energy Laboratory (2011).

Sparrow, E. M. and A. Haji-Sheikh (1965), "Laminar Heat Transfer and Pressure Drop in Isosceles Triangular, Right Triangular, and Circular Sector Ducts," *Journal of Heat Transfer* Vol. 87 pp. 426-427.

Thomas, M. et al. "A New Study of Hot Water Use in Canada" Natural Resources Canada. Presented at ASHRAE Winter Meeting, Las Vegas, NV (2011).

Wallis, G. B. (1969). *One Dimensional Two Phase Flow*. New York, McGraw-Hill.

15.0 List of Acronyms

AHRI	Air-Conditioning, Heating, and Refrigeration Institute
AOS	A.O. Smith
ASHRAE	American Society of Heating Refrigeration and Air-Conditioning Engineers
CEC	California Energy Commission
CFD	Computational Fluid Dynamics
CO	Carbon Monoxide
CO_2	Carbon Dioxide
COND	Condenser
COP	Coefficient of Performance
CWH	Commercial Water Heater
DEG	Davis Energy Group
DES	Desorber
DOE	U.S. Department of Energy
EEV	Electronic Expansion Valve
EF	Energy Factor
EHPWH	Electric Heat Pump Water Heater
EVAP	Evaporator
FEA	Finite Element Analysis
GAX	Generator Absorber Heat Exchanger (cycle)
GEN	Generator
GHPWH	Gas-fired Heat Pump Water Heater
GIT	Georgia Institute of Technology
GPM	Gallons Per Minute
GT	Georgia Institute of Technology
GTI	Gas Technology Institute
HCA	Hydronically Cooled Absorber
HPWH	Heat Pump Water Heater
HVAC	Heating, Ventilation and Air-Conditioning
ID	Inside Diameter
LBNL	Lawrence Berkeley National Laboratory
LiBr-H_2O	Lithium Bromide – Water (cycle)
LMTD	Log-Mean Temperature Difference
MOT	Method of Test
NAECA	National Appliance Energy Conservation Act
NH_3-H_2O	Ammonia – Water (cycle)
NIST	National Institute of Standards and Technology
NOx	Oxides of Nitrogen (NO2 + NO)
OD	Outside Diameter
PG&E	Pacific Gas & Electric
PLC	Programmable Logic Controller
RFI	Request for Information
RHX	Refrigerant Heat Exchanger
RTD	Resistance Temperature Detectors
RWH	Residential Water Heater
SCAGAX	Solution Cooled Absorber – Generator Absorber Heat Exchanger
SCAQMD	South Coast Air Quality Management District
SE	Single Effect (cycle)

SHD	Solution Heated Desorber
SHX	Solution Heat Exchanger
SL	Standby Loss
SMTI	Stone Mountain Technologies, Inc.
SPC	Standard Projects Committee
SUT	Simulated Use Test
TC	Thermocouple
TE	Thermal Efficiency
UA	Overall Heat Transfer Coefficient x Heat Transfer Area
UA	Standby Heat Loss Coefficient (EF Test)
WC	(of) Water Column